POLITECNICO DI TORINO

Collegio di Ingegneria Chimica e dei Materiali

Corso di Laurea Magistrale
in Ingegneria Chimica e dei Processi Sostenibili

Tesi di Laurea Magistrale

Studio sperimentale sull'impatto del processo di spray freeze-drying sulla morfologia del prodotto finito

Relatori
Prof. Roberto Pisano
Dott. Gianluca Boccardo
Dott.ssa Adali Merve Betul

Candidato
Antonio Jesús Clemente Ramírez

Marzo 2021

ACKNOWLEDGMENTS

This thesis marks the culmination of a period in my life, a period full of unknowns and challenges that I could not have overcome without the help of very special people in my life. This work is dedicated to those people, the ones that never stopped believing I could do it and were with me the whole way.

To my dad for giving me the strength of character and perseverance.

To my mom for showing me it is ok to look for emotional support in those who love you.

To my brother for showing me the value of hard work and for teaching never to be satisfied until I reach greatness.

To my girlfriend and her family for cheering me up, always believing I could do it, and for giving me a different outlook for life.

To Manuel, Miguel, Rafael, and Daily for keeping me grounded when my head was in the clouds.

To my friends for being there when I needed them.

To my teachers and advisors, for sharing your knowledge and cultivating a sense of curiosity and love for engineering in me, without you this would not have been possible.

And to you, the reader, for giving life to my words.

TABLE OF CONTENTS

SOMMARIO

I prodotti farmaceutici hanno degli standard industriali sempre più rigorosi in termini di sicurezza e salute del consumatore, richiedendo metodi di produzione sempre più efficienti. In particolare, nel campo dei preparati iniettabili si è alla ricerca di nuove metodologie che permettano la produzione in continuo di prodotti termolabili. In questo progetto di tesi ci si focalizzerà sullo studio del processo di spray freeze-drying come metodo per l'essiccamento in continuo di biofarmaci in massa.

Tecniche di essiccamento

Seppure esistano vari metodi di essiccamento, la maggior parte di questi metodi è incompatibile con le caratteristiche termolabili dei prodotti farmaceutici. A questo scopo si può utilizzare il processo di liofilizzazione che permette di separare il solvente in condizioni di bassa temperatura e alto vuoto. Nel seguito ci si soffermerà sulla tecnica dello spray freeze-drying che sarà approfondita in questo progetto di tesi.

Spray-drying

Questa tecnica è usata abbondantemente nell'industria di cibo e bevande (soprattutto nel settore di produzione di latte in polvere) per la sua facilità di uso e di scale-up. Il metodo consiste in una prima fase di atomizzazione della soluzione e successivo congelamento per esposizione aduna corrente gassosa avente bassa temperatura. Il prodotto congelato è poi trasferito in un contenitore e caricato in una camera di essiccamento in cui è esposto a condizioni di alto vuoto e blando riscaldamento, che promuove la separazione del solvente congelato per sublimazione.

Come già detto, questa tecnica ha il vantaggio di essere semplice da utilizzare e di essere ben consolidata nell'industria alimentare. Le stringenti esigenze di sterilità, e le basse temperature richieste dal prodotto, hanno però finora impedito l'affermarsi di questa tecnica nel campo farmaceutico.

Liofilizzazione

I prodotti che sono sensibili alle temperature però, non possono essere essiccati usando lo spray-drying dovuto alle alte temperature, relative al limite di questi componenti, usate. Quindi, il processo di liofilizzazione, il cui opera a temperature criogeniche, emerge come alternativa. La liofilizzazione (o "freeze-drying") si compone di tre fasi che sono descritte nel seguito

- Congelamento

Durante questa fase, l'acqua viene separata dalla soluzione per cristallizzazione. Questo, però, non avviene spontaneamente al suo punto di congelamento termodinamico, ma la soluzione rimane liquida fino a quando non raggiunge una temperatura molto più bassa. La temperatura alla quale si forma il primo cristallo è definita come la temperatura di

nucleazione e la differenza tra essa e il punto di congelamento termodinamico è definita "supercooling" o grado di sottoraffreddamento (Pisano, Alternative methods of controlling nucleation in freeze drying, 2019).

In un convenzionale processo di congelamento, la soluzione è gradualmente raffreddata al di sotto della temperatura di congelamento termodinamico fino alla formazione dei primi nuclei stabili. Essendo quest'ultimo fenomeno esotermico, si osserva un aumento improvviso della temperatura fino a quella di equilibrio termodinamico. Durante questa fase, i ripiani del liofilizzatore sono mantenuti a bassa temperatura per consentire una costante rimozione del calore che si libera durante la fase di accrescimento dei nuclei in cristalli di ghiaccio. (Rey e May, 2010). Una volta che tutta l'acqua "libera" si è separata per cristallizzazione e, quindi, viene meno il calore liberato dall'accrescimento, la temperatura del prodotto decresce progressivamente fino a raggiungere quella del ripiano del liofilizzatore.

- Essiccamento primario

Dopo il congelamento comincia l'essiccamento primario, la fase più impegnativa in termini di tempo e di energia del processo di liofilizzazione. Questa fase elimina la maggior parte dell'acqua attraverso la sublimazione del ghiaccio formatosi nella fase di congelamento. Quando le fiale vengono caricate nella camera di essiccamento, la camera è depressurizzata in modo da creare a condizioni di alto vuoto e la temperatura dei ripiani è aumentata per fornire il calore necessario per la sublimazione, facendo attenzione a mantenere il prodotto al di sotto del suo valore critico che, in genere, varia tra -40 e -10 °C Il vapore prodotto per sublimazione è rimosso dalle fiale attraverso un gruppo a vuoto che si compone da un condensatore e una pompa a vuoto.

- Essiccamento secondario

L'essiccamento primario elimina l'acqua "libera" si è separata in forma di cristalli di ghiaccio durante la fase di congelamento. Al termine di questa fase, il campione contiene ancora un quantitativo significativo di acqua che è intimamente legata al prodotto liofilizzato. Quest'ultima è rimossa grazie ad un riscaldamento più spinto che ne favorisce la separazione per desorbimento. Ciò permette il desorbimento dell'acqua "legata" al prodotto e permette al processo di raggiungere i livelli di umidità desiderati.

Spray freeze-drying

Il processo di liofilizzazione è piuttosto lungo e può richiedere anche alcune settimane per essere completato. Pertanto, si stanno studiando varie soluzioni che permettono di ridurne la durata. Lo spray freeze-drying è una di queste soluzioni. Come illustrato in Figura 1, il processo si compone di più fasi. La soluzione è dapprima nebulizzata attraverso un sistema di atomizzazione. La soluzione così nebulizzata è poi esposta ad una corrente di gas criogenico e posta a contatto diretto con un liquido criogenico che promuove il congelamento delle gocce di liquido prima formate. Le particelle congelate sono quindi trasferite in una camera di essiccamento dove sono esposte a condizioni di alto vuoto:

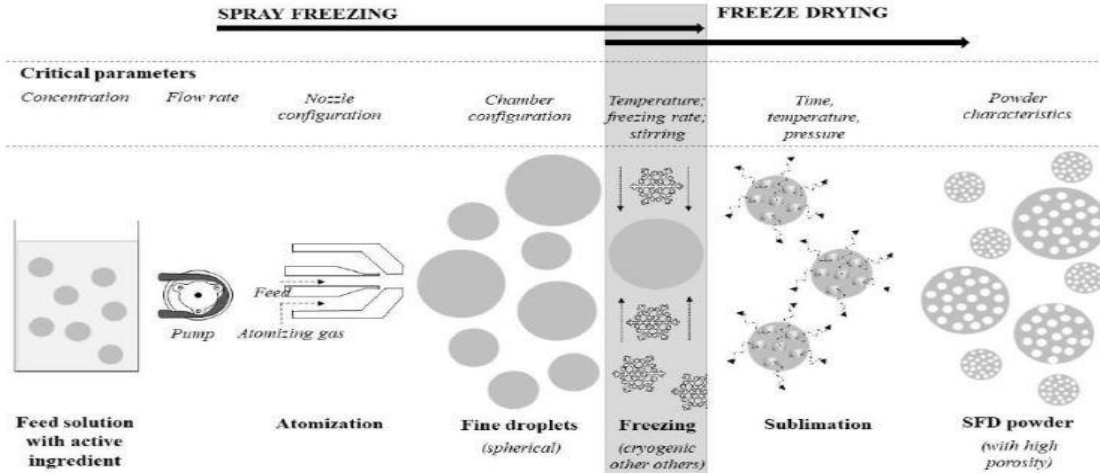

Figura 1. Schema del processo di spray freeze-drying. Figura tratta da: Vishali, Monisha, Sundari, Moses, e Chinnaswamy, 2019, con modifiche

Uno dei limiti del processo di liofilizzazione è legato alla formazione di una matrice solida che, seppure sia molto porosa, oppone un'elevata resistenza al flusso di vapore che si libera per sublimazione del ghiaccio. La liofilizzazione di particelle congelate di piccola dimensione, alcune decine di µm, permette di ridurre in modo significativo la resistenza al trasferimento di materia opposta dal materiale che deve essere essiccato.

Atomizzazione

Siccome è la fase più influente nella morfologia finale del prodotto, è indispensabile conoscere gli atomizzatori più communi a livello commerciale e le sue applicazioni. Bayvel e Orzechowski (1993) ne descrivono alcuni tra i quali si ricordano:

- Atomizzatore a getto:

Produce un getto di liquido che si disintegra dopo lo scarico dall'atomizzatore. Questo getto si produce facendo passare il liquido pressurizzato attraverso un orificio piuttosto piccolo, come quelli rappresentati dalla figura 2, lo cui trasforma la pressione in energia cinetica e di conseguenza atomizza il fluido. Sono molto economici e diffusi, ma non funzionano bene quando si lavora con un liquido viscoso.

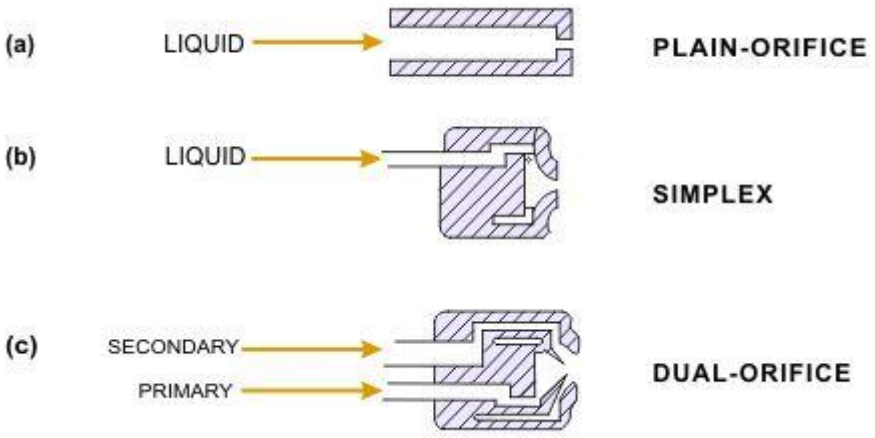

Figura 2. Schemi di diversi tipi di atomizzatori a getto. Figura tratta da: https://www.thermopedia.com/content/573, con modifiche

- Atomizzatore a vortice:

  Come rappresentato in figura 3, invece di essere iniettato direttamente il fluido viene inserito in modo tale da generare un movimento vorticoso che fa uscire lo spruzzo non come un getto compatto, ma come un ampio foglio di forma conica. Questo aiuta a garantire una corretta atomizzazione del flusso a pressioni medio-basse. Se la velocità con cui il fluido è introdotto è bassa, l'atomizzazione sarà dovuta allo stesso fenomeno dall'atomizzatore a getto (cioè alla trasformazione della pressione in energia cinetica dovuta al cambio di diametro). Quando invece ne ha una velocità media-alta, l'atomizzazione avverrà in parte per fenomeni ondulatori generati dal movimento vorticoso. Finalmente, per valori di velocità molto alte l'atomizzazione sarà dovuta all'azione dell'aria ambientale introdotta per il movimento a vortice (Bayvel e Orzechowski, 1993). Questo ugello, così come quello a getto, è molto usato quando il fluido e poco viscoso ma non trova molte applicazioni quando la viscosità aumenta.

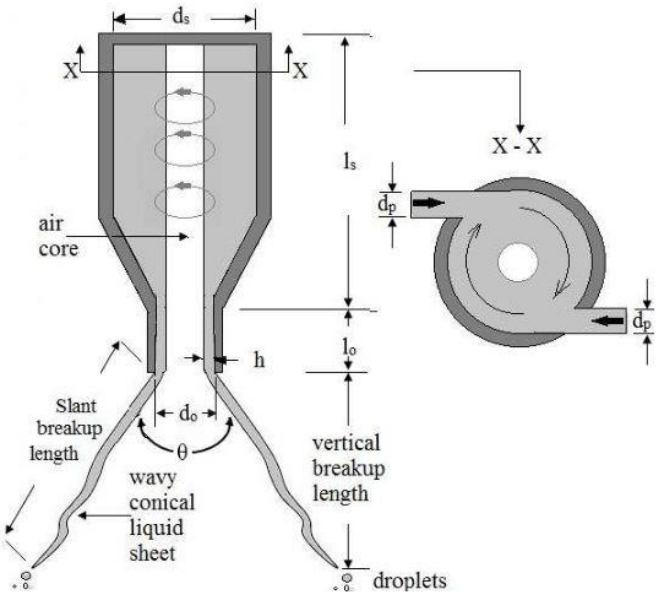

Figura 3. Schema di un atomizzatore a vortice di categoria simplex. Figura tratta da: Vijay, Moorthi, e Manivannan, 2015, con modifiche

- Atomizzatore ad ultrasuoni:

Questi sono tipi relativamente moderni di ugelli, principalmente usati nell'industria farmaceutica e della chimica fine perché producono un getto molto raffinato, che può poi essere essiccato in una polvere con qualità molto soddisfacente. Ci sono due teorie principali che esplorano i meccanismi di funzionamento coinvolti in questo ugello, la teoria della cavitazione e quella dell'onda capillare. Nel lavoro di Bouguslavskii ed Eknadiosyants (1969) si descrive l'intero processo come un accoppiamento dei due modelli, suggerendo che lo shock idraulico periodico della cavitazione interagisce ed eccita le onde capillari, producendo goccioline. Vale la pena notare che, mentre le goccioline prodotte dalle onde capillari hanno una distribuzione eccezionalmente uniforme, la disintegrazione causata dallo shock di cavitazione (che è essenzialmente un fenomeno casuale) è molto irregolare e porta ad una distribuzione non uniforme. La figura 4 fornisce una rappresentazione visiva del funzionamento dell'ugello.

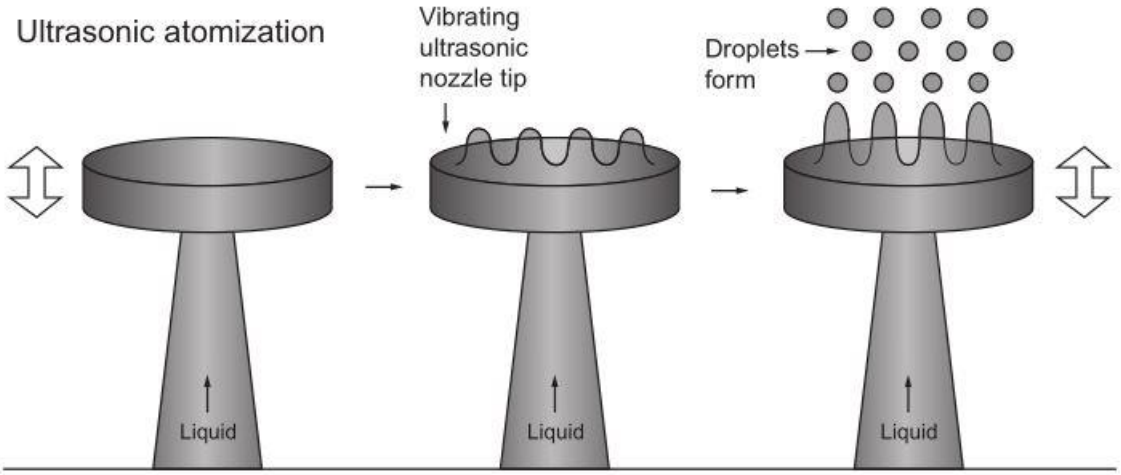

Figura 4. Schema di un atomizzatore ad ultrasuoni. Figura tratta da: Gogate, 2015, con modifiche

Congelamento

Il metodo con cui avviene il congelamento deve essere decisamente diverso da quello utilizzato per un normale processo di liofilizzazione, in quanto il prodotto a essiccare non si trova come un liquido contenuto in flaconi o come pezzi solidi, ma come uno spray fino. La figura 5 riporta i tre metodi utilizzati per questo processo.

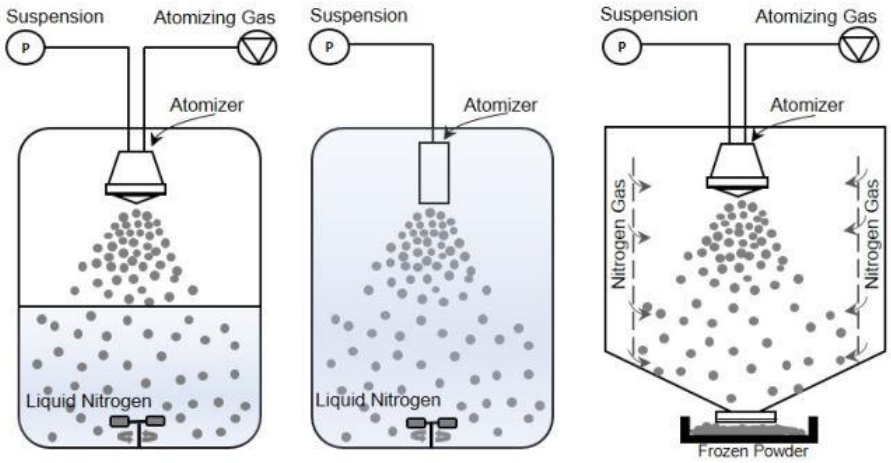

Figura 5. Modalità di spray-freezing: SFV/L (sinistra), SFL (centro) and SFV (destra). Figura tratta da: Adali, Barresi, Boccardo e Pisano, 2020 con modifiche

- Spray-freezing into vapor (SFV)

In questa modalità di congelamento a spray, la soluzione e nebulizzata direttamente in una camera contenente un fluido criogenico in fase vapore, generalmente fatto fluire in direzione controcorrente allo spray. Questo però genera dei problemi con il recupero della polvere liofilizzata e la loro elutriazione (Leuenberger H. , 2002). Quindi, alcuni studi si sono occupati di risolvere il problema; una soluzione interessante è quella proposta per Wang, Finlay, Peppler, e Sweeney (2006), la cui fa passare il criogeno in direzione co-corrente attraverso buchi disposti nella parete della camera, migliorando considerevolmente il recupero di prodotto.

- Spray-freezing into liquid (SFL)

In questo processo l'ugello è immerso nel fluido criogenico che, a differenza dallo SFV, si trova in fase liquida. Operare in questo modo ci permette di lavorare con fluidi più economici (come la CO_2 pressurizzata) invece di azoto, ed è più efficiente nel suo processo di trasferimento d'energia perché il coefficiente di scambio dei liquidi è molto elevato rispetto a quelli dai gas. Inoltre, il limitato contatto con l'aria aumenta la stabilità dei componenti attivi, e avere un congelamento più veloce diminuisce i loro processi di segregazione (Yu, Johnston, e O.Williams III, 2006).

- Spray-freezing into vapor over liquid (SFV/L)

Questo metodo consiste in nebulizzare la soluzione su di un liquido criogenico bollente, così da avere un piccolo strato di vapore che faccia uno stadio di raffreddamento prima di congelarsi nel liquido. Lo strato di vapore che fa d'innesco al processo di congelamento potrebbe, potenzialmente, proteggere le particelle ottenute della contaminazione causata dal contatto intimo fra il prodotto in fase liquida e il fluido criogenico, perché al momento di arrivarci alla superficie la goccia è già parzialmente (oppure completamente) congelata.

Essiccamento

Una volta eseguito lo "spray-freezing", si può utilizzare il normale processo di liofilizzazione, ma il principale vantaggio che ha questo processo è il suo potenziale per lavorare in continuo e a condizioni atmosferiche, togliendo la necessità di un vuoto estremo per raggiungere gli obiettivi di umidità del prodotto e la natura batch del processo tradizionale. Alcuni dei nuovi metodi per l'essiccamento sono riportati a continuazione.

- Spray freeze-drying atmosferico (ASFD)

Questa modalità di operazione basato sugli studi di Meryman (1959) e da Lewin e Mateles (1962, come citato in Ishwarya et al., 2015) propone di operare a pressione atmosferica. Il metodo si basa sul fatto che la forza spingente del processo di liofilizzazione non è esclusivamente il gradiente di pressione totale nella camera, ma anche la differenza di pressione parziale dell'acqua fra questa e le particelle. In un'operazione normale di liofilizzazione, i prodotti generano una resistenza al trasferimento di materia dovuta alle loro dimensioni, facendo molto difficoltoso questo processo (Quast e Karel, 1968). Quindi, lo step di atomizzazione dello spray freeze-drying fa si che questa resistenza venga eliminata, permettendo di lavorare anche in queste condizioni di pressione.

Ulteriori studi hanno trovato che, sebbene il processo genera un risparmio di tempo nella fase di carico-scarico (togliendo il bisogno di "airlocks" e apparecchiature aggiuntive per tenere il vuoto) e di energia rispetto alla liofilizzazione tradizionale, l'essiccamento è piuttosto lento a queste condizioni, e anche utilizza i gas essicanti in una quantità e velocità cosi elevata da far sparire i risparmi ottenuti in precedenza (Ishwarya et al., 2015).

- Modello di Rey

Nel loro libro, Rey e May (2010) suggeriscono l'adozione di un sistema che utilizza l'atomizzazione del prodotto come primo step per poter operare in continuo. Nella figura 6 si riporta il disegno proposto per Rey. Si può osservare che l'alimentazione al processo è formata da un passaggio di nebulizzazione e congelamento iniziale (1). Seguitamente, le particelle congelate passano ad una camera al vuoto (2) dove si realizza l'essiccamento primario. L'essiccamento secondario si esegue nel terzo stadio (3), dove si fanno incidere delle onde infrarosse (o microonde) e si diminuisce la pressione per togliere l'acqua "legata" al prodotto, e finalmente nel quarto stadio (4) si raccoglie il prodotto secco e si mette in flaconi.

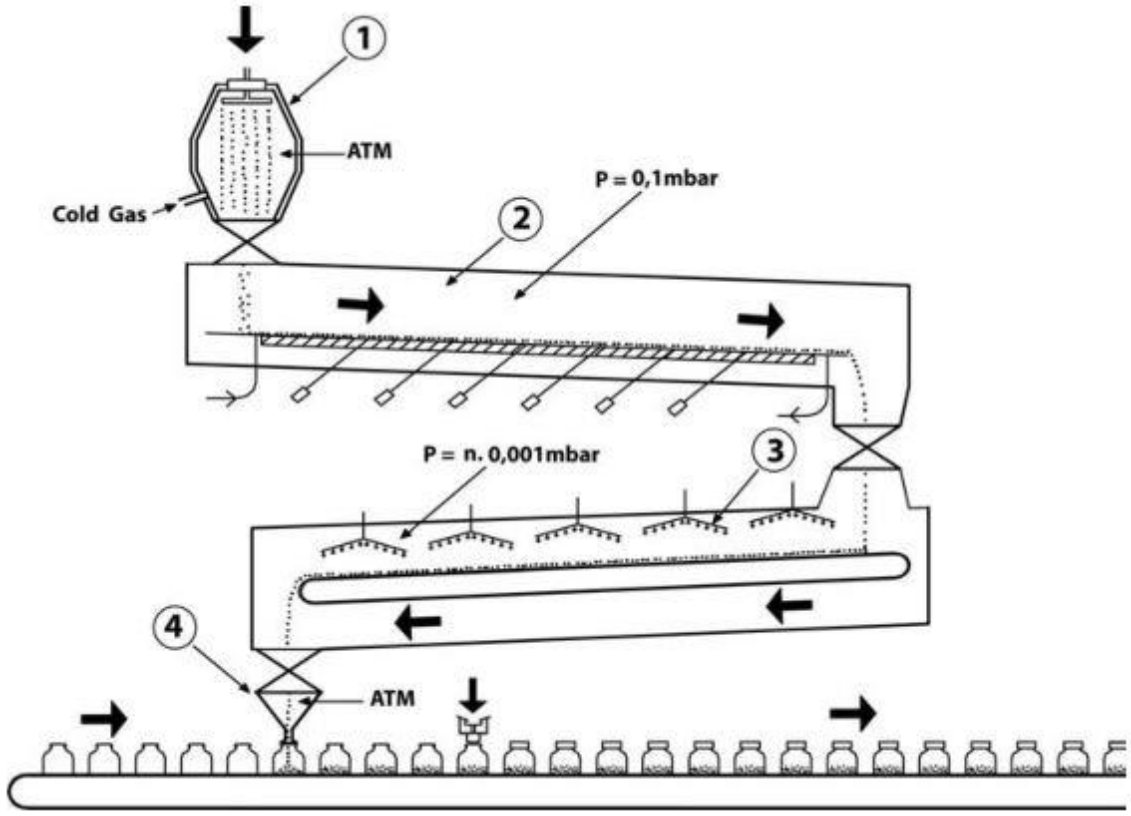

Figura 6. Schema del modello di Rey per operazioni di liofilizzazione in continuo. Figura tratta da: Rey e May, 2010, con modifiche

Tecniche di caratterizzazione

Esistono diversi metodi per la caratterizzazione morfologica delle particelle liofilizzate, ma fra quelli più comuni si trovano la microscopia elettronica a scansione (SEM) e l'adsorbimento di gas sulla superficie (BET).

Microscopia elettronica a scansione (SEM)

Quest'analisi è ormai diventata uno standard per l'analisi morfologica delle strutture grazie alla sua semplicità e precisione. La tecnica consiste nel focalizzare un fascio di elettroni sulla superficie di un campione per ottenere un modello di diffrazione che può essere elaborato in una fotografia ad alta risoluzione della sua topografia superficiale. Un esempio di immagine SEM è riportato in figura 7.

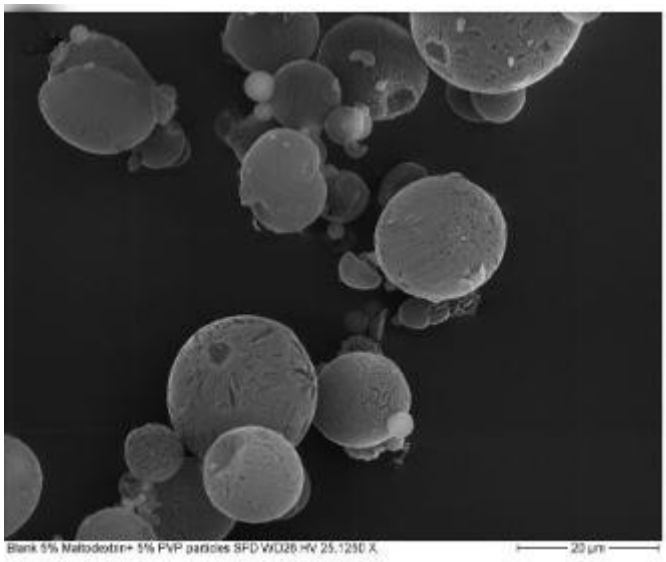

Figura 7. Immagine al SEM di particelle di maltodestrina + PVP prodotte tramite spray freeze-drying. Figura tratta da: Alia e Lamprecht, 2014, con modifiche.

Poiché questo metodo si basa sulla capacità di un materiale di condurre e disperdere elettroni, un tipico campione per l'analisi al SEM è costituito da sostanze che sono di natura metallica perché gli elettroni possono scorrere liberamente al loro interno, producendo quindi i risultati desiderati. Per una sostanza non metallica, però, è necessario eseguire un processo di metallizzazione (che consiste nel rivestire il campione con una pellicola conduttiva) prima di iniziare l'analisi.

Adsorbimento di gas (BET)

Un solido con un'area superficiale elevata può scambiare massa e calore a un ritmo accelerato, che nel caso dell'industria farmaceutica è auspicabile perché il prodotto può essere ricostituito rapidamente prima dell'uso. È anche interessante notare che i solidi porosi hanno un'aerodinamica che può essere sfruttata per i farmaci ingeriti dal polmone.

L'uso di gas inerti per determinare l'area superficiale deriva dalla teoria dell'adsorbimento fisico proposta da vari scienziati nel corso degli anni. La teoria più degna di nota è quella di Langmuir, che afferma che una sostanza adsorbita lo farà in un monostrato che raggiunge ogni angolo della particella. Sulla base di questa teoria,

Brunauer, Emmet e Teller svilupparono la loro equazione omonima (equazione Brunauer-Emmet-Teller o BET) che mette in relazione diversi parametri che possono essere usati per determinare il volume adsorbito e di conseguenza trovare l'area superficiale attraverso la seguente equazione: $P/[V*(P_0-P)] = 1/(V_m*C)+(C-1)*P/(V_m*C*P_0)$ dove P è la pressione parziale dell'adsorbato, V è il volume di gas adsorbito a P, Vm è il volume adsorbito come monostrato, P0 è la pressione di saturazione alla temperatura sperimentale e C è una costante.

Ci sono sei diversi modelli che l'isoterma di adsorbimento risultante può produrre, tutti rappresentati in figura 8:

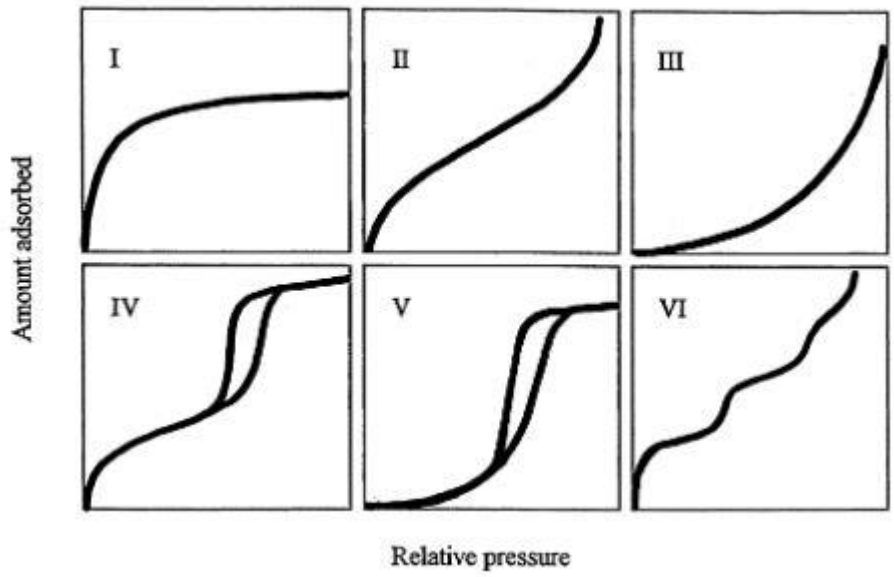

Figura 8. Classificazione IUPAC delle isoterme di adsorbimento. Figura tratta da: Donohue e Aranovich, 1998, con modifiche.

Secondo Donohue e Aranovich (1998), ogni tipo di curva può essere classificato in base al tipo di adsorbato che descrive.

> "*L'isoterma di tipo I "si avvicina a un valore limite" e di solito è usata per descrivere l'adsorbimento su adsorbenti microporosi. I tipi II e III descrivono l'adsorbimento su adsorbenti macroporosi con interazioni adsorbato-adsorbente forti e deboli rispettivamente. I tipi IV e V rappresentano l'adsorbimento mono e multistrato più la condensazione capillare Il tipo VI, che non era incluso nella classificazione di Brunauer, illustra che le isoterme di adsorbimento possono avere uno o più stadi di adsorbimento*."

Obiettivi della tesi

Questa tesi ha l'obiettivo di studiare l'influenza delle condizioni operative utilizzate per la fase di atomizzazione sulla morfologia, dimensione ed eterogeneità delle particelle prodotte per spray freeze-drying. Nello specifico si è studiato l'influenze della potenza fornita all'atomizzatore ad onde ultrasonore, la portata di alimentazione e la viscosità della soluzione da atomizzare.

Materiali e metodi

Questa sezione fornirà una spiegazione dettagliata della procedura sperimentale utilizzata per ottenere i risultati sperimentali di questa tesi, da come i campioni sono stati preparati a come sono stati analizzati utilizzando le tecniche precedentemente menzionate.

Materiali e preparazione dei campioni

Le sostanze utilizzate per condurre gli esperimenti sono D-mannitolo (Sigma-Aldrich, Germania) con una purezza riportata maggior o uguale 99% e saccarosio (Sigma-Aldrich, Germania) di grado puriss. Entrambi sono eccipienti comuni usati nell'industria farmaceutica per assicurare che la morfologia e le proprietà del prodotto finale siano all'altezza di un determinato standard.

Le formulazioni di mannitolo sono state preparate per ottenere una concentrazione di 5% p/p e quelle di saccarosio di 5% p/p e di 40% p/p. Utilizzando una bilancia elettronica, il componente è stato introdotto in un becher da 250 ml fino a raggiungere la massa necessaria per produrre 200 ml di soluzione alla concentrazione desiderata. Per la preparazione di tutte le soluzioni è stata utilizzata acqua pura. Dopo aver diluito la polvere del componente, le formulazioni sono state messe su un agitatore magnetico finché non c'erano grumi visibili. Dopo aver raggiunto questo risultato, il becher è stato sigillato con carta paraffinata per evitare la contaminazione dei campioni e l'agitatore è stato tenuto acceso fino all'iniezione della miscela.

Processo di atomizzazione e congelamento

La soluzione è stata introdotta in una siringa di capacità di 100 mL, facendo attenzione che non ci fossero bolle d'aria. La siringa è poi stata alimentata al sistema di atomizzazione ad ultrasuoni tramite una pompa a siringa. Nella fase di avvio, si è alimentato l'atomizzatore con una portata progressivamente crescente di soluzione fino alla formazione di un flusso continuo di gocce. A valle di quest'operazione preliminare, si sono avviate le prove oggetto di studio che sono state condotte utilizzando un volume costante di soluzione (30 mL) ed una portata di 1 mL/min, 2.5 mL/min, 5 mL/min, 7.5 mL/min e 10 mL/min. Durante questa fase, le potenze utilizzate per l'atomizzazione delle soluzioni di mannitolo sono state 1W, 3W e 4,5W, mentre per le preparazioni di saccarosio è stata 3W.

Nella figura 9 si può visualizzare che il metodo di congelamento scelto in questo sperimento è stata lo "spray-freezing into vapor over liquid" (SFV/L). Questa modalità comprende la atomizzazione dei campioni in un "dewar" contenente azoto liquido, lasciando uno spazio moderato fra l'ugello e il liquido criogenico bollente per averci uno strato di vapore. Durante l'atomizzazione, il fluido criogenico è stato mantenuto in agitazione tramite un agitatore magnetico allo scopo di evitare l'aggregazione delle particelle congelate. Dopo aver iniettato il volume impostato, la pompa si è spenta automaticamente, l'atomizzatore e l'agitatore magnetico sono stati spenti, e il dewar contenente le particelle congelate è stato svuotato in un vassoio uguale a quello rappresentato in figura 9, dove sono state lasciate ad asciugare fino alla completa evaporazione dell'azoto.

Figura 9. Sistema Dewar-atomizzatore (sinistra) e vassoio con il prodotto (destra)

Raccolta dei campioni, caricamento e processo di essiccamento

Mentre si produceva il primo lotto, la temperatura dello "shelf" dell'essiccatore è stata impostata a -50 °C per mantenere i campioni congelati prima di essiccarli. I vari campioni sono stati poi caricati nei vari compartimenti del vassoio riportato in figura 10, e questo a sua volta è stato caricato all'interno del liofilizzatore. Una termocoppia è stata inserita nell'apparecchio e posta in un portacampioni per monitorare la temperatura del prodotto durante il processo.

Figura 10. Vassoio segmentato

Una volta che il vassoio è stato completamente caricato con i campioni, è stato introdotto nel liofilizzatore e lo "shelf" è stato raffreddato al valore di temperatura specifico per il campione ad essere analizzato. Nei lotti di mannitolo, la temperatura per l'essiccazione primaria è stata impostata a 10 °C e la pressione a 200 µbar; per i lotti di soluzione di saccarosio, la temperatura è stata impostata a -20 °C e la pressione a 100 µbar. Quando la temperatura dello "shelf" ha raggiunto il set-point, il processo di essiccazione primaria è stato avviato.

Il tempo di essiccamento non è stato preimpostato ma è stato determinato per ciascuna prova confrontando il segnale di pressione di un sensore capacitivo e di uno termo-conduttivo. Dopo quel punto, è iniziata l'essiccazione secondaria; sono state mantenute le stesse condizioni di pressione e la temperatura è stata aumentata a 20 °C per favorire il desorbimento dell'acqua legata. Il processo è stato eseguito per cinque ore.

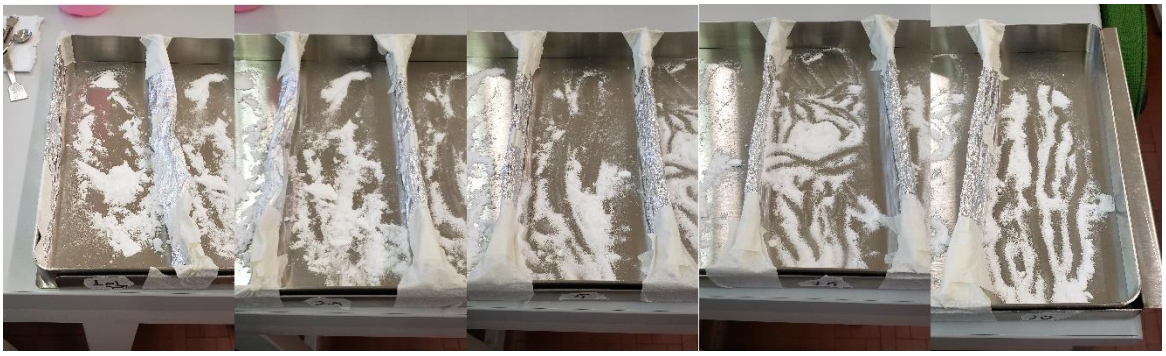

Figura 11. Immagine del vassoio contenente la polvere essiccata della soluzione di saccarosio al 40% ottenuta usando una diversa portata di alimentazione all'atomizzatore ultrasuoni.

Caratterizzazione della polvere liofilizzata

Dopo che i campioni sono stati liofilizzati e partizionati in flaconi, essi sono stati caratterizzati tramite analisi BET e SEM.

Per quanto riguarda l'analisi BET, circa 200 mg di polvere sono stati introdotti nella cella di carico dello strumento e si è poi effettuata una fase preliminare di degassaggio a circa 40°C per 3 ore. Questo pretrattamento ha lo scopo di eliminare ogni contaminante gassoso eventualmente adsorbito sulla superficie del campione. Per quanto riguarda l'analisi SEM, i campioni sono stati metallizzati per permettere agli elettroni di muoversi liberamente sulla superficie.

Le immagini acquisite al SEM sono state elaborate utilizzando ImageJ per misurare le dimensioni delle particelle visibili. Per la maggior parte delle immagini, il numero di misure realizzate per ogni particella sono state cinque, ma per la soluzione di saccarosio al 40% il numero di misure è stato cambiato da cinque a otto per compensare il fatto che le particelle non erano perfettamente sferiche. I dati grezzi sono stati poi utilizzati per calcolare la media e la deviazione standard. Tutti i calcoli e le analisi sono stati fatti attraverso il software OriginLab pro.

Risultati

Questa sezione si concentrerà sulla presentazione dei risultati ottenuti dalla procedura sperimentale e sulla loro discussione, dando particolare attenzione alle condizioni che potrebbero influenzare le proprietà morfologiche delle particelle ottenute.

Dimensioni delle particelle

Le figure 12 e 13 riportano le immagini SEM per i campioni a base di mannitolo al 5% (p/p), atomizzati sia a 3 W che a 4,5 W, per portate di 1 mL/min e 10 mL/min.

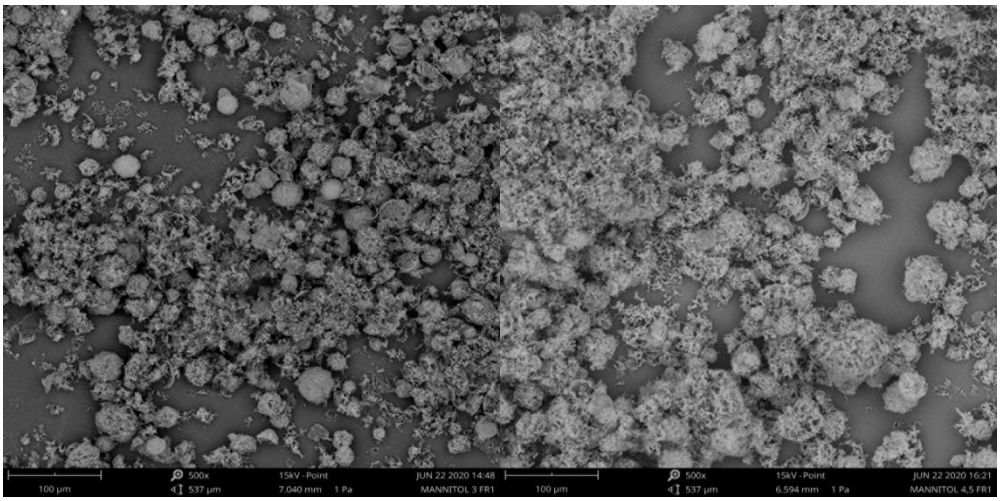

Figura 12. Immagini SEM dei campioni di mannitolo prodotti a 1 mL/min ad una potenza utilizzata di 3 W (sinistra) e 4,5 W (destra)

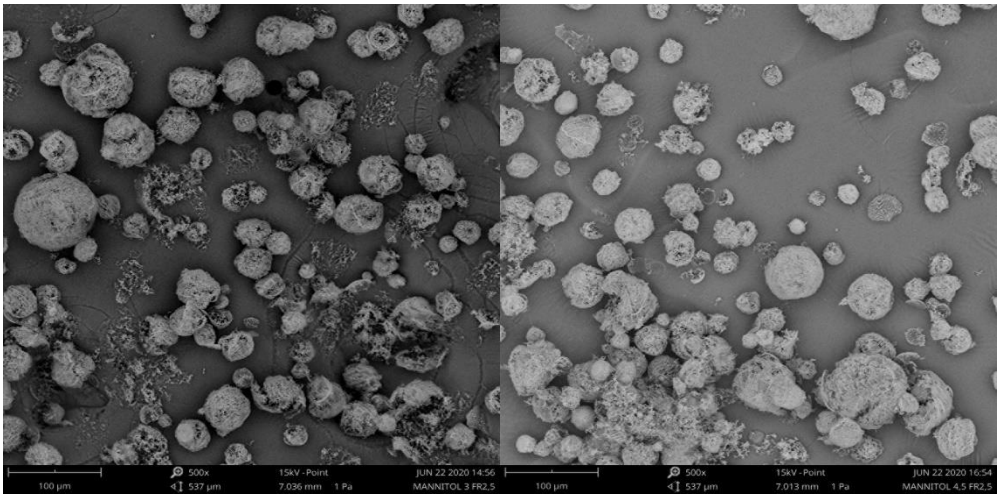

Figura 13. Immagini SEM dei campioni di mannitolo prodotti a 10 mL/min ad una potenza utilizzata di 3 W (sinistra) e 4,5 W (destra)

La prima cosa che possiamo osservare è che, quando si utilizza una potenza maggiore, i campioni formano una struttura a spugna sia a 1 mL/min che a 10 mL/min. Appoggiandoci al fatto che l'atomizzatore usato per questo studio aveva una frequenza impostata di 60 kHz, possiamo analizzare la situazione in base alla teoria della cavitazione per l'atomizzazione ultrasonica. Come evidenziato da Avvaru et al. (2006), una parte della potenza utilizzata per questo tipo di atomizzazione è utilizzata per far oscillare il film liquido, causando quindi

un film più sottile di quello che il valore teorico suggerirebbe. Allo stesso tempo, i film più spessi generati da un aumento della portata corrispondono ai loro valori teorici perché le forze gravitazionali hanno più influenza delle forze viscose.

Ulteriori ricerche come quella di Rajan e Pandit (2001) indicano che c'è una portata limite alla quale la potenza andrà interamente verso l'atomizzazione del fluido perché la gravità avrà una notevole influenza nell'oscillazione del fluido. Pertanto, quando tutta l'energia viene utilizzata per questo scopo (quando lo spessore è oltre il suo limite), il campione potrebbe essere disintegrato se viene impiegata troppa potenza. Questo offre una possibile spiegazione del perché, mentre a 3 e 4,5 W i campioni da 10 mL/min presentavano le stesse strutture amorfe di quelli formati a 1 mL/min, quelli generati a 1 W non le hanno generate. Le altre velocità di flusso hanno formato particelle piuttosto definite, nel senso che si possono osservare goccioline sferiche chiare.

È stato trovato che il modello statistico più appropriato era la distribuzione LogNormal, che ha costantemente fornito un fattore r^2 vicino a 0,99 per tutte le formulazioni. La media e la deviazione standard che derivavano da tale distribuzione sono riportate nella tabella 1.

Tabella 1. Media e deviazione standard delle dimensioni delle particelle di mannitolo al variare della potenza erogata all'atomizzatore

	Mannitolo 1 W		**Mannitolo 3 W**		**Mannitolo 4.5 W**	
Portata (mL/min) [Q]	**Media (µm) [M]**	**Deviazione Std. (µm) [σ]**	**Media (µm) [M]**	**Deviazione Std. (µm) [σ]**	**Media (µm) [M]**	**Deviazione Std. (µm) [σ]**
1.0	18.89	0.37	11	0.25	14.5	0.29
2.5	21.95	0.41	15.1	0.4	14.57	0.34
5.0	27.65	0.49	20.02	0.47	25.77	0.69
7.5	26.26	0.65	13.34	0.37	14.76	0.48
10.0	25.07	0.77	51.88	0.9	-	-

Questi risultati mostrano che le particelle prodotte a maggior potenza impiegata sono più uniformi, in termini di dimensione, rispetto ai lotti prodotti utilizzando una potenza minore. Questo ha senso perché una potenza impiegata maggiore riduce il tempo di residenza del fluido (Avvaru et al., 2006), questo a sua volta fa sì che la dissipazione di energia sia inferiore e diminuisce la disparità di energia dal fenomeno della cavitazione.

Inoltre, le particelle prodotte a 1 W sono, come previsto, più grandi di quelle generate a 3 e 4,5 W. Tuttavia, quelle prodotte a 3 W non sono significativamente più piccole di quelle prodotte a 4,5 W, tranne quelle prodotte a 5 mL/min. Questo è probabilmente un prodotto del basso numero di particelle che potevano essere misurate in quest'ultimo caso perché il surplus di energia impiegato per atomizzare i campioni ha deteriorato la loro qualità.

Un risultato degno di nota è che quando si usa una potenza inferiore, il diametro medio delle particelle non è sceso drasticamente come quando si usano quantità maggiori di energia. Questo è meglio rappresentato in figura 14.

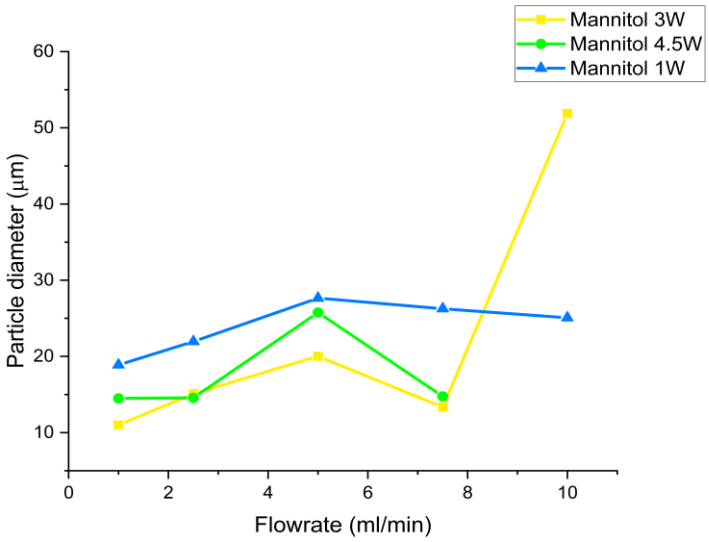

Figura 14. Dimensioni delle particelle di mannitolo formate a diverse portate e diverse potenze utilizzate

Da questo grafico, possiamo osservare che dopo aver superato il limite di potenza, che nel caso del mannitolo ha un valore compreso tra 1 e 3 W, la dimensione media delle particelle crolla una volta raggiunto il limite di spessore denotando un picco marcato. Da un'altra parte, quando si è utilizzato una potenza inferiore, si osserva che l'andamento delle dimensioni delle particelle prima del raggiungimento del limite di flusso è quasi identico nella sua forma a quello osservato per le potenze superiori. Tuttavia, dopo che il limite di spessore è stato superato, la dimensione delle particelle rimane quasi costante. Questa sorta di effetto di smorzamento potrebbe essere presente perché l'energia fornita non è così elevata come negli altri due casi, e quindi è sufficiente per atomizzare il fluido correttamente ma non per disintegrarlo. Le grandi dimensioni a 10 mL/min sono causate dalla bassa disponibilità di particelle generate a questa portata

La prossima sezione dell'analisi si è occupata dei cambiamenti nella distribuzione delle dimensioni delle particelle quando la viscosità della soluzione da atomizzare è stata modificata per effetto dell'aumento della concentrazione di soluto. La Tabella 2 riporta la media e la deviazione standard ottenuta tramite OriginLab.

Tabella 2. Media e deviazione standard delle dimensioni delle particelle di saccarosio a diversa concentrazione

Portata (mL/min) [Q]	**Saccarosio al 5%**		**Saccarosio al 40%**	
	Media (µm) [M]	**Deviazione Std. (µm) [σ]**	**Media (µm) [M]**	**Deviazione Std. (µm) [σ]**
1.0	9.58	0.37	21.93	0.29
2.5	11.22	0.43	22.14	0.39
5.0	17.00	0.43	26.51	0.34
7.5	23.60	0.46	28.07	0.45
10.0	16.93	0.74	29.82	0.57

Questi risultati indicano che un aumento della viscosità ha un effetto maggiore di quello della potenza esibita nei campioni a bassa concentrazione, e leggermente maggiore di quello della portata. Questo ha senso perché mentre più alta sia la viscosità, maggior sarà l'energia dispersa nel fluido e quindi ci sarà meno energia per poter atomizzare le particelle, facendole essere più grosse. Inoltre, la tendenza a raggiungere un valore di picco non è stata vista per la soluzione al 40%, lo cui potrebbe significare due cose, o dopo un determinato valore di viscosità le dimensioni delle particelle tenderà ad aumentare indefinitamente con la portata, o la portata alla quale il valore di picco può essere trovato aumenterà con questo parametro.

La terza sezione si è concentrata nell'influenza della influenza che la portata di alimentazione ha avuto sul prodotto finito.

Dai risultati precedenti, possiamo vedere che l'aumento della portata generalmente aumenta la dimensione finale delle particelle della polvere. Questo ha senso, dato che una maggiore quantità di fluido entra nel sistema, dando luogo a un film liquido più spesso che aiuta a dissipare parte dell'energia fornita. Un aumento indefinito della portata però, non causerà un aumento della dimensione delle particelle, come si è visto per le polveri di mannitolo al 5% (p/p) e di saccarosio al 5% (p/p). Come commentato prima, dopo aver raggiunto una determinata portata le forze gravitazionali che agiscono nel fluido saranno in grado di compensare la quantità di energia che viene utilizzata per far oscillare l'ugello, permettendo all'energia di andare nella sua interezza verso l'atomizzazione del fluido.

La figura 15 illustrerà i cambi nell'uniformità della distribuzione delle particelle con il cambio di portata nelle particelle di mannitolo al 5% (p/p) prodotte a diverse portate utilizzando 1 W.

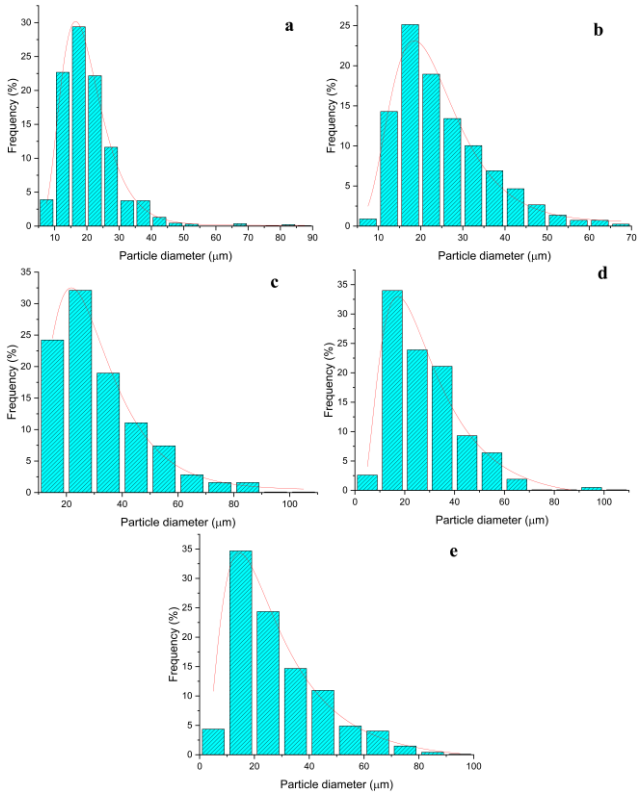

Figura 15. Distribuzione delle dimensioni delle particelle prodotte dalla soluzione di mannitolo al 5% (p/p) atomizzate a 1 mL/min (a), 2.5 mL/min (b), 5 mL/min (c), 7.5 mL/min (d) e 10 mL/min (e)

Dalla figura si osserva che aumentare la portata ha causato una diminuzione nell'uniformità della distribuzione granulometrica. Questo può essere spiegato considerando lo stesso principio che abbiamo usato nell'argomento precedente. Una maggiore quantità di fluido nel sistema significa che più energia viene dissipata nel film liquido e quindi fa che il sistema si comporti come se la potenza fornita fosse inferiore al valore reale. Come l'uniformità dell'atomizzazione ad ultrasuoni deriva dalla regolarità con cui si formano le bolle di cavitazione e le onde capillari, le forze gravitazionali, pur permettendo di trasmettere più energia netta al fluido, non hanno influenza sull'uniformità della distribuzione.

Area superficiale specifica

La seconda parte dello studio si è concentrata sui cambiamenti nell'area superficiale specifica della particella, con gli stessi parametri utilizzati per l'analisi della distribuzione granulometrica. Le isoterme di adsorbimento risultanti dallo studio BET hanno per lo più seguito un modello tipico di tipo II, con le eccezioni delle curve del saccarosio a 1 mL/min e 2,5 mL/min, entrambe mostrate in figura 16.

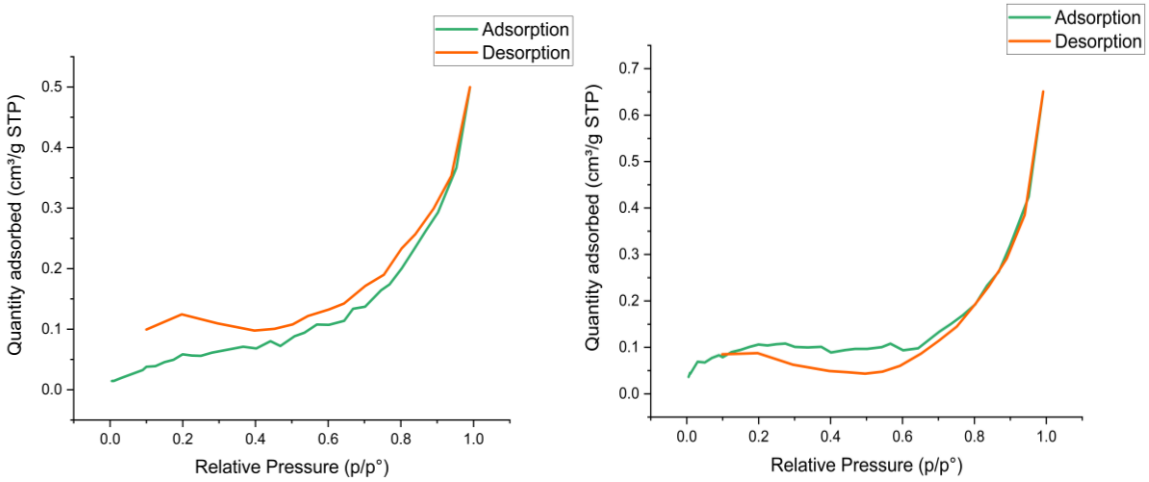

Figura 16. Isoterme di adsorbimento dei campioni della soluzione di saccarosio al 5% prodotte a 1mL/min (destra) e 2.5 mL/min (sinistra)

La prima immagine mostra un ciclo di adsorbimento-desorbimento incompleto, questo potrebbe indicare che il tempo utilizzato assegnato al processo non è stato sufficiente per consentire all'azoto di desorbire/adsorbire, e questo ha senso dato che il campione aveva una rete intricata di cluster che ha reso il processo di diffusione del gas più difficile a questa velocità di flusso. La seconda immagine denota un'isteresi, che secondo Gleysteen e Deitz (1945) potrebbe significare che si è verificata una condensazione capillare o che c'è stato un adsorbimento multimolecolare. In questo caso, l'opzione più probabile sarebbe la seconda perché nei casi in cui si forma uno strato multimolecolare, il processo di desorbimento dovrebbe avvenire dallo strato modificato, facendo sì che l'isoterma di desorbimento sia superiore a quella di adsorbimento per un certo tempo fino a quando non si raggiunge una pressione relativa sufficientemente bassa (Gleysteen e Deitz, 1945). La Tabella 3 mostra i risultati ottenuti con il metodo BET.

Tabella 3. Area superficie specifica della polvere ottenuta dalla soluzione di mannitolo al 5% (p/p) e quella di saccarosio al 5% (p/p) prodotte a diverse portate con una potenza impiegata di 3 W

Portata (mL/min) [Q]	**Mannitolo (m^2/g) [S_{BET}]**	**Saccarosio (m^2/g) [S_{BET}]**
1.0	7.5798 ± 0.0580	0.2292 ± 0.0102
2.5	6.1389 ± 0.0861	0.3659 ± 0.0107
5.0	7.5269 ± 0.0538	1.3706 ± 0.0251
7.5	6.3668 ± 0.0434	1.2832 ± 0.0207
10.0	5.5516 ± 0.0248	2.3091 ± 0.0164

Da questi risultati, possiamo osservare che il mannitolo ha, in media, una superficie maggiore del saccarosio a causa della sua porosità superiore. Anche se questo era previsto, il fatto che entrambe le soluzioni abbiano una tendenza opposta. non lo è. I risultati mostrano che mentre il valore del mannitolo diminuisce continuamente con la portata (tranne quello ottenuto a 5 mL/min), quello del saccarosio aumenta.

Il comportamento del saccarosio potrebbe essere spiegato ipotizzando che i cluster formati a basse velocità di flusso abbiano ostruito i pori presenti nelle particelle più grandi, abbassando così la loro area superficiale. Inoltre, l'effetto di de-clustering dell'aumento della velocità di flusso ha avuto un profondo impatto sull'area superficiale.

D'altra parte, la tendenza del mannitolo ha seguito il modello previsto per una soluzione cristallina, ovvero che le particelle più grandi spesso risultano in valori di superficie specifica più piccoli, ad eccezione del campione prodotto a 5 mL/min. Questa eccezione potrebbe essere a causa della maggiore integrata trovata nelle particelle prodotte a questa portata.

Per quanto riguarda ai risultati ottenuti con il cambio di concentrazione, possiamo osservare che un aumento della concentrazione causa una diminuzione della formazione di cluster. Questo al suo tempo fa sì che le isoterme di adsorbimento abbiano un modello di tipo II dalla prima portata e anche un aumento radicale dell'area superficiale specifica risultante. Questi risultati sono riportati nella tabella 4.

Tabella 4. Area superficie specifica della polvere ottenuta dalle soluzioni di saccarosio al 5 % (p/p) e al 40% (p/p) prodotte a diverse portate con una potenza impiegata di 3 W

Portata (mL/min) [Q]	**Saccarosio al 5% (m^2/g) [S_{BET}]**	**Saccarosio al 40% (m^2/g) [S_{BET}]**
1.0	0.2292 ± 0.0102	1.4737 ± 0.0142
2.5	0.3659 ± 0.0107	1.9659 ± 0.0276
5.0	1.3706 ± 0.0251	4.5365 ± 0.0201
7.5	1.2832 ± 0.0207	8.5312 ± 0.0412
10.0	2.3091 ± 0.0164	8.9679 ± 0.0489

Possiamo osservare dai risultati sperimentali che un aumento della concentrazione incrementa drasticamente la superficie specifica. Possiamo attribuire questo al minore numero di cluster che si sono formati nelle concentrazioni più alte. Questo si può osservare nelle figure 17 e 18, le cui mostrano le immagini SEM ottenute a 1 mL/min e a 7,5 mL/min. Queste immagini mostrano che c'è una diminuzione prominente nel numero di cluster in questo valore di portata, lo cui spiegherebbe l'improvviso salto nell'area superficiale a questa particolare velocità di flusso.

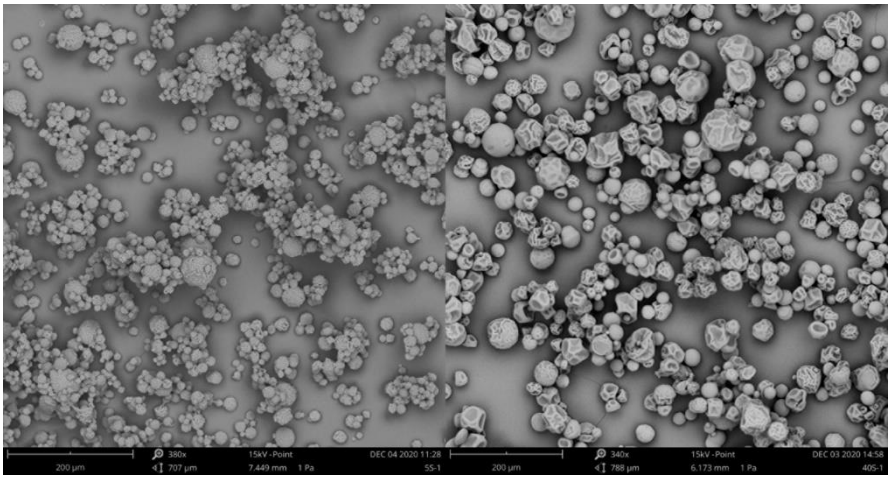

Figura 17. Immagini SEM dei campioni di saccarosio prodotti a 1 mL/min ad una concentrazione di 5% p/p (sinistra) e 40% p/p (destra)

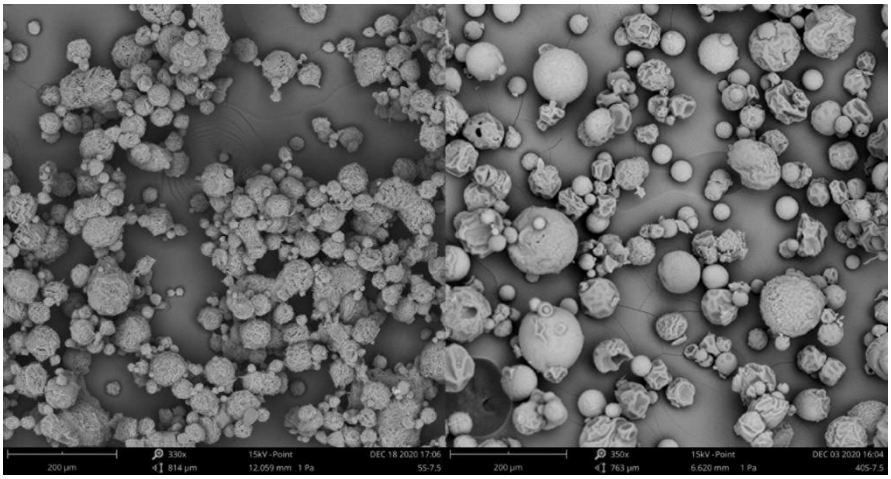

Figura 18. Immagini SEM dei campioni di saccarosio prodotti a 7.5 mL/min ad una concentrazione di 5% p/p (sinistra) e 40% p/p (destra)

Conclusioni

Dopo aver realizzato gli esperimenti e analizzato i risultati, si possono trarre le seguenti conclusioni:

- Entro un intervallo specifico, un aumento della potenza impiegata per l'atomizzazione diminuisce le dimensioni medie delle particelle e rende la loro distribuzione più uniforme. Una volta superato l'intervallo, non ci sarà alcuna diminuzione notevole delle dimensioni delle particelle e il campione potrebbe essere disintegrato.

- L'aumento della viscosità di una soluzione aumenta anche le dimensioni medie delle particelle prodotte, ma ne diminuisce leggermente la loro uniformità. La tendenza di una soluzione a formare aggregati viene anche diminuita.

- Aumentando la portata di alimentazione si ottengono particelle più grandi e meno uniformi. Tuttavia, esiste una portata critica dopo la quale la dimensione delle particelle tenderà a diminuire con un aumento della portata senza aumentare la loro uniformità. Questo valore critico è indipendente dalla potenza, aumenta con la viscosità e, in minor grado, è modificato dal soluto utilizzato.

- La superficie specifica di soluti come il saccarosio incrementa con un aumento della portata di alimentazione e di un aumento della viscosità. Per soluti come il mannitolo, l'area superficiale specifica diminuirà con un aumento della portata di alimentazione.

Suggerimenti e ricerca futura

Prendendo in considerazione i risultati ottenuti, ci sono alcuni ulteriori test che potrebbero essere eseguiti per avere un'idea più chiara dell'effetto che questi parametri hanno sul prodotto finale. Per capire meglio l'effetto che questi parametri hanno sulle soluzioni amorfe, si dovrebbe usare un soluto diverso come il trealosio. Inoltre, i test successivi dovrebbero lavorare con sistemi contenenti una combinazione di saccarosio e mannitolo e valutare eventuali effetti di interazione tra i due componenti nella formazione delle particelle liofilizzate. Un altro aspetto di interesse riguarda l’influenza del processo di atomizzazione-congelamento sull’attività biologica residua di un biofarmaco. Infine, potrebbe essere di interesse estendere l’intervallo di portate con cui le soluzioni di saccarosio sono alimentate al sistema di atomizzazione.

.

CHAPTER 1: THEORETICAL FRAMEWORK

Modern pharmaceutical goods have increasing standards for health and safety, from the properties they need to have to how long they should be able to be safely stored without modifying said properties. Moisture is, in most cases, one of the main causes of deviation from industrial standards because it facilitates biological processes like bacterial proliferation occurring inside the preparations, changes a material's properties, and causes other effects that are detrimental to the product's shelf life. Hence, it is of the utmost importance that it is reduced as much as possible to mitigate the consequences of its presence.

Industrial drying processes have been developed for little more than a century and the scientific community is striving to find better, innovative ways to achieve optimal moisture. Among many drying techniques, spray-drying and freeze-drying have become an industry standard because they provide satisfactory results across multiple fields and are easily scaled-up, however, the two of them have some limitations regarding their energy usage and the kind of substances they can be applied to.

To compensate for those limitations, a novel technique called spray freeze-drying has captured the attention of researchers because of its potential to produce better results than the other two techniques while spending less energy. The technique itself tries to reduce the time and energy consumed by the drying process of traditional freeze-drying by modifying the product's morphology from a cake inside a vial to droplets; this has been shown to reduce the mass transfer resistance and consequently diminish drying times and the need for a high vacuum.

1.1. Background

Drying is defined as the process of removing water (or other solvents) from a solid, leaving powders, continuous sheets of product, and flakes, as a product. This allows the desiccated items to be packaged, stored, and shelved, preventing things such as mold, bacteria, and fungi to grow on them and making them safe for human consumption. Drying is also an essential operation in most chemical processes since its efficiency will determine a products' overall quality and will have an impact on the total cost of the process.

This technique is relevant in a plethora of fields, such as the concrete production industry, the food and beverage industry, the lumber industry, etc. In the pharmaceutical field, for example, a poorly desiccated powder can bring catastrophic consequences for the product. According to Dawoodbhai and Rhodes (1989), moisture in high enough quantities will cause an increased attraction force between the particles, hindering their flow and making handling more difficult. Moreover, while it is necessary to have a certain amount of moisture present to increase the properties of the powder, too much of it can be the root of the loss of it and can trigger changes in the products' properties.

The most intuitive procedure of achieving the desired level of drying is by evaporating the liquid that is contained inside the product at high temperatures, resulting in a cake or a sheet. This method is useful when drying concrete or for the pottery industry because the

materials used can handle the temperatures without losing the desired properties. However, for heat-sensitive materials, reaching the boiling temperature of water can damage or change the properties of the product, giving it a limited use for mid to high-value products such as the ones produced in the fine chemicals field. This, together with the fact that it is not very energy efficient, makes the need to develop newer and better drying technologies a necessity. The most relevant conventional ones are spray drying and Freeze-drying.

1.2. Spray drying

This process can be briefly summarized as a technique that "involves formation of droplets from the bulk liquid followed by the removal of moisture from the liquid droplets" (Chen X. D., 2008, p. 115). The removal of the moisture is typically achieved using a drying gas at a set temperature which, in the case of food-related applications, typically ranges from 50 to 80°C to limit thermal degradation of the end-product (Gharsallaoui, Roudaut, Chambin, Voilley, and Saurel, 2007).

1.2.1. Involved phenomena

In this operation, the moisture inside the particle is removed via a fast and simultaneous heat and mass transfer, a quick observation of a particle during this process can provide insight into how it is carried out. A basic scheme of the drying process of a particle is provided by figure 1. The air that surrounds the particle transfers a certain amount of heat to the particle and causes the temperature to rise, therefore making the moisture inside the particle evaporate and escape; the released vapor will then be carried out by the air current. This makes obtaining a solution for a coupled heat and mass transfer balance imperative for the study and modeling of this phenomenon.

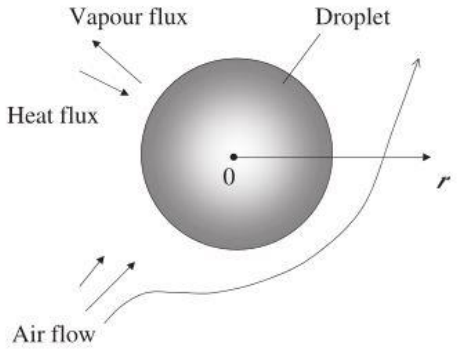

Figure 1. Transport phenomena in a droplet. Reprinted from: Chen X. D., 2008, with modifications.

1.2.2. Components of a spray drying system

In his book, Chen (2008) explains that a standard spray-drying apparatus consists of at least 4 main units:

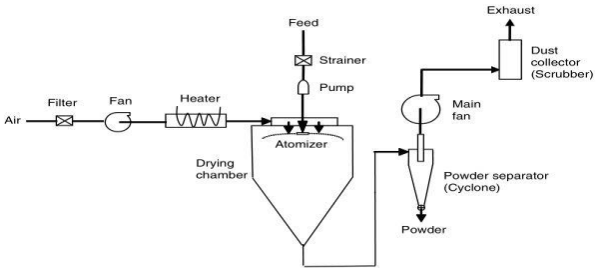

Figure 2. Single-stage spray dryer scheme. Reprinted from: Bhandari, Patel, and Chen, 2008, with modifications.

1.2.2.1. Drying gas and heating unit

In a typical spray drying system, air, water vapor, or inert gas is used both to heat the spray of liquid and to carry away the moisture released from it. The gas is introduced to the system with the help of fans that force it to pass through a heating unit, that will adjust the temperature of the gas until it reaches the desired value (usually around 150-270 °C). In case atmospheric air is used, a prior dehumidification step must be added to ensure that the process is carried out efficiently. The gas can be heated in many ways (from an electric resistant to oil-powered furnaces) and it enters the chamber with the help of gas dispersers to provide a homogenous flow inside the drying chamber and to promote mixing between the hot gas and the droplets.

1.2.2.2. Atomization system

Perhaps the most crucial unit in the whole process, the atomization system turns a continuous stream of liquid into small droplets, effectively increasing the surface area and making the process more efficient. In their book, Bayvel and Orzechowski (1993) note that one cubic meter of liquid can be transformed into approximately $2x10^{12}$ uniform droplets of 100 µm diameter, this results in a surface area of circa 60,000 m^2. As we know, mass transfer phenomena benefit greatly from a reduced surface area, and therefore atomizing the bulk liquid increases the drying speed and reduces the energy required to perform the process.

1.2.2.3. Drying chamber

The spray then goes through a drying chamber to complete the dehydration process. The design of the chamber will depend on the type of atomizer used, as well as the properties of the material that needs to be desiccated, the required capacity, the cost, the number of stages to be implanted, and the type of airflow with respect to the feed. The most common configuration of this unit is a cylindrically shaped drying chamber with a cone at the bottom, the spray is fed in co-current with the air, and gravity makes the dry powder fall down the aperture of the cone where it will be collected (Chen X. D., 2008)

1.2.2.4. Powder separator

After the drying stage, as much as 50% of the product can remain in the exhaust current under certain conditions (for example, in the milk powder's industry case if the product has a high protein and low lactose content, it will easily reach this value) which introduces the need for a separation stage (Pisecký, 2012).

There are numerous ways to separate these two components, the most common one being introducing a cyclone at the exhaust. In this method, the powder and air mix enter the apparatus with a certain velocity and collides with a curved wall; the centrifugal and gravitational forces make the powder move in a vortex motion that causes it to drop down the center while the air exits from the top. This device is so widespread because, if it is properly built, the maintenance is almost negligible, and the lack of mechanical parts makes it very hard for the equipment to be damaged.

1.2.3. Current challenges and limitations

As it has been stated, spray drying is a widespread technique capable of easy scale-up, a lot of flexibility in the materials that can be dried, as well as extensive documentation. Conversely, this method also has some limitations that restrict its use for heat-sensitive materials. Some studies have shown that, when applying this process to enzyme-containing solutions, almost 40 to 50% of the enzymes segregate themselves to the surface which brings them into proximity to the hot drying air (Chen X. D., 2008). As it is known, proteins, in general, are extremely heat sensitive, and a minimum variation of the temperature can deactivate them and make the product almost worthless.

Another limitation of this process is its low powder yield when using amorphous solutions. This was pointed out in an article authored by Maury, Murphy, Kumar, Shi, and Lee (2005), which suggested that the low yield in one of the most popular models of spray dryer (in this case the Büchi model 190 and its successors) was a consequence of the cyclone's design, and inadequate process condition. The final challenge for this method is that it is not very energy efficient, with some studies reporting a thermal efficiency of less than 20 % (Liu, 1992, as cited in Cheng, Zhou, and Liu, 2018).

1.3. Freeze-drying

As early as 1906, a paper published to the Académie des Sciences in Paris by Bordas and D'Arsonval suggested that it was possible to take a delicate substance from a frozen state using a moderate vacuum. They asserted that in that state, the product would be stable at room temperature for an extended amount of time (as cited by Rey and May, 2010). Working at low temperatures removes the main limitation for drying heat-sensitive materials, as they stay under a temperature that can cause thermal degradation of the product or changes in the desired properties without adding additional substances that may affect the purity of the powder.

1.3.1. Involved phenomena

As it was the case for spray drying, freeze-drying is the result of simultaneous action of mass and heat transfer that cannot be modeled without a coupled solution for both equations, however, it is completely different from the previous case. Some of the major differences between these two methods are the absence of a carrier gas that can simultaneously heat the particle and carry away the moisture, and the geometry of the system. A scheme of a close-up to the system is provided by figure 3.

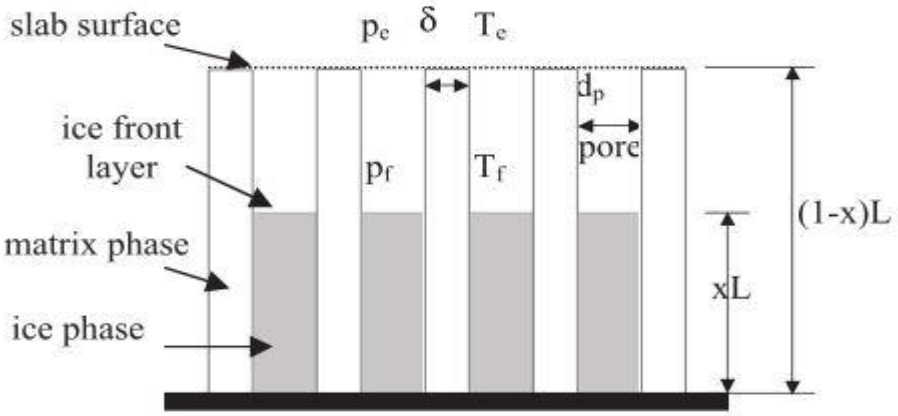

Figure 3. Scheme of the freeze-drying process of a slab. Reprinted from: Alzamora, Vergara-Balderas, and Welti-Chanes, 2008, with modifications.

The drying process is carried out by sublimating the ice phase of the porous matrix by subjecting the slab to a moderate vacuum and supplying it with energy. This can be done through conduction from the dry layer or the ice phase, which implies getting a heating plate or shelf over the slab or under it respectively, or through heat generation within the frozen layer via microwaves (Alzamora, Vergara-Balderas, and Welti-Chanes, 2008).

1.3.2. Stages of a traditional freeze-drying process

A freeze-drying system does not consist of a single stage, but rather an assembly of several steps. These are:

1.3.2.1. Freezing

The freezing step is the most important step for this operation as it is the primary dehydration stage, and it determines a lot of important factors for the final product; this means there must be a deep comprehension of everything that happens during this stage to allow proper control. During this step, the water is separated from the solution when it forms crystals; this, however, does not occur spontaneously at its thermodynamic freezing point, instead, the solution remains liquid until it reaches a much lower temperature. The temperature at which the first crystal is formed is defined as the nucleation temperature and the difference between it and the thermodynamic freezing point is termed supercooling (Pisano, 2019).

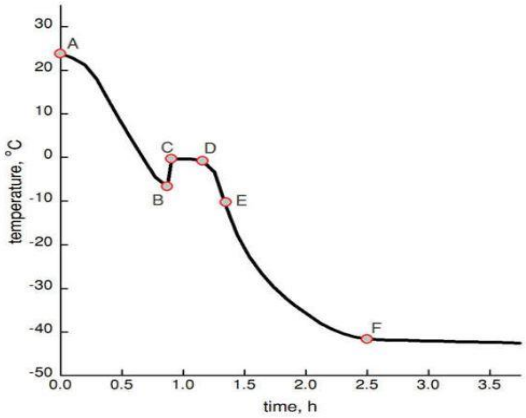

Figure 4. Temperature profile for a pharmaceutical product freezing process. Reprinted from: Pisano R., 2019, with modifications.

In figure 4, we can see how a normal freezing process occurs. First, the product is taken from the ambient temperature to its nucleation point (AB segment). After reaching this point, a slight increase in the product's temperature can be noticed (BC segment), this is due to the exothermal nature of the nucleation process which causes an increase every time a crystal is formed (Rey and May, 2010). At the end of the nucleation stage, there is an ulterior solidification stage (CD segment) that transpires at a comparatively constant rate when compared to the nucleation stage and a final cooling stage (DE segment) which serves as a final conditioning step to stabilize the product at a determined temperature.

The process conditions at which this stage is performed can affect the final product. An example of this can be found in a research paper authored by Franks (1992), which indicates that the rate-decreasing effect of low temperatures is often null compared to the rate-enhancing effect of concentration. Since the freezing step is the main dehydration stage of the freeze-drying technique, we can expect that a cooler temperature will increase the concentration of the product dramatically until it reaches an asymptote, as depicted in figure 5. This means that a labile compound could still suffer from degradation or start an undesirable reaction if the freezing process is not conducted with the appropriate measures and techniques.

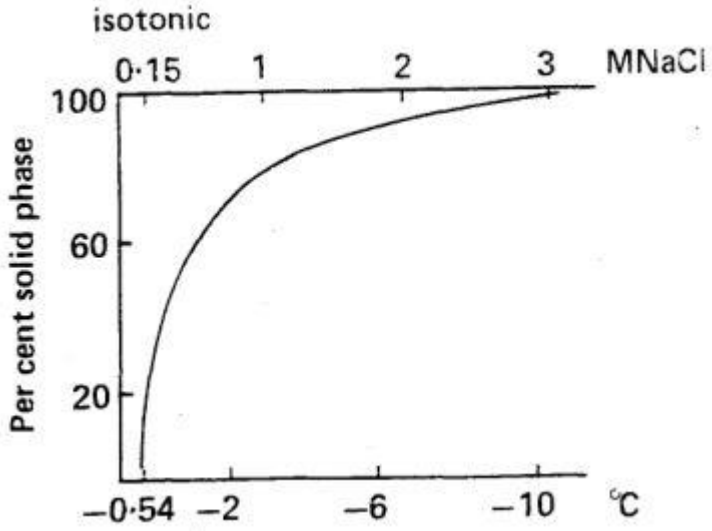

Figure 5. Concentration profile of a 0.144 M isotonic saline solution regarding changes in its temperature. Reprinted from: Franks, 1992, with modifications.

Furthermore, proteins could also suffer from diverse effects such as denaturation and aggregation according to how the process is carried out, this is significant given that proteins are one of the main products made through lyophilization. A study by Eckhardt (1991) showed that increasing the cooling rate at which this stage was done caused a surge, albeit to various degrees, in the formation of insoluble aggregates in the resulting product. It is also well documented that protein denaturation occurs at the ice-freeze-concentrate interphase, and several studies such as the one performed by Bhatnagar (2008) have tried to provide insight into when the maximum destabilization is obtained and its main factors.

1.3.2.2. Primary drying

By far the most time and energy-intensive step of a freeze-drying operation, the primary drying stage eliminates most of the water. This is done through the sublimation of the ice layer of the product formed. When the vials are loaded in the drying chamber, it is depressurized to start the sublimation process, and its temperature is lowered to values ranging from -40 ~ -10 °C to ensure the integrity of the product. Since sublimation requires energy to be carried out, a coiled tray is used to supply it through the use of a heating fluid (Pisano, Fissore, and Barresi, 2011). The moisture that is removed from the vials is then collected in a condenser unit that disposes of it.

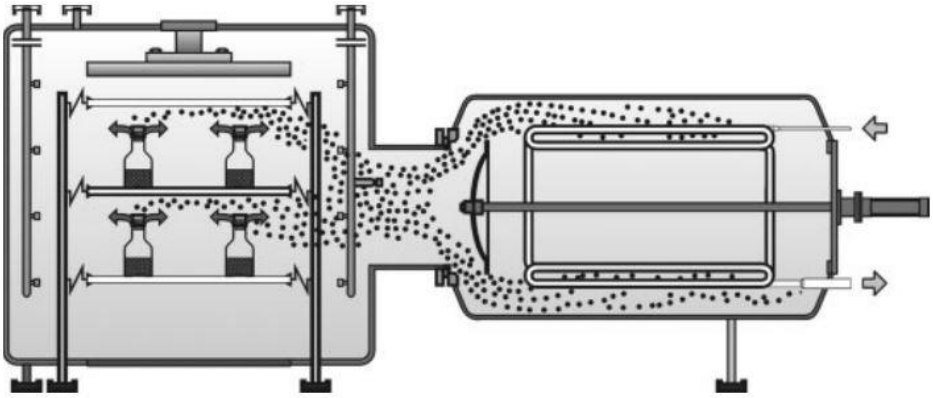

Figure 6. Typical drying chamber scheme. Reprinted from: Oetjen and Haseley, 2018, with modifications.

Numerous parameters influence the drying rate of a freeze drier, nevertheless, according to Haseley and Oetjen (2018) the two most critical parameters are the operating pressure and the shelf temperature. This becomes obvious from a basic transport phenomena point of view because, as illustrated in figure 7, if the chamber has less pressure the ice can sublimate at a lower temperature since the favored state of the matter will be gaseous. Conversely, the higher the shelf temperature is, the more heat flux will there be in the system, which will accelerate the sublimation process by providing more energy.

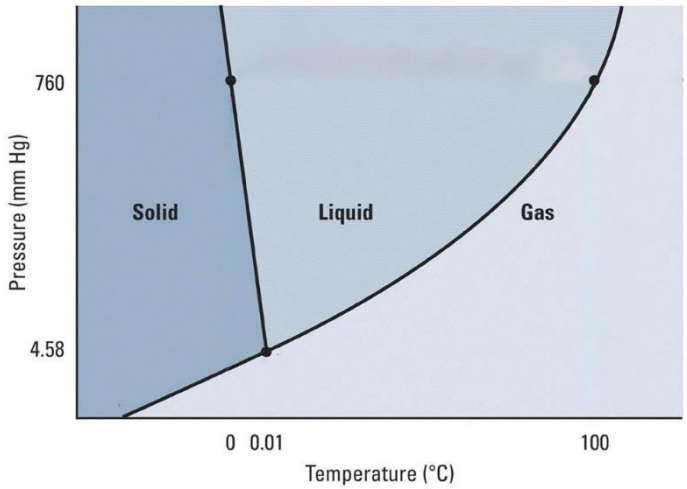

Figure 7. Phase diagram of water. Adapted from: https://useruploads.socratic.org/z82Fue33S0ee26X6a8bX_phase_1.jpg.

Deciding the operating temperature of the chamber must be done while considering the glass transition temperature (Tg') when drying amorphous compounds, and the eutectic point when the solute is crystalline in nature. In order to have adequately shaped products that can be commercialized, to avoid protein seggregation, and to preserve activity, the chamber is generally be kept below these temperatures, however, current research such as the one produced by Bjelošević et al. (2018) suggests that aggressive drying conditions like operating above Tg' or even the collapse temperature of the product (Tc), do not necessarily damage to the final product in terms of its properties, which could potentially offer some optimization possibilities.

Pressure and heat-flux are also related in freeze-drying. In an article by Jennings (1988) it is stated that, when the chamber pressure was greater than the one on the ice surface, there was little to no difference between the shelf's temperature and the ice. As soon as the chamber's pressure dropped to a lower value, the temperature at the ice surface decreased meaningfully which increased the heat-flux that was entering the vial and, therefore, accelerated the sublimation process.

Additionally, since this process is crutial to the final aspect and properties of the product, a considerable amount of control has to be implemented. If the operator fails to maintain them for the duration of the cycle, back melting, puffing, and collapse could occur (Rey and May, 2010). Therefore, determining the end point of the primary drying is crutial because a longer cycle will require sustaining controls for a longer period, swelling costs and increasing the possibility of damage being done to the products.

In order to determine this point, a reliable data set about the status of the drying process must be obtained, and measuring the humidity conditions on the chamber can provide relevant information about it, which is why most of the end-point determination techniques that exist today are based on this measure. In their article, Patel, Doen, and Pikal (2010) describe some of the most widespread tecniques used to this end:

- Comparative pressure measurement:

In this method, a capacitance manometer measures the true pressure of the whole chamber while a Pirani vacuum gauge quantifies pressure by measuring the changes in the

heat capacity of the gas, which varies with the partial pressure of the evaporated water. This makes the Pirani gauge measures circa 60% higher than the capacitance manometer reading, as can be seen in figure 8. Both curves are constantly monitored, and at the point where there is less water inside the chamber, the Pirani gauge measured value plummets and reaches the pressure value of the capacitance manometer, thus indicating the end of the process.

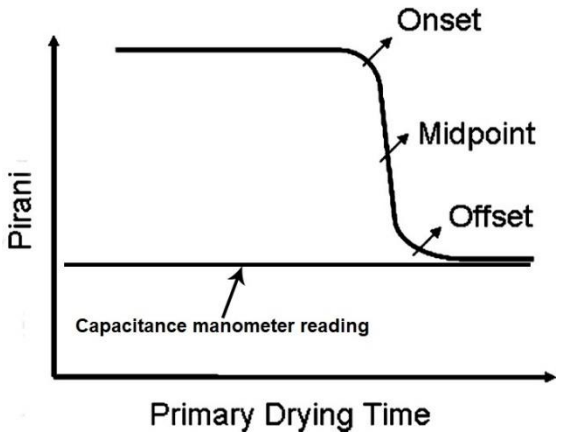

Figure 8. Pirani gauge pressure profile for primary drying. Reprinted from: Patel et al., 2010, with modifications.

- Dew point:

This technique consists in measuring the frost point of the process, which according to Patel et. al (2010) is the temperature at which the equilibrium pressure on the ice surface is equal to the measured partial pressure. A sensor can be installed to constantly measure the partial pressure and compare it to the dew point and, similarly to the comparative pressure method, once the partial pressure starts dropping below the frost point the process in considered finished.

- Product temperature:

Because the temperature at which the sublimation process is carried out differs considerably from the shelf's temperature, another indication that the process is nearing its completion is the temperature different between these two. Therefore, by introducing a thermocouple within several parts of the tray one can visualize this curve and compare the temperature of the product to the set-point of the shelf. The moment the temperature of the sample reaches the set-point of the shelf, the process can be considered finished.

Other parameters can also play a significant role in the time primary drying takes. An example of this can be the mass transfer resistance created by the existence of a thick solid layer (also known as cake) like the one represented in figure 9. The gas flow that comes from the sublimation of the ice will be impeded by the porous matrix that resulted from the drying process, which means that the more the drying advances, the harder it will be for the moisture to be eliminated at the same conditions. Another implication of this effect is that vials cannot be filled indefinitely, because at a certain point the cake will be too thick to be effectively dried.

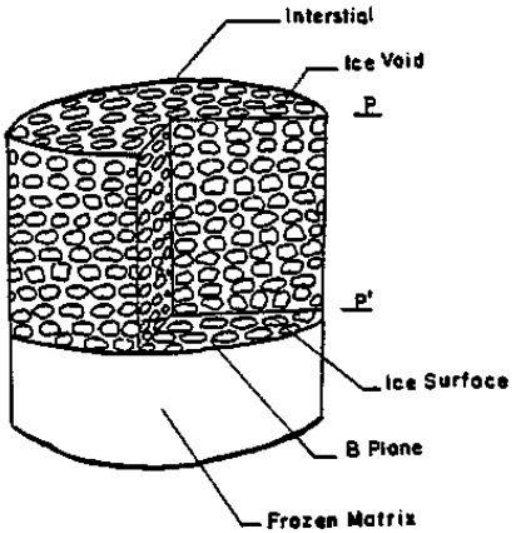

Figure 9. Schematic representation of freeze-dried vials. Reprinted from: Jennings, 1988, with modifications.

Besides its thickness, the nature of the material of the cake will play a key role in the diffusion of the water vapor because, as is the case in any mass transport phenomenon, if the solid matrix has a relatively high affinity for water the necessary energy to cause sublimation will dramatically increase. The same is true for any solvent that needs to be removed via this method, which is why a good understanding of the solid that will be dried is of the utmost importance.

1.3.2.3. Secondary drying

Primary drying is never enough to completely eliminate moisture from a product due to the different resistances that water vapor can encounter, and due to the presence of bound water inside the dry matrix. Therefore, a secondary drying process is performed after the primary stage to ensure that the standards have been achieved. The remaining moisture content in the product is usually low at this stage, which is why this operation is generally done by raising the temperature and lowering the pressure of the chamber. Nevertheless, this step is not as extensively documented in literature as primary drying, as commented by Pikal, Shah, Roy, and Putman (1990). This is important to know because while primary drying is essentially the sublimation, removing bound water with insufficient knowledge could prove a challenge since it does not necessarily follow the same drying kinetics.

According to Pikal et al (1990) findings, operating at a pressure under a certain limit, usually 0.2 mmHg, does not cause an increase the water removal rate significantly. Additionally, they found temperature to be the most influential parameter, greatly reducing drying times with slight increases in its value. This could seem like a problem since freeze-drying main objective is avoiding degradation of the active ingredient caused by high temperatures, however, the study found that as long as the activation energy of the deactivation process is equal or close to the activation of the drying process,the secondary drying was independent from the temperature.

Another difficulty that this stage faces is that it does not expel a great amount of water vapor, thus the end-point of the process cannot be determined by monitoring the humidity content inside the chamber as it was one for the primary drying. Therefore, a finite amount of time must be set beforehand which provides an additional challenge. Initially, most of

the drying times were obtained through heuristical methods like the one proposed by Pikal, Tang and Nail (2005), but most of the modern research focuses on obtaining a mathematical model that can accurately measure the optimal drying time.

1.3.3. Current challenges and limitations

This process, though effective when drying heat-sensitive materials, is much too expensive to use for general products which confine its spread in the industry to only the most valuable products. The costs from this technique are due to many factors, such as its energy-intensive nature due to the use of vacuum conditions and low temperatures, its long drying times, its batch nature, etc. This means that there is a significant effort by the research community to search for ways to improve upon the process.

There have been efforts to develop mathematical models that can accurately describe the mass and heat transfer phenomena involved, thus allowing for the optimization of the process via computational simulations. An example of this is a study done by Trelea, Passot, Fonseca, and Marin (2007), which proposed the use of interactive software to optimize the process based on the desired quality of the product. The result of this study was a reduction of around 12 h of the drying time for a sample solution, however, even this significant reduction represented only 33% of the drying, which means that the drying process could still take more than 24 h to finish.

Additionally, several efforts have been made to automatize the process and change the mode to operation mode from batch to continuous. Not only it reduces production time, but also it limits human error in the process. As stated in the work of Capozzi, Trout, and Pisano (2019) new regulations push processes towards a continuous operation to diminish deviations from the standards.

Another attempt to reduce drying time was made by Quast and Karel (1968), who discovered that for big samples, an impermeable layer of frozen material forms at the top of the sample which impedes vapor from escaping the solid matrix. Their solution for this problem was mechanically breaking the frozen slab to allow water vapor to escape the solid matrix at an increased rate or change the freezing mode to slush freezing.

1.4. Spray freeze-drying

While robust and widespread, the traditional freeze-drying suffers from a lot of limitations. One of the first approaches at optimizing the process was trying to operate in atmospheric conditions, which was proven possible in a couple of studies done by Meryman (1959) and by Lewin and Mateles (1962, as cited by Ishwarya, Anandharamakrishnan, and Stapley, 2015). These studies proposed that the mass transfer not only depended on the degree of the vacuum, but also on the humidity of the desiccant used and, therefore, if the partial pressure of the water was kept sufficiently low, operating at atmospheric pressure was possible.

However, the methods proposed by those studies were not suitable for bulk liquids or pureed products because of their slow drying time. Woodward (1963, as cited by Ishiwarya et al., 2015) studied the process to see if it could be possible to implement at a commercial

level and found that the main parameters that affected the drying time were the product's dimensions and the gas temperature.

Taking this study and the one done by Quast and Karel (1968) into consideration, Malecki, Shinde, Morgan, and Farkas (1970, as cited by Ishwarya et al., 2015) hypothesized that atomizing the liquid into a cryogenic medium could reduce drying times by a great degree, without varying the operating parameters (i.e. pressure and temperature of the chamber). The resulting sublimation rate after atomizing the fluid was greater than the one in its slab counterpart, and it proceeded in an unrestricted matter. From these studies, the basis for spray freeze drying was cemented.

1.4.1. Involved phenomena

By reducing the particle size from a slab to a droplet, mass and heat transfer phenomena are greatly accelerated because the temperature is more evenly distributed inside the single particles and its water content will be significantly lower. However, new considerations such as the porosity of the bed that is formed by the stacked particles, the geometry of the particles, and other factors must be considered to understand the phenomenon. A visual representation of a bulk spray freeze-drying process is provided in figure 10.

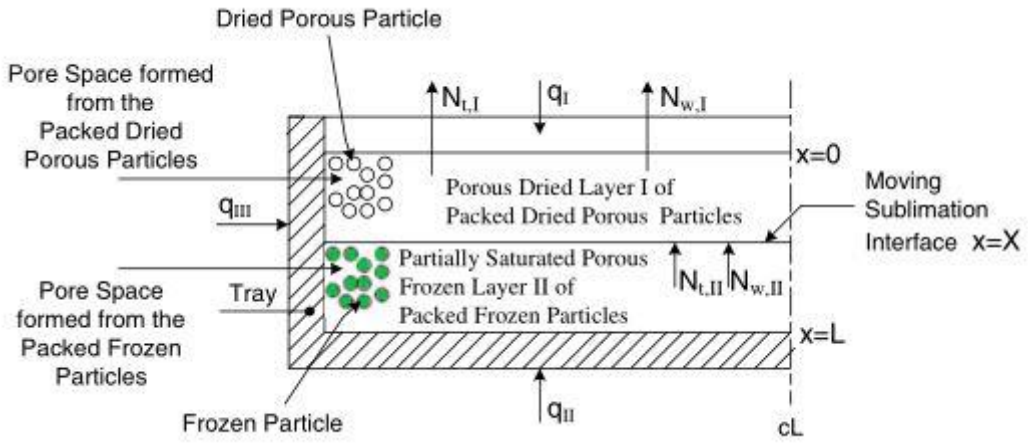

Figure 10. Scheme of a material being dried via bulk spray freeze-drying. Reprinted from: Liapis and Bruttini, 2009, with modifications.

The first observation that comes into mind, is that the whole system resembles a vial of increased dimensions with a clearly defined interphase between the frozen and dry layers. However, that is where the similarities finish since both layers are more akin to a packed bed than a block of frozen product. Another interesting observation is that the glass walls no longer act as a resistance to mass transfer phenomena, this is advantageous because it allows for a more distributed flow of vapor, avoiding a single exit point. From a heat transfer perspective, the lack of walls would potentially allow for a more uniform temperature in the particle. Nevertheless, if the tray is sufficiently large the heat will not be evenly distributed along its length, which could potentially bring problems to the drying process. Therefore, while the reduced dimensions do accelerate the process for the individual particles if the bed is not well distributed a resistance analogous to that of the vial might appear.

1.4.2. Stages of the spray freeze-drying process

This process consists of three main steps, each of them with different approaches and variations. These are:

1.4.2.1. Atomization

The inclusion of an atomization step is the defining factor that differentiates a traditional freeze-drying system from a spray freeze-drying one. It allows the whole process to be more efficient by reducing the resistance of dry cake and increases the uniformity of the heat transfer process, as well as allowing the elimination of the resistance coming from the glass wall of the vial.

As was the case for spray-drying, the type of nozzles utilized during the process and the density of the fluid determine how finely dispersed the spray will be. This makes classifying and choosing between different types of nozzles an important step when designing a spray freeze-drying system. While they can be classified in a great variety of ways, sorting them based on the type of energy used can be valuable for the visualization of the process. Each nozzle uses a different kind of approach to produce droplets for specific applications, size range, and fluids, from those that use liquid energy to modern ones that depend on ultrasonic waves. Bayvel and Orzechowski (1993) describe some of the most common types.

- Jet atomizer:

The most straightforward of the three sub-classes, it can operate continuously and intermittently. As illustrated in figure 11, it produces a jet of fluid that disintegrates after the discharge from the atomizer by transforming the pressure into kinetic energy through a change in diameter. They are very cheap and widespread but do not perform well when working with a viscous liquid.

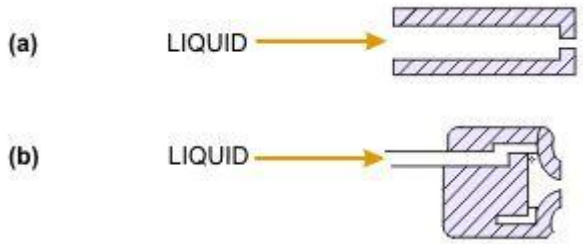

Figure 11. Schemes for different kinds of jet atomizers: a) Plain orifice, b) Simplex. Retrieved from: https://www.thermopedia.com/content/573, with modifications.

- Swirl atomizer:

As depicted in figure 12, this kind of atomizer introduces the fluid in such a way that a swirling motion is generated which makes the spray leave, not as a compact jet, but as a wide conically shaped sheet. This helps ensure a proper atomizing of the stream at medium to low pressures. Depending on the discharge velocity, the disintegration will advance in different approaches "For small velocities the sheet disintegration is due to perforation, for higher velocities it is due to wave phenomena, and for very high

velocities it is due to aerodynamic action of an ambient gas" (Bayvel and Orzechowski, 1993, p. 4).

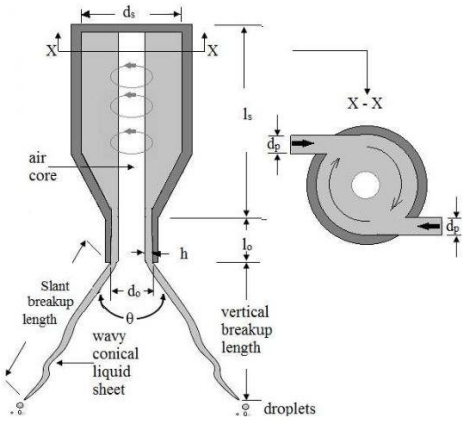

Figure 12. Scheme of a simplex swirl atomizer. Retrieved from Vijay, Moorthi, e Manivannan, 2015, with modifications.

- Jet-swirl atomizer:

This type of atomizer combines some features of a jet and a swirl atomizer, which results in an adjustable spray. Part of the fluid is introduced as an unswirled axial jet and the other as a swirled annular jet, the resulting momentum from the interaction between the two streams determines the distribution and the quality of the spray.

- Pneumatic atomizer

Another extensively used sort of atomizer is the pneumatic variety, which transfers a gas's kinetic energy to the liquid and disintegrates it. Since gases have a high amount of energy, the use of this type of atomizer usually guarantees good disintegration of the liquid, and thus are particularly useful when dealing with viscous fluids. On the other hand, the multiple ways in which the liquid and gas can interact can complicate the flow's study.

- Ultrasonic atomizer

An alternative type of atomizer is the ultrasonic kind. These are relatively modern types of nozzles that are chiefly used in the pharmaceutical and the fine chemicals industries because they produce a very refined spray, which can then be desiccated into a powder with very satisfactory qualities. Two major theories that explore the functioning mechanisms involved in this nozzle are the cavitation and the capillary wave theories.

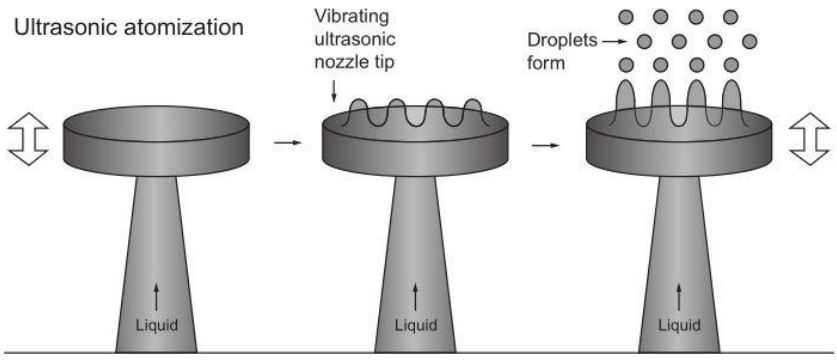

Figure 13. Scheme of an ultrasonic nozzle. Reprinted from: Gogate, 2015, with modifications.

In his paper, Lang (1962) proposed that the atomization process consisted of exciting a liquid film with a directed ultrasound wave to generate capillary waves in the liquid. When a certain point is reached, the crests of these waves expelled droplets of a defined diameter which depended on the wavelength of the capillary wave through the following equation $D = 0.34 * (8 * \pi * T)/(\rho * F^2)$ where D is the particle's diameter in cm, T is the surface tension, and F is the atomizer frequency in cps, and ρ is the density.

While accurate in most conventional procedures, Lang's theory produces less than satisfactory results for high frequency and high-energy intensity systems which introduces the need for another model. Rajan and Pandit (2001) describe cavitation theory as a phenomenon that generates cavitation bubbles when sonic waves are applied to a liquid film of a certain thickness; the collapse of these cavities (especially near the surface) generates high-intensity hydraulic shocks that disintegrate and eject droplets out of the nozzle. The same study then produced a modified equation to calculate the resulting droplet size $D = (\pi * \sigma/(\rho * f^2))^{0.33} * [1 + A * (N_{We})^{0.22} * (N_{Oh})^{0.166} * (N_{In})^{-0.0277}]$ where $N_{We} = f * Q * \rho/\sigma$ is the modified Weber number, $N_{Oh} = \mu/(f * A * m^2 * \rho)$ is the modified Ohnesorge number, $N_{In} = f^2 * A * m^4/(C * Q)$ is the intensity number, D is the droplet diameter, f is the frequency, σ is the surface tension, ρ is the density, Q is the flowrate, μ is the viscosity, A is the surface area of the droplet, and m^4 is the mass of the droplet.

The work of Bouguslavskii and Eknadiosyants (1969) described the whole process as a coupling of the two models, suggesting that the periodic hydraulic shock from the cavitation interacts and excites the capillary waves, producing droplets. It is worth noticing that, while droplets produced by capillary waves have an exceptionally uniform distribution, the disintegration caused by cavitation shock (which is essentially a random phenomenon) is very irregular and leads to a non-uniform distribution. This fact, together with the conjunction theory, can explain why at higher frequencies the droplets' diameter starts to differ from the one obtained by Lang's equation but remain relatively uniform during the atomization process (Avvaru, Patil, Gogate, and Pandit, 2006).

- Rotary atomizer

An additional type of atomizer that is broadly used for large-scale industrial applications is the rotary kind. In this case, the kinetic energy does not come from a fluid (like on the pneumatic or liquid energy atomizer) but from the centrifugal force generated by a small electric motor that causes a disk or wheel to rotate. The fluid is introduced near the axis of rotation, and when it reaches the surface of the disk is ejected and atomized because of the energy transfer. One of the drawbacks of this category is that it requires high speeds to produce sufficient energy for the disintegration process which can be problematic because, since the system is mechanical in its nature, the parts used can break if not maintained correctly.

1.4.2.2. Spray-freezing

The techniques used for spray-freezing applications are different from the ones used in traditional freezing because the process no longer involves vials and other large products, but fine sprays. Image 14 illustrates the three main methods.

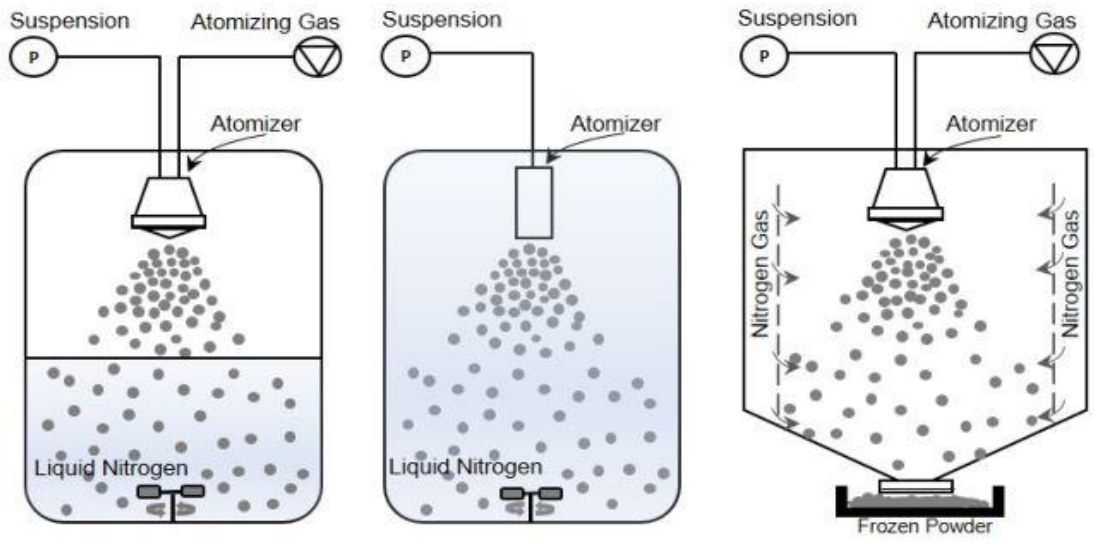

Figure 14. Spray-freezing methods: SFV/L (left), SFL (center) and SFV (right). Reprinted from: Adali, Barresi, Boccardo, and Pisano, 2020, with modifications.

- Spray-freezing into vapor (SFV):

The atomized fluid is injected into a chamber that makes cold gas flow inside of it to freeze the droplets. This process depends on many different mechanisms that act at the same time. These are briefly described in a study done by Anandharamakrishnan, Gimbun, Stapley, and Rielly (2009):

> *"(1) the formation and the motion of individual drops with respect to each other and the gas, is determined by the fluid mechanics of the spray; (2) heat transfer between the gas and the droplets depends on the local conditions; e.g., gas temperature, droplet temperature, and droplet–gas slip velocity; and (3) freezing and ice crystallization within the drops (p. 1)."*

This method allows for the least amount of nitrogen to be introduced inside the primary drying process, as well as the best recovery of the cryogen, because it freezes the droplets without entering the pores in its liquid stage and it can be easily filtrated. While counter-current flow is the traditional mode of operation, powder recovery, and elutriation can become a problem; therefore, new developments in co-current operation are being researched with promising results (Adali, Barresi, Boccardo, and Pisano, 2020).

- Spray-freezing into liquid (SFL):

In this method, the spray is injected directly into the cryogenic liquid. This allows for a flexible selection of mediums because a traditional fluid, like nitrogen, can be used if the operation has to be carried out at atmospheric pressure, but if the use of pressurization is an option, other (more economical) fluids like CO_2 can be used. The advantage of this method is that the freezing rate is the highest of them all (since a liquid's heat transfer coefficient is generally higher than that of a gas), therefore, it is logical to assume that phase separation would be the lowest of the three methods since the solution does not have the time to separate. Additionally, studies have shown that lower exposure to the air-water interphase that is obtained through this method might help increase the stability and residual activity of heat-sensitive materials (Yu, Johnston, and O.Williams III, 2006).

- Spray-freezing into vapor over liquid (SFV/L):

This method consists of spraying the solution onto a boiling cryogenic liquid, so as to have a small vapor layer that acts as a cooling stage before freezing into the liquid. The vapor layer triggers an initial freezing process that protects the particles from contamination caused by intimate contact between the product in the liquid phase and the cryogenic fluid because by the time it reaches the surface the droplet is already partially (or completely) frozen.

1.4.2.3. Drying

To end the process, a traditional freeze-drying operation can be performed to dry the particle. Since the particle size is much lower than that of a slab or a vial, the sublimation process happens at a much higher rate compared to a typical operation. However, newer methods have been proposed with promising results. Some of them are:

- Atmospheric spray freeze-drying (ASFD):

As stated in the name, this type of freeze-drying does not work in vacuum conditions, but at atmospheric pressure instead. It is based on Meryman's theory, and the fact that it works at such conditions greatly reduces the energy consumption of the process, as well as cutting some of the time required to operate in a vacuum (a purge stage, installing interlocking systems, etc). However, many studies have found that the drying time required for this type of process is considerably larger than the one for conventional freeze driers, which is why most of the atmospheric driers work together with a spray freezing system.

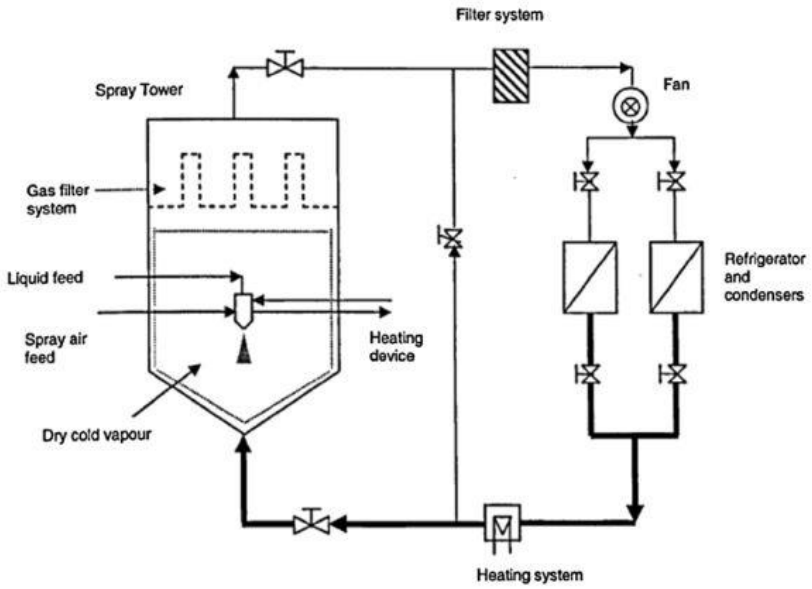

Figure 15. Atmospheric spray freeze-drier scheme. Reprinted from: Ishwarya et al., 2015, with modifications.

- Atmospheric fluidized bed spray freeze drying (AFBSFD):

To further improve the drying rates, Leuenberger, in the United States of America Patent No. 4608764 (1986) proposed the implementation of a dry ice fluidized bed unit over which the solution was atomized. The frozen powder was then dehydrated by a stream

of desiccated fluidizing air, injected at a rate that was higher than the terminal velocity of the particles, which were then transported to the filter system. This method, while efficient, consumes a huge amount of cold gas.

- Sub-atmospheric pressure spray freeze drying (SASFD):

According to Ishwarya et al. (2015), this method was invented to circumvent the high consumption of cold gas by working in a partial vacuum. Some studies found that the drying time and the gas usage were greatly reduced even when a total vacuum was not reached. This gives some leeway for process optimization.

1.4.3. Current research and possible applications

One of the main advantages of using a spray freeze-drying process is that it could provide the pharmaceutical industry with the opportunity to operate continuously. In his review of the advantages and challenges of making freeze-drying a continuous operation, Pisano (2020) mentions that even though lyophilization is a widespread and robust method, the inherent flaws of its batch nature (need for sterilization and cleaning processes, the loading-unloading stages, etc.) impacts negatively on the profitability and efficiency of the process. Therefore, switching to a continuous operation would represent an advantage in terms of quality control, ease of operation, and final product throughput and homogeneity.

Operating in this manner with traditional techniques and processes is near impossible due to mass and heat transfer constraints. Spray freeze-drying, however, decreases said limits up to a point where it is feasible to make the switch. One evidence of this can be found in Rey and May's (2010) concept, which can be seen in the following figure.

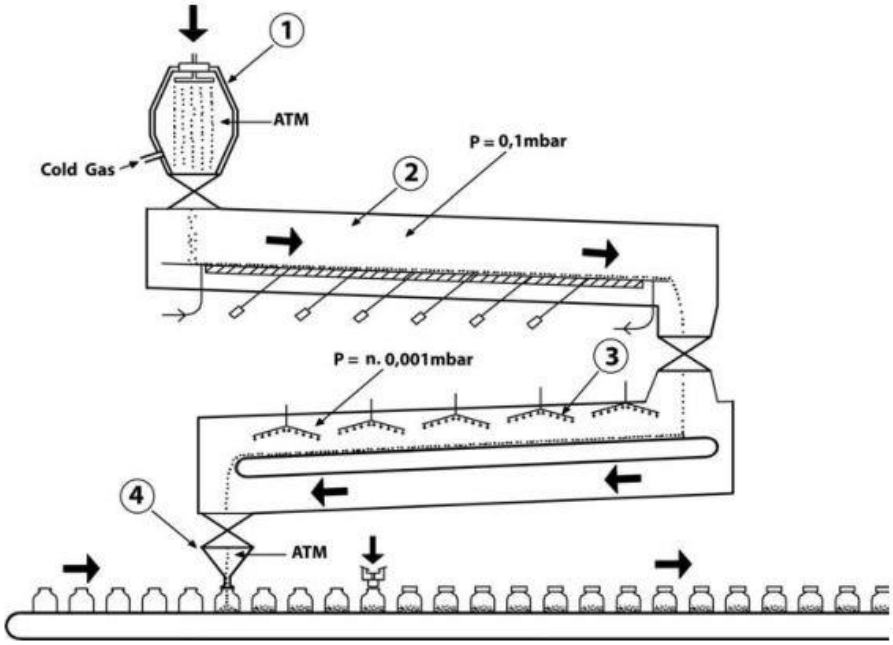

Figure 16. Rey and May's proposal for continuous lyophilization. Reprinted from: Rey and May, 2010, with modifications.

We can see in their model that the first operation consists of an atomization and freezing stage (1), the frozen particles would then go through an airlock towards the primary drying

chamber (2) where they would be moved through an ultrasonic conveyor belt. After finishing the primary drying stage, the dried particles would pass through another airlock into the secondary drying chamber (3), where microwave and/or infrared radiation would be directed towards the particles to force, together with the vacuum, the escape of bound water from the product. Finally, the finished product would go to a collection station where vials would be filled and stoppered (4). While this design could be optimized with modern knowledge, this shows that with an initial atomization step operating continuously is possible.

Besides Rey's model, Adali et al. (2020) make reference to several different approaches with the potential to operate continuously.

- Spray-freezing and dynamic freeze-drying.

The main idea behind this model is spray-freezing the particles and then introducing them to a LyoMotion unit. This technology consists of a rotary drum at vacuum conditions with heated walls and an infrared radiation source in the middle of it to provide the necessary energy for the sublimation process. A scheme of the process can be seen in figure 17.

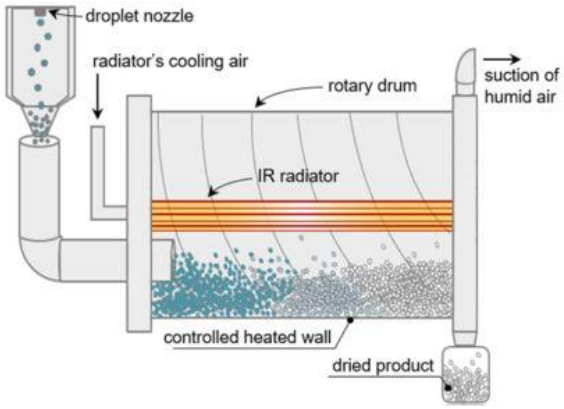

Figure 17. Spray-freezing into a LyoMotion unit. Retrieved from: Adali, Barresi, Boccardo, and Pisano, 2020.

While the spray freezing is continuous, the LyoMotion unit is not, which therefore makes the concept unfit for continuous operation in its current state. However, Adali et al. (2020) propose solutions to this problem in the form of adding more than one tumble drying stage to continuously collect dry powder without interrupting the drying process.

- Stirred freeze-drying.

In this process, the particles are frozen inside a stirred chamber by mixing the particles with a freezing agent. Once they are frozen, they fall into a continuously stirred tank where the freeze-drying operation occurs, the heat is supplied by the heated walls, and its kept uniform via continuous mixing. Once they are dry enough, the finished product is transported into the integrated filter chamber, where they can be collected. According to Adali et al. (2020), the advantage of this system is that it is completely continuous and highly uniform in its drying process, so it would allow for the full automatization of the process. A schematic representation of the process can be seen in the following figure.

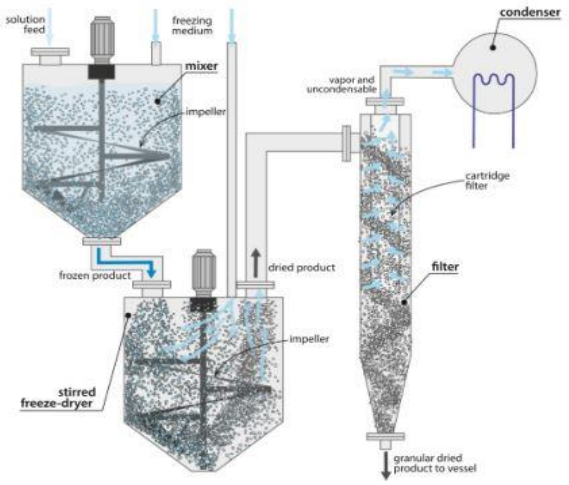

Figure 18. Scheme of a stirred freeze-drying process. Retrieved from: Pisano, Arsiccio, Capozzi, and Trout, 2019, with modifications.

1.5. Characterization of samples

After obtaining a spray-freeze dried sample, it is important to characterize the properties of the resulting powder so as to have an objective view of its quality. For this purpose, several characterization techniques such as SEM, BET, and others are implemented frequently and, therefore, it is convenient to have a thorough understanding of the working principles, the apparatuses involved, and the information they can provide. Most of the methods are described in the book Principles of instrumental analysis by Skoog, Crouch, and Holler (2017).

1.5.1. Scanning electron microscope (SEM)

This analysis has become a standard for the morphological analysis of structures because of its simplicity and accuracy. The technique consists in focusing a fine beam of electrons on a sample's surface to obtain a diffraction pattern that can be processed into a high-resolution photograph of its surface topography. The images obtained through SEM analysis have a resemblance to the following figure.

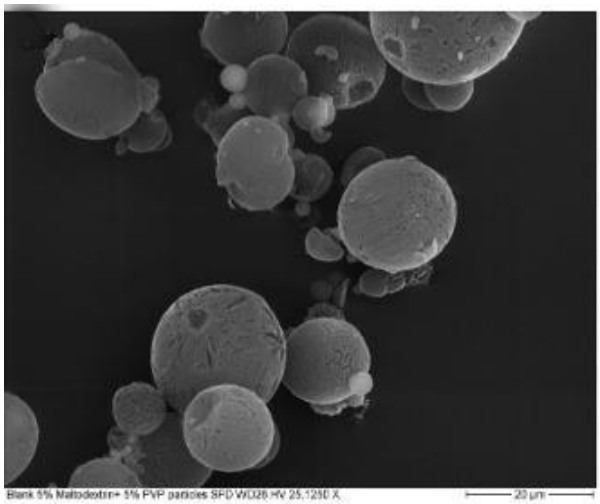

Figure 19. SEM image of maltodextrin + PVP particles produced via spray freeze-drying
Reprinted from: Alia and Lamprecht, 2014, with modifications

Since this method is based on a material's ability to conduct and scatter electrons, a typical SEM analysis sample consists of substances that are metallic in nature because electrons can freely flow inside them, therefore producing the desired results. For a non-metallic substance though, a metallization process (which consists of coating the sample with a conductive film) must be carried out before starting the analysis.

The apparatus used for this method consists of individuals parts that can be modified and assembled. These are reported in Skoog et al (2017) as:

- Electron gun and optics system:

As stated before, this technique makes use of a concentrated beam of electrons to bombard the sample's surface with it, therefore, it is intuitive to assume that the apparatus must have an electron source and an instrument that can focus and accelerate them. The source is usually a tungsten filament, or a field emission gun for high-resolution images, connected to a high-voltage power source. When current hits the emitter with sufficient energy, electrons jump from the source.

The free electrons must be directed towards the objective after being condensed into a beam of a determined size and energy. The condenser lens system is the one that determines the total energy throughput of the beam that reaches the objective lens system, which is then in charge of directing and sizing the beam.

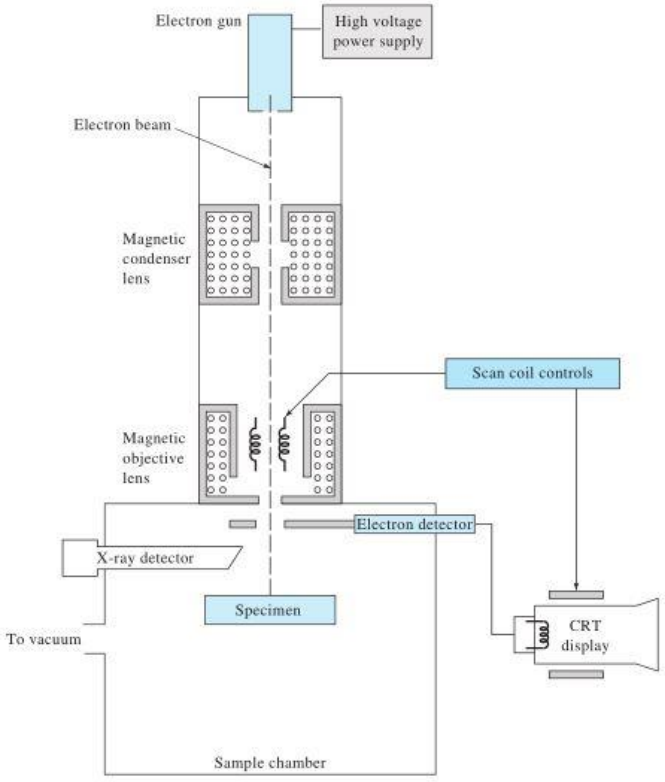

Figure 20. Typical scheme of an SEM apparatus with an electron and an x-ray detector. Reprinted from: Skoog, Crouch, and Holler, 2017, with modifications

- Additional detectors:

When the electron beam collides with the sample, radiation and electrons jump from it which can be then captured and measured by detectors added to the apparatus. To

understand which kind of detectors should be added, a basic understanding of the interaction between the sample and the electron beam is required. When the beam crashes against the sample two categories of interactions can be observed, the elastic kind which bounces off the sample in a different direction and loses a not so significant amount of energy, and the inelastic type that transfers the electron's energy partially or totally to the sample. A schematic representation of this can be observed in figure 21.

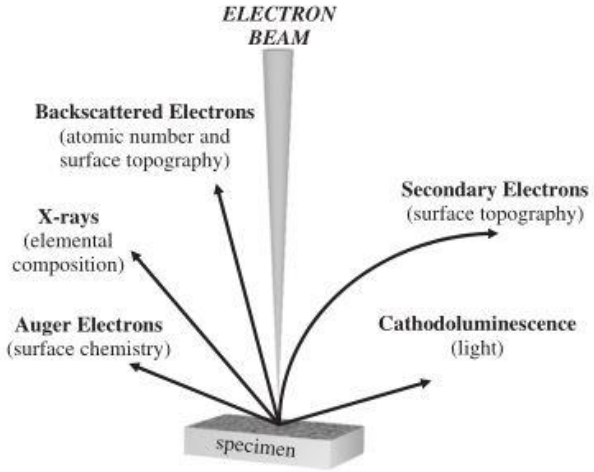

Figure 21. Different signals produced from the interaction between the beam of electrons and the sample. Reprinted from: Storey and Ymen, 2011, with modifications.

Numerous signals derive from the beam-sample interaction, some of the more relevant ones are backscattered electrons, which are the result of a superficial and elastic collision and are characterized by only having their direction modified and keeping their kinetic energy. When the impact is inelastic instead, X-ray radiation, photons (in the form of cathodoluminescence) and loosely bound electrons can jump from the sample; These electrons are called secondary electrons, and they jump together with the backscattered electrons with different energy and diameter.

The ability to introduce detectors for these signals is one of the features that make this type of analysis so versatile. Backscattered electrons and secondary electron detectors will give information on the sample's surface topography by transforming this signal into flashes of light that can then be translated into shapes. The detector usually captures both kinds of electrons (cannot capture secondary electrons exclusively because it is sensitive to the highly energetic backscattered electrons) but can also be calibrated to filter the secondary electrons.

Installing an X-ray detector can give the researcher clues about the chemical nature of the compound that is being studied. According to Storey and Ymen (2011), when the beam collides inelastically with the sample, a vacancy is created and then filled with a free electron, the excess energy is then released as radiation. The amount of energy released is unique to a specific compound, and therefore can be used to identify it.

- Sample holder

1.5.2. Surface area determination (BET)

Since spray freeze-dried particles become porous solids, it is within the researchers' interests to know the total surface area of the particles, because it provides an indicator of the quality obtained through the process. A solid with a high surface area can exchange mass and heat at an accelerated rate, which in the case of the pharmaceutical industry is desirable because the product can be quickly absorbed by the body. It is also interesting to notice that porous solids have aerodynamics that can be exploited for lung ingested pharmaceuticals.

The use of inert gases to determine surface area comes from the physical adsorption theory proposed by various scientists over the years. The most noteworthy theory is that of Langmuir (other studies are usually based on Langmuir's theory), which states that an adsorbed substance will do so in a monolayer that reaches every corner of the particle. Based on this theory, Brunauer, Emmet, and Teller developed their homonymous equation (Brunauer-Emmet-Teller or BET equation) which correlates several parameters that can be used to determine the volume adsorbed and, using that, the surface area through the following equation: $P/[V*(P_0-P)] = 1/(V_m*C)+(C-1)*P/(V_m*C*P_0)$ where P is the partial pressure of the adsorbate, V is the volume of gas adsorbed at P, V_m is the volume adsorbed as a monolayer, P_0 is the saturation pressure at the experimental temperature and C is a constant.

There are 6 different patterns the resulting adsorption isotherm can produce, all of which are represented in figure 22.

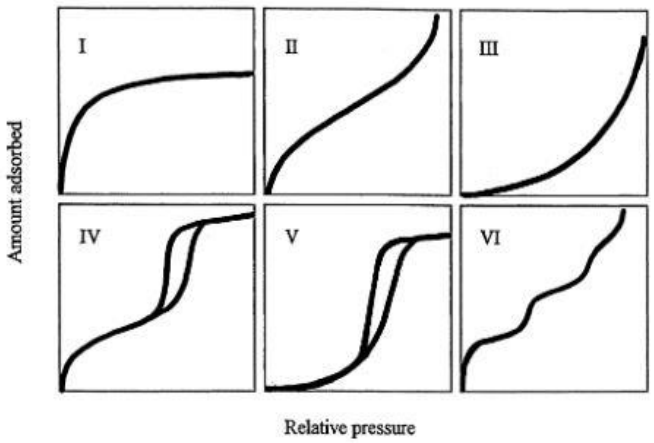

Figure 22. IUPAC classification of adsorption isotherms. Reprinted from: Donohue and Aranovich, 1998, with modifications

According to Donohue and Aranovich (1998), each type of curve can be classified according to which kind of adsorbate they describe:

> *"Type I isotherm "approaches a limiting value" and usually is used to describe adsorption on microporous adsorbents. Types II and III describe adsorption on macroporous adsorbents with strong and weak adsorbate-adsorbent interactions respectively. Types IV and V represent mono and multilayer adsorption plus capillary condensation Type VI, which was not included in the Brunauer classification, illustrates that the adsorption isotherms can have one or more steps."*

1.5.3. Additional common studies

1.5.3.1. Differential Scanning Calorimetry (DSC).

This technique focuses on changes in the glass transition temperature of the studied sample which, as we now know, is useful when studying the nucleation phase of the freezing process and the phase separation phenomena. It is the most used thermal analysis method because it is quick, simple, and widely available in laboratories. Skoog et al. (2017) describes three different types of DSC: power-compensated DSC, heat-flux DSC, modulated DSC.

1.5.3.1.1. Possible studies performed with this technique.

This technique can be used for quality control purposes since they provide information, through the melting point identification and other properties, about the purity of a substance as well as its identity. Some of its most common applications are, as described by Skoog et al (2017):

- Glass transition temperature studies:

The determination of the glass transition temperature of a species is one of the most relevant studies performed with this technique and the one most closely related to freezing processes since it determines when nucleation will start occurring in a crystalline material. Many of the substance's properties change at this temperature, which makes, and knowing the onset of this change can be of paramount importance when developing a method for freezing it.

- Crystallinity and crystallization rates:

Know to which degree the substance is crystalline and the rate at which it goes from a liquid to a crystal is relevant when studying freezing phenomena. This technique is effective because, as stated earlier, nucleation is an exothermal phenomenon, so it is remarkably identifiable by a peak in the thermogram.

- Reaction kinetics, and protein stability and structure

1.5.3.2 X-ray diffraction (XRD)

This is one of the most widespread techniques for identifying crystalline materials and substances since its discovery in 1912, because of its relative simplicity and accuracy in results. This method has provided abundant information about the behavior and arrangement of this type of material since each crystalline material has a unique x-ray diffraction pattern and it is, therefore, easy to individuate and classify single components and register them on a database for future analysis.

We can see that when a beam passes through a sample, it is diffracted and it scatters into a particular direction, therefore allowing the resulting scattered electrons to be captured by a photosensitive film. The undiffracted beam passes straight out of the camera into an

appropriately designed tube. The film is successively revealed, and the diffraction pattern is identified.

1.5.3.2.1. Identification of the diffraction pattern and applications

The diffraction pattern is identified using Bragg's equation, which can provide the angle of the diffracted beam and thus the crystalline plane orientation, together with the intensity of the beam. After revealing the planes, the resulting graphs are contrasted with information held in an empirical dataset containing more than 800000 materials. If the sample is supposed to be a pure material, then the researcher looks for an exact match inside the database, if it is a mixture of two or more components, then combinations of the more intense lines are used to find a match.

CHAPTER 2: THESIS OBJECTIVES

This project aims to study the influence of the operating conditions on the final product of a spray freeze-drying process. This goal was redefined and focused on the evaluation of the impact of the atomization stage, which controls the morphology, size, heterogeneity, and the number of the particles. Therefore, this thesis assessed the influence that changes on the power supplied to the ultrasonic atomizer, the feed flowrate, and the concentration of the solution to be atomized have on the final morphology of the obtained particles. The properties evaluated for this were the particle size and specific surface area.

The individual chapters are briefly discussed in this section:

- Chapter one gives a comprehensive theoretical base for the principles of the process, the set of analyses that are usually performed, and the current research being done for it.

- Chapter two states the objectives and motivations of the thesis

- Chapter three provides the materials a methodology with which the experiment was conducted.

- Chapter four will focus on the presentation and discussion of the results.

- Chapter five will state the conclusions reached by the study and will provide recommendations for future research.

CHAPTER 3: MATERIALS AND METHODS

This chapter will provide a detailed explanation of the experimental procedure used to obtain the experimental results of this thesis, from how the samples were prepared to how they were analyzed.

3.1. Materials and sample preparation

The substances used to carry out the experiments were D-mannitol (Sigma-Aldrich, Germany) with a purity of more than 99% and puriss grade sucrose (Sigma-Aldrich, Germany). Both are common excipients used in the pharmaceutical industry to ensure that the final product's morphology and properties are up to a determined standard. It is important to know the usage these materials have in the industry and their properties to understand why they were chosen as cases of study.

According to the compound summary of the National Center for Biotechnology Information (2004), "Mannitol is a naturally occurring alcohol found in fruits and vegetables and used as an osmotic diuretic". It is usually used as a sweetener, and as a caking or bulking agent for lyophilized preparations since it produces well-defined cakes of product (Kumar, Mallik, and Sarkar, 2017).

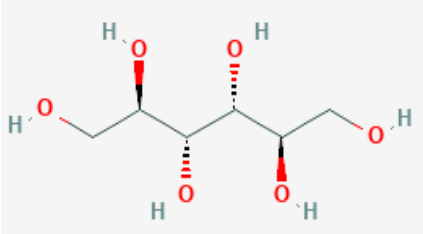

Figure 23. 2D structure of D-mannitol. Retrieved from: https://pubchem.ncbi.nlm.nih.gov/compound/6251#section=2D-Structure.

Sucrose, on the other hand, is widely used as a cryoprotectant for freezing operations. It is very effective when protecting living tissue and proteins because it prevents their denaturation by partially dehydrating them, therefore avoiding the formation of ice crystals that would otherwise damage the sample (Bhattacharya, 2018). Sucrose, however, is prone to collapse on itself and it requires a lower temperature to achieve an acceptable sublimation rate.

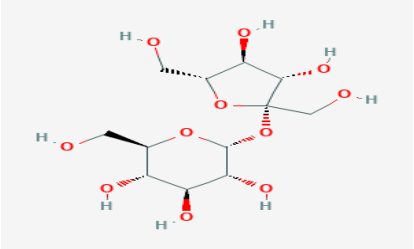

Figure 24. 2D structure of sucrose. Retrieved from: https://pubchem.ncbi.nlm.nih.gov/compound/Sucrose#section=2D-Structure.

Mannitol formulations were prepared to obtain a 5% (w/w) solution while sucrose preparations were set at a concentration of 5% (w/w) and 40% (w/w). Using the electronic

scale reported in figure 25, the mass of solute necessary to produce 200 ml of solution at the desired concentration was introduced into a beaker. Pure water was used to dilute all the preparations. After diluting the component, the formulations were placed on a magnetic stirrer until there were no visible lumps, and when this point was reached the beaker was sealed with paraffin to avoid contamination of the samples until the mixture was injected.

Figure 25. Electronic scale and beaker with sucrose

3.2. Atomization and freezing process

The samples were introduced one at a time into a 100 mL capacity syringe that had plastic tubing connected to the tip, taking special precautions to ensure that no air bubbles were present inside of the system; the other end of the tubbing was then connected to the feed line of a 60 kHz ultrasonic atomizer. The syringe was then placed on a syringe pump to control the total volume introduced to the system and its flowrate.

An initial curing process was performed by starting the pump at a slow flowrate and starting the atomizer with a power of 3 W until a continuous stream of atomized particles was expelled from the tip. Following this preliminary operation, the tests were carried out using a constant volume of solution (30 mL) and a flowrate of 1 mL/min, 2.5 mL/min, 5 mL/min, 7.5 mL/min, and 10 mL/min. During this phase, the powers used for atomization of the mannitol solutions were 1W, 3W, and 4.5W, while for the sucrose preparations it was kept at 3W.

As figure 26 illustrates, the chosen mode of spray-freezing was SFV/L. This operation consisted of filling the dewar with liquid nitrogen up until the mid-section, leaving enough space between the nozzle and the surface of the liquid to allow the formation of a vapor stratum. The dewar was placed over a magnetic stirrer to avoid clumping and aggregation of the particles during the freezing process. After the set volume was atomized into the dewar, the pump automatically shut down, the atomizer and the magnetic stirrer were turned off, and the dewar containing the frozen particles was emptied into the tray shown in figure 26, where they were left to dry until the nitrogen was completely evaporated.

Figure 26. Spray-freezing system set-up (left) and collection tray (right)

3.3. Sample collection, loading, and freeze-drying process

The freeze-drying operation was set to dry all the particles produced for a single preparation at different atomization conditions to make the process less time-consuming. Consequently, as depicted in figure 27, the tray that was used for the freeze-drying process was divided into different segments to accommodate the different samples. After all the nitrogen was evaporated, the particles were transferred to the tray segment corresponding to their flowrate and immediately introduced into the shelf of the freeze-drier, which was pre-cooled at a temperature of -50 °C. This was done to keep the samples from melting before all the particles were loaded and to ensure the same starting temperature for all the samples.

Figure 27. Segmented tray

Once the tray was loaded with all the samples, the freeze-drying process was initiated. The equipment used was a REVO freeze-dryer (Millrock Technology). Primary drying was performed at 10 °C and 200 µbar for the mannitol particles and was changed to -20 °C and 100 µbar for the sucrose particles. When the shelf temperature reached the set-point, the primary drying process was started. The endpoint of the primary drying process was obtained when the pressure reading of the Pirani gauge installed in the freeze-dryer was equal to the one in the capacitance manometer. Secondary drying was carried out for 5 hours at 20 °C at the same pressure conditions as primary drying for all the formulations. The resulting powder was collected in marked vials, sealed with aluminum caps, and stored at -20°C until they were used for the analysis.

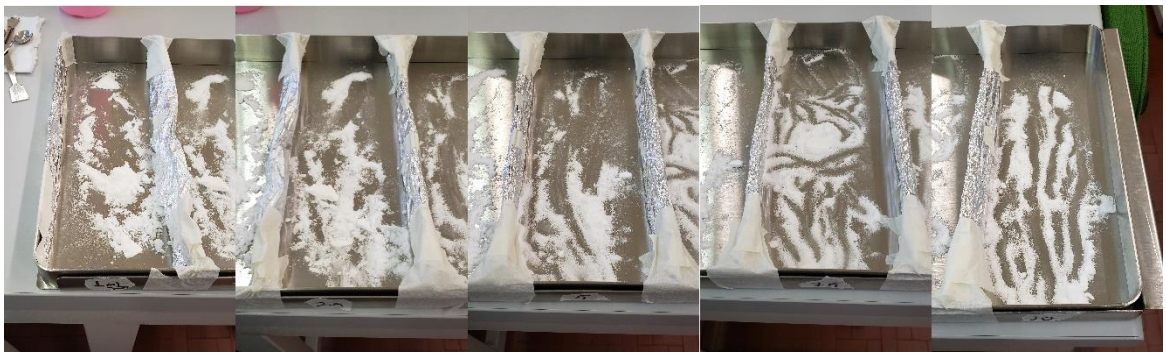

Figure 28. Tray containing the spray freeze-dried powder of the 40% (w/w) sucrose solution at different flow rates.

3.4. Powder characterization and analysis

The effects of process variables (feed flowrate and concentration) on particle size and specific surface area were investigated. Therefore, the resulting dried particles were characterized by the following experimental methods:

- Specific surface area (BET)
- Scanning electron microscopy (SEM)

3.4.1. Specific surface area (BET)

The specific surface area was determined by the adsorption of nitrogen to the surface of a solid material. The adsorption of nitrogen, known as adsorption isotherm or Brunauer, Emmett, and Teller (BET) isotherm, was measured using the Accelerated Surface Area and Porosimetry System (ASAP 2020) supplied by Micromeritics (USA). The ASAP 2020 includes two independent vacuum systems, one for sample degassing and one for sample analysis. A known amount of powder (200 mg) was placed in a glass sample container and connected to the degassing step in which the sample was degassed for 3 hours at 40 °C prior to analysis to remove any contaminants from the sample. After degassing, the sample was weighed to obtain its dry mass for further analysis and connected to the analysis stage where the adsorption process takes place. The nitrogen adsorption-desorption isotherms were measured at the temperature of 77K over a relative pressure (P/P0) between 0.05–0.30. The surface area of a sample was calculated from the adsorption isotherm using the BET equation by ASAP 2020 software.

The BET analyses were conducted by Dr. Merve Betul Adali at the Department of Applied Science and Technology (DISAT) at Politecnico di Torino.

3.4.2. Scanning electron microscope (SEM)

For the SEM analysis, since the samples consisted of organic matter, an initial metallization step was performed to allow electrons to move freely around the surface. The SEM images were captured in the microscopy and surface analysis laboratory of the DISAT at Politecnico di Torino.

Once the SEM images were obtained, ImageJ software (NIH, USA) was used to determine the geometric diameter of the dried particles, and approximately 200-300 particles were measured for each sample by taking an average of 5 measurements within the particle. The raw data was then used to calculate the mean and the standard deviation following the best model available, and to plot the results in histograms. All the calculations and analyses were done through OriginLab pro software. For the 40% (w/w) sucrose solution, the measures were changed from 5 to 8 to compensate for the non-sphericity of the particles.

CHAPTER 4: RESULTS AND DISCUSSION

This chapter will focus on presenting the results obtained from the experimental procedure and discussing them, giving particular attention to the conditions that could influence the morphological properties of the obtained particles.

4.1. Particle size distribution

The first part of the analysis will focus on the effect the diverse factors had on the particle size distribution. The parameters that were changed were the power used to atomize the solution, the concentration of the solution, and the flowrate at which they were injected.

4.1.1. Influence of the power input

Images 29 to 33 illustrate the resulting SEM images obtained for the mannitol preparations at 5% (w/w), when supplying the atomizer with power equal to 1W, 3W, and 4.5 W at different flowrates.

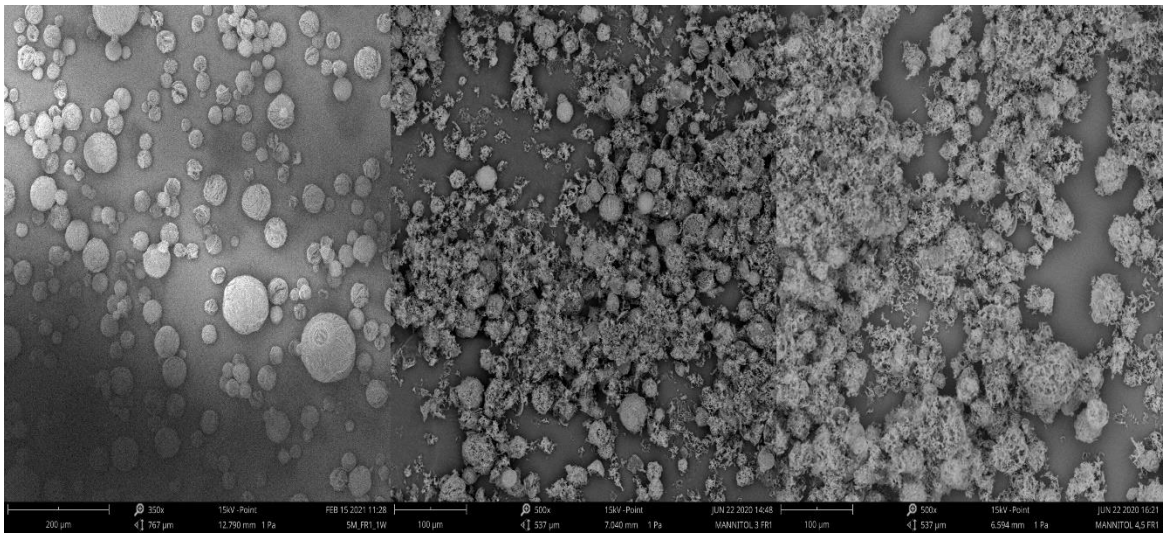

Figure 29. SEM images of mannitol powder obtained from the 5% (w/w) solution, atomized at a flowrate of 1 mL/min with different power inputs, 1W (left), 3W (center), and 4.5W (right)

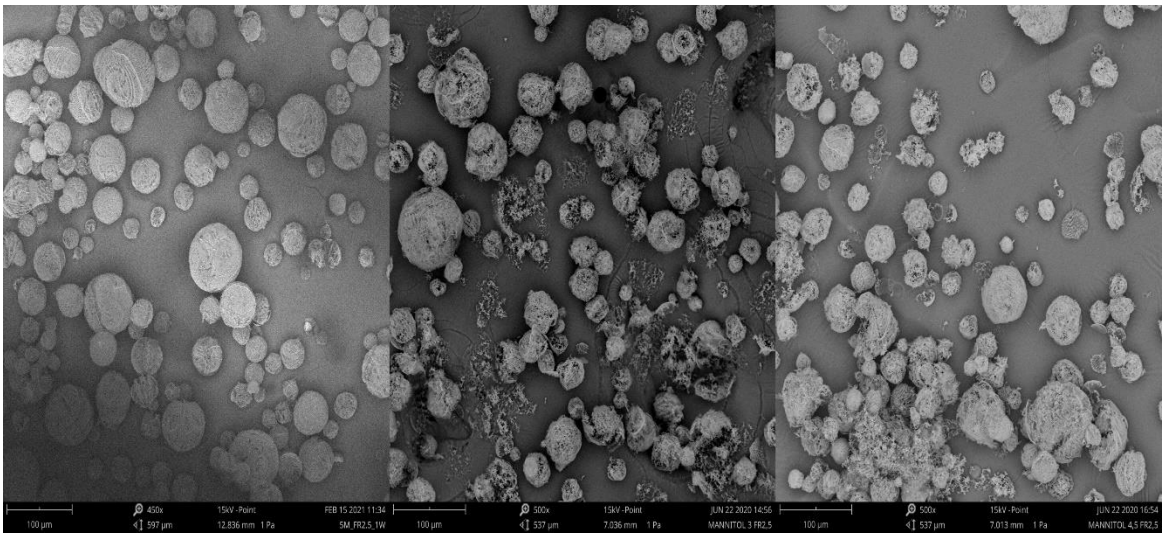

Figure 30. SEM images of mannitol powder obtained from the 5% (w/w) solution, atomized at a flowrate of 2.5 mL/min with different power inputs, 1W (left), 3W (center), and 4.5W (right)

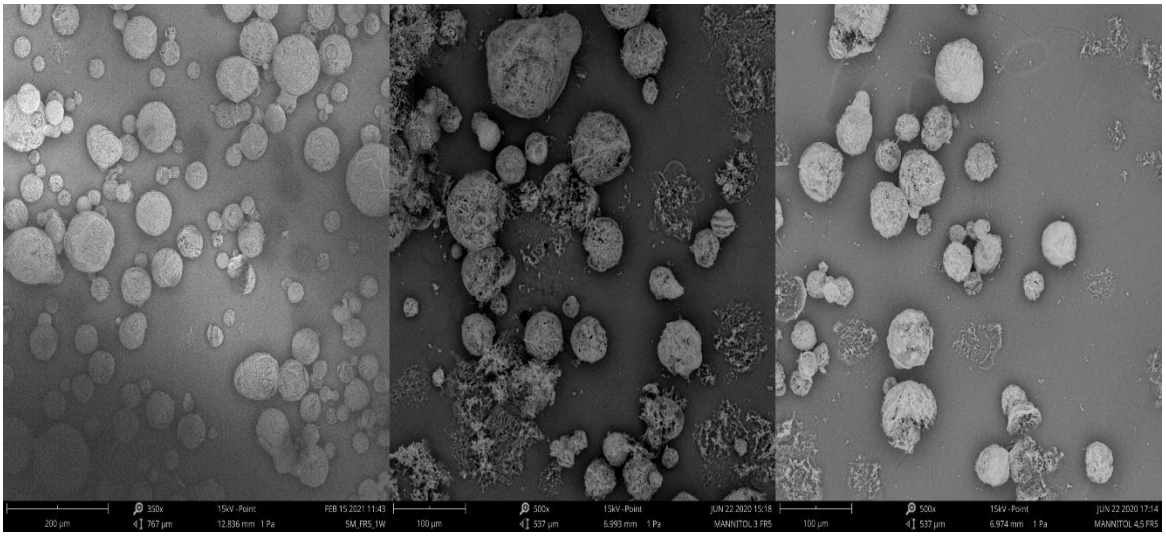

Figure 31. SEM images of mannitol powder obtained from the 5% (w/w) solution, atomized at a flowrate of 5 mL/min with different power inputs, 1W (left), 3W (center), and 4.5W (right)

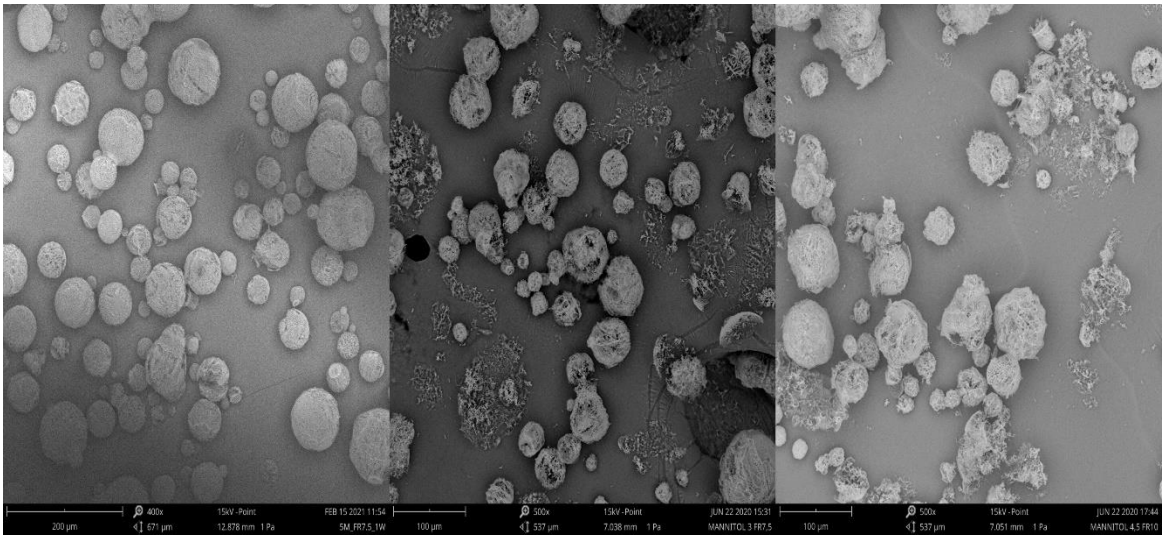

Figure 32. SEM images of mannitol powder obtained from the 5% (w/w) solution, atomized at a flowrate of 7.5 mL/min with different power inputs, 1W (left), 3W (center), and 4.5W (right)

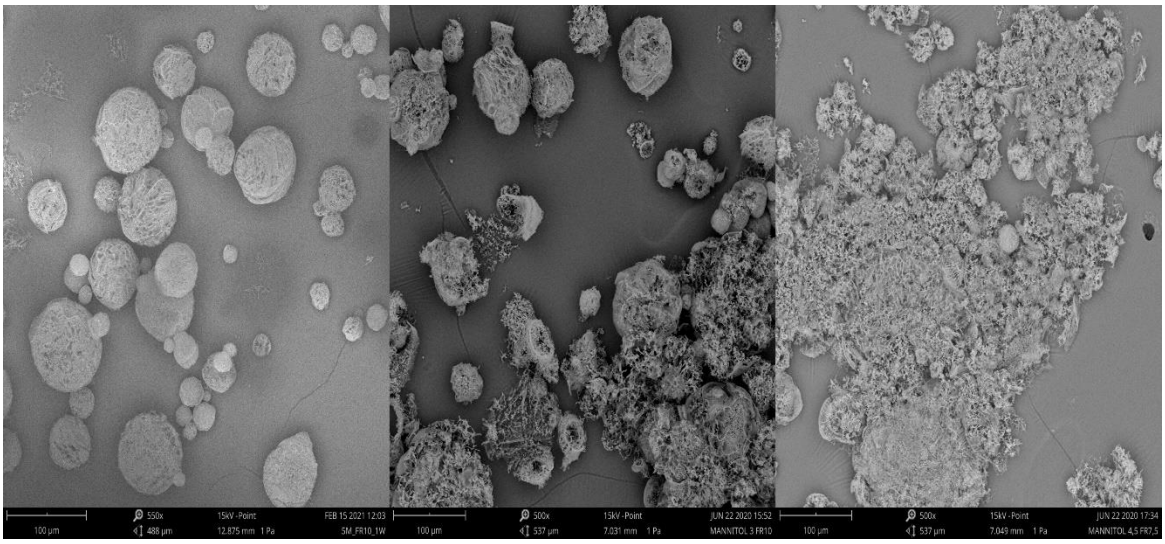

Figure 33. SEM images of mannitol powder obtained from the 5% (w/w) solution, atomized at a flowrate of 10 mL/min with different power inputs, 1W (left), 3W (center), and 4.5W (right)

The first thing we can observe is that, whereas using a power input of 1 W generated perfectly spherical particles at every flowrate, supplying a power input of 3 W and 4.5 W caused the formation of a sponge-like structure at both 1 mL/min and 10 mL/min, and caused the particles produced in the flowrates outside these values to considerably deteriorate when compared to the ones produced at 1 W.

The formation of sponge-like structures at 1 mL/min using a power input 3 W and 4.5 W can be explained by analyzing the liquid film that wets the surface of the nozzle. At low flowrates, the thickness of this film is not enough to withstand the amount of power that is being supplied to the system, which would then cause the disintegration of the sample. While this may explain why the lowest flowrate produced this kind of structure, it does not provide a satisfactory explanation as to why at 10 mL/min the same phenomenon occurred. The studies of Avvaru et al. (2006) could offer a viable explanation as to why this happened. Their study proposes that after a critical flowrate, part of the power used for the atomization of the fluid is used to make the liquid film oscillate, and an increase in flowrate will decrease the amount of energy used for this purpose because gravitational forces will help with the oscillation process. Consequently, after a certain flowrate, the energy from the gravitational forces will contribute enough to compensate for the power fraction that goes into making the nozzle oscillate.

Table 1 provides the geometrical size of the particles made from the 5% (w/w) mannitol solution at different flowrates and atomized at 1 W, 3 W, and 4.5 W. While fitting the results, it was found that the most appropriate statistical model was the LogNormal distribution. This model is widely used for particle size analysis in the characterization of aerosols and sieved particles because it consistently provides a close fit for a wide array of particulate populations (International Atomic Energy Agency, 1978). An r^2 factor close to 0.99 was obtained for all the formulations and fitted closely with the dataset obtained.

Table 1. The geometric particle size of mannitol powder produced from a 5% (w/w) solution atomized at different flowrates using an ultrasonic atomizer operated at 1 W, 3 W, and 4.5 W.

Flowrate (mL/min) [Q]	Mannitol 1 W		Mannitol 3 W		Mannitol 4.5 W	
	Mean (µm) [M]	Std. Deviation (µm) [σ]	Mean (µm) [M]	Std. Deviation (µm) [σ]	Mean (µm) [M]	Std. Deviation (µm) [σ]
1.0	18.89	0.37	11	0.25	14.5	0.29
2.5	21.95	0.41	15.1	0.4	14.57	0.34
5.0	27.65	0.49	20.02	0.47	25.77	0.69
7.5	26.26	0.65	13.34	0.37	14.76	0.48
10.0	25.07	0.77	51.88	0.9	-	-

We can observe that increasing the power from 1 W to 3 W resulted in a considerable decrease in particle size, which is consistent with previous experiences. After increasing the power supplied from 3 W to 4.5 W, however, no significant decrease was found apart from those produced at 5 mL/min. The deviation at this flowrate could have its roots in the low number of particles available for measuring, which therefore skewed the average value. Therefore, the results suggest that there is a power limit after which the sample will not show a decrease in size and will start to disintegrate.

When using a lower power input, we can observe that the particle size trend before 5 mL/min was reached was almost identical to the one obtained for the higher powers, with a considerable increase in its base size. However, whereas the particles obtained at 1 W of supplied power remained quasi-constant in size after overcoming the critical flowrate, the 3 W and 4 W samples plummeted in size. The reason for this sort of dampening behavior could be that the energy supplied is not as high as it was in the other two cases, and it was therefore enough to atomize the fluid but not completely disintegrate it, supporting the previous hypothesis. Another noteworthy result is that the largest particle size was obtained at 10 mL/min and 3 W. This could be a product of the low number of particles that were available for measuring at this flowrate.

Images 34 to 39 illustrate the changes in particle size distribution obtained for the 5% (w/w) mannitol powder produced at 1 W, 3 W, and 4.5 W at different flowrates.

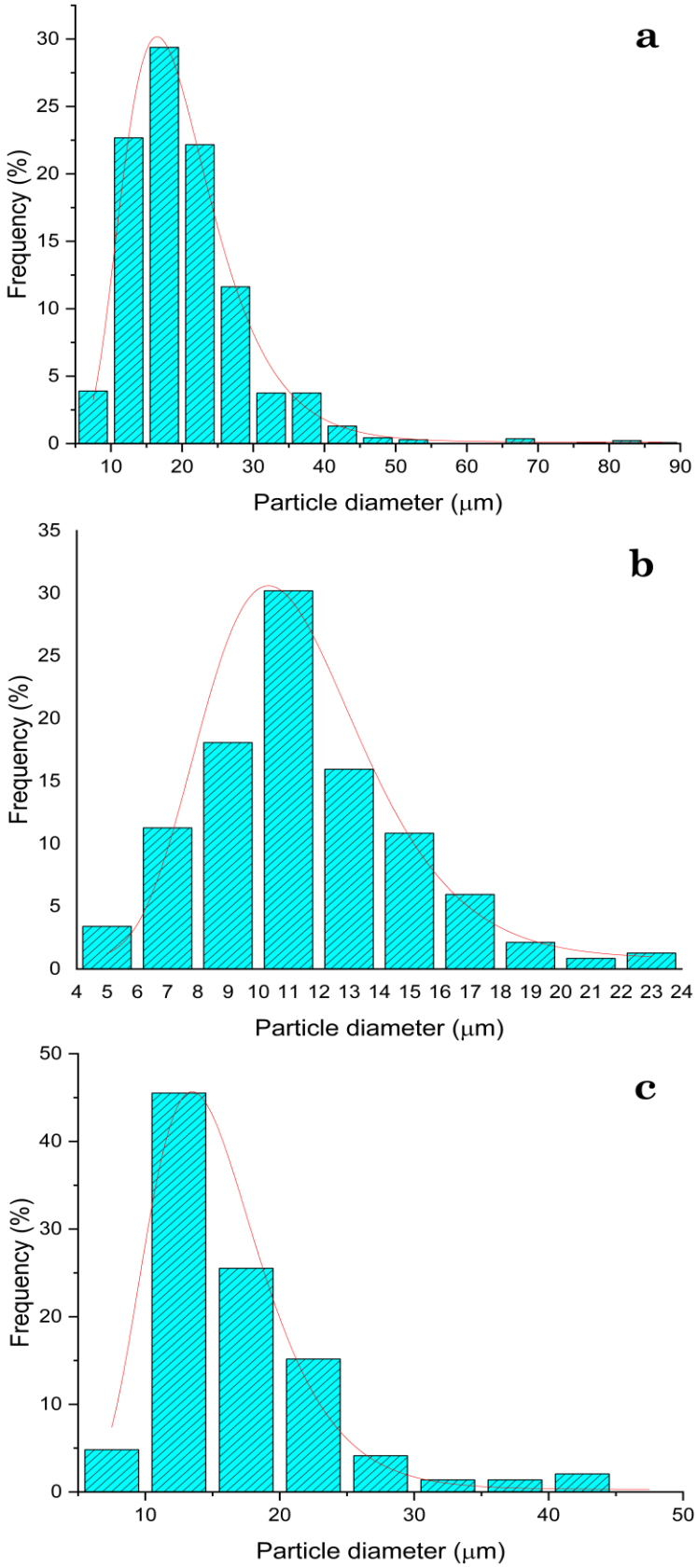

Figure 34. Particle size distribution of mannitol powder obtained from the 5% (w/w) solution, atomized at a flowrate of 1 mL/min with a power input of 1W (a), 3W (b), and 4.5W (c).

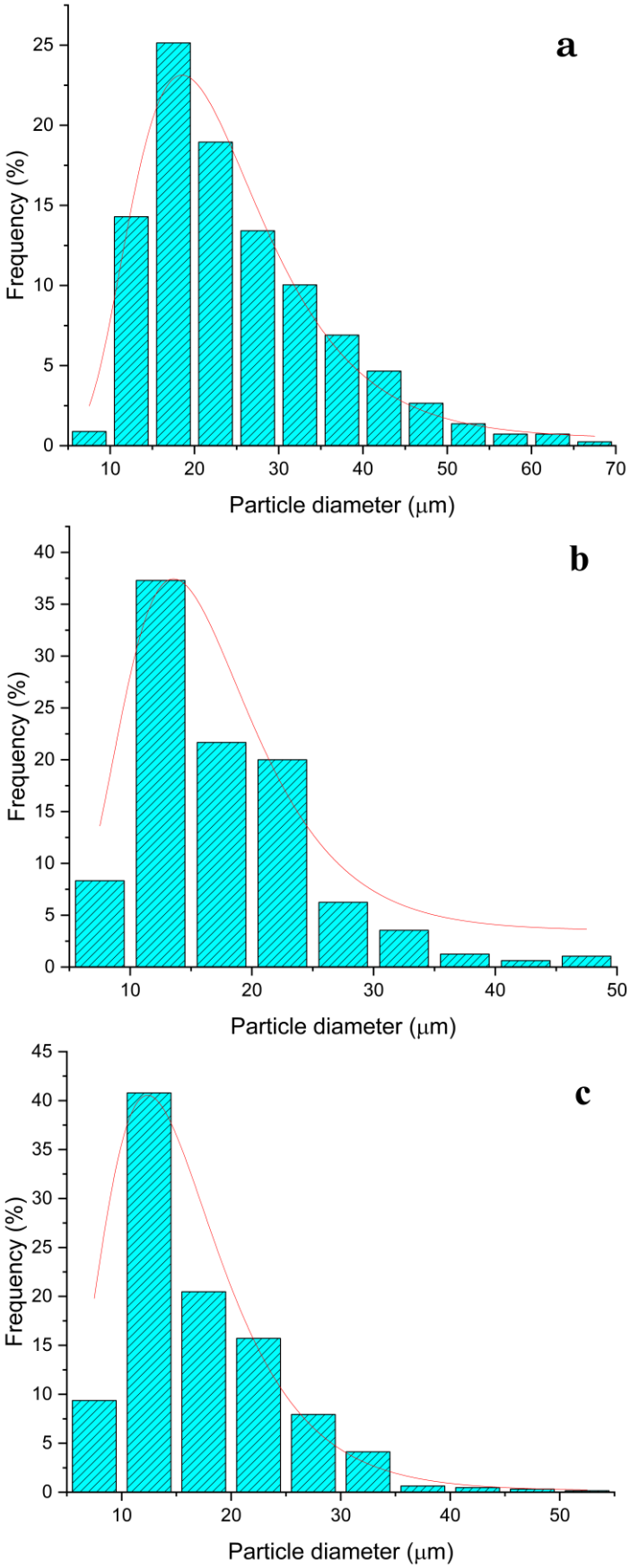

Figure 35. Particle size distribution of mannitol powder obtained from the 5% (w/w) solution, atomized at a flowrate of 2.5 mL/min with a power input of 1W (a), 3W (b), and 4.5W (c).

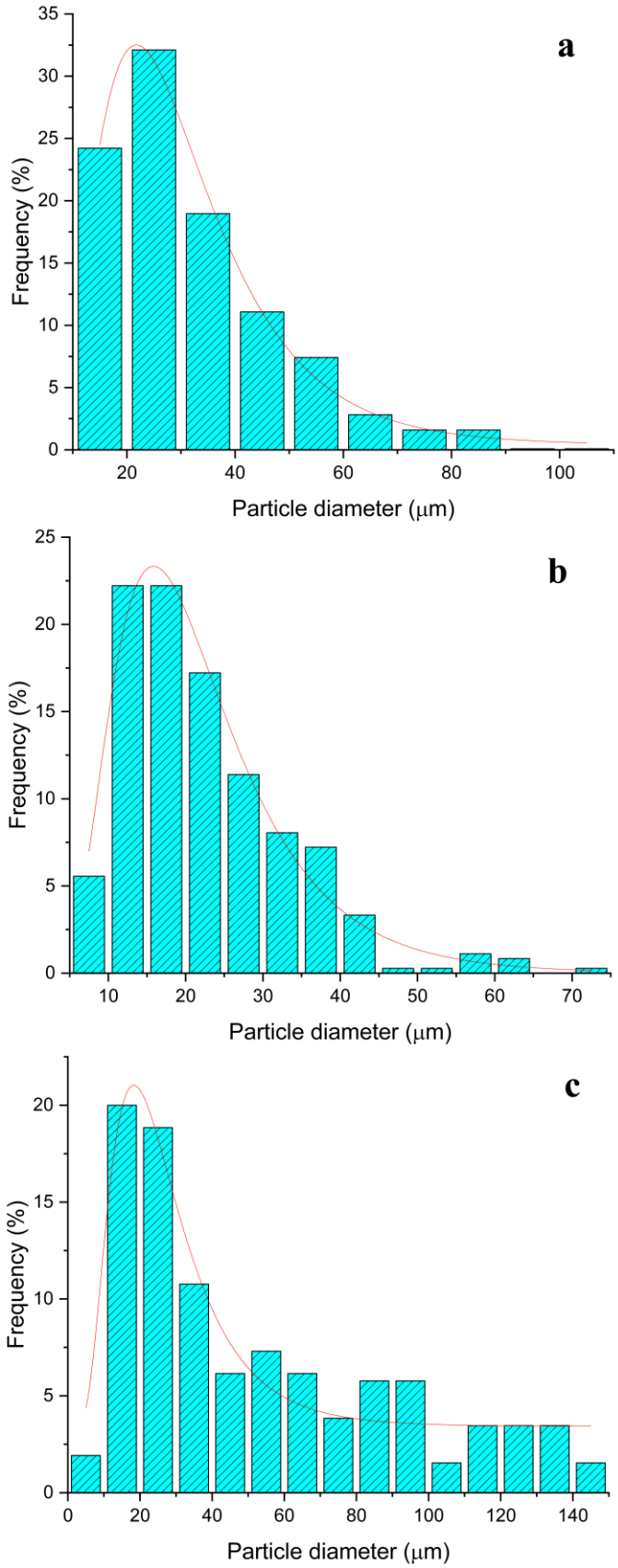

Figure 36. Particle size distribution of mannitol powder obtained from the 5% (w/w) solution, atomized at a flowrate of 5 mL/min with a power input of 1W (a), 3W (b), and 4.5W (c).

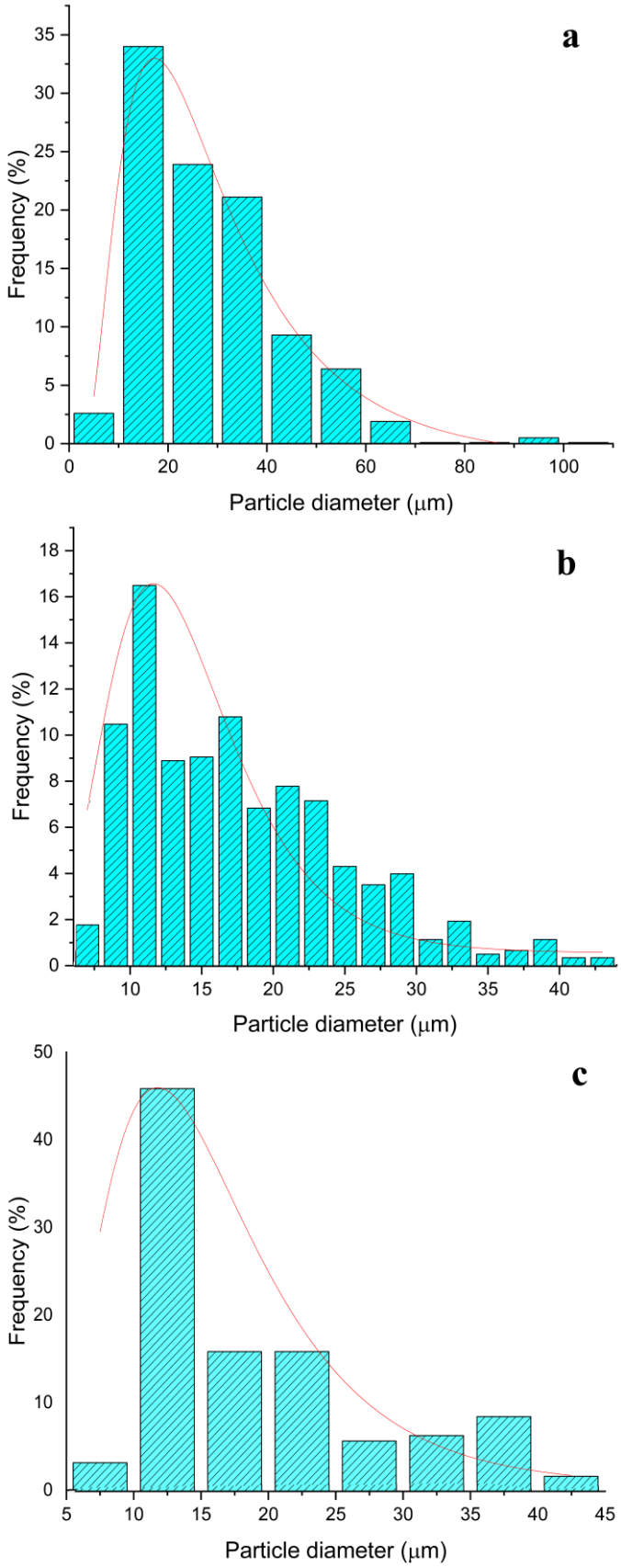

Figure 37. Particle size distribution of mannitol powder obtained from the 5% (w/w) solution, atomized at a flowrate of 7.5 mL/min with a power input of 1W (a), 3W (b), and 4.5W (c).

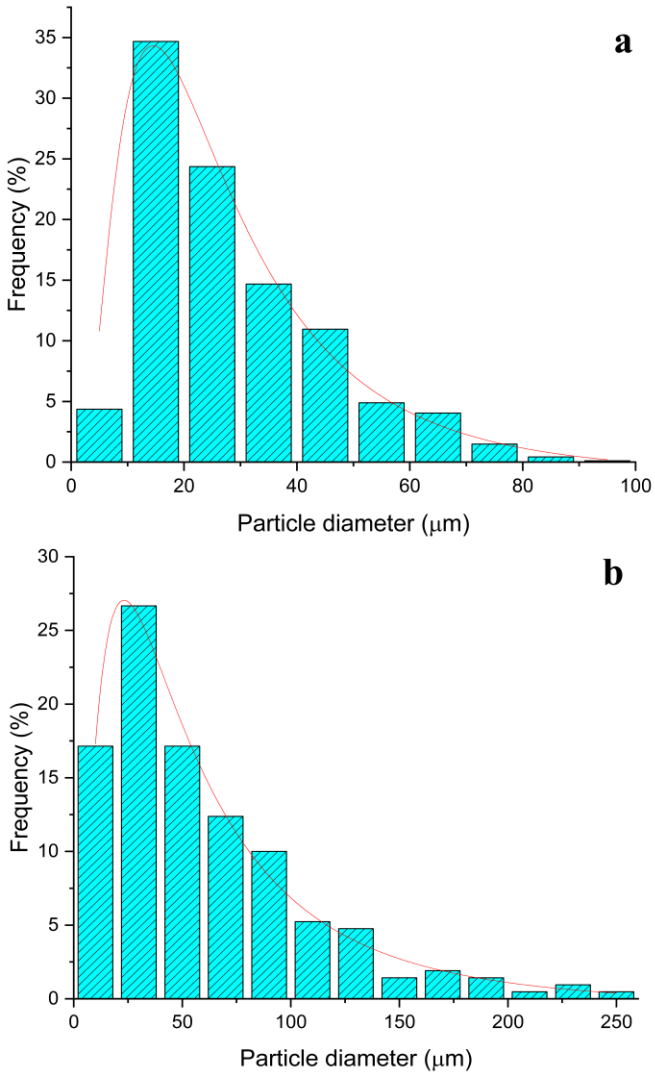

Figure 38. Particle size distribution of mannitol powder obtained from the 5% (w/w) solution, atomized at a flowrate of 10 mL/min with a power input of 1W (a), and 3W (b).

The results obtained denote that increasing the power input for the atomizer will help obtain more uniform particles. This makes sense since a higher power input reduces the residence time of the fluid (Avvaru et al., 2006). This in turn causes the dissipation of energy to be lower and decreases the energy disparity from the cavitation phenomenon.

4.1.2. Influence of the viscosity

This section will focus on analyzing the changes in the particle size distribution when the viscosity of the solution is increased from 1.144 mPa.s for the sucrose solution at 5 % (w/w), to 6.167 mPa.s for the solution at 40% (w/w). The viscosity data were calculated by Swindells (1958) at 20°C, which is the average temperature at which the atomizer tip was kept during the spray-freezing process. Figures 39 to 43 report the SEM images obtained for the 5% (left) and 40% (right) sucrose solutions at different flowrates.

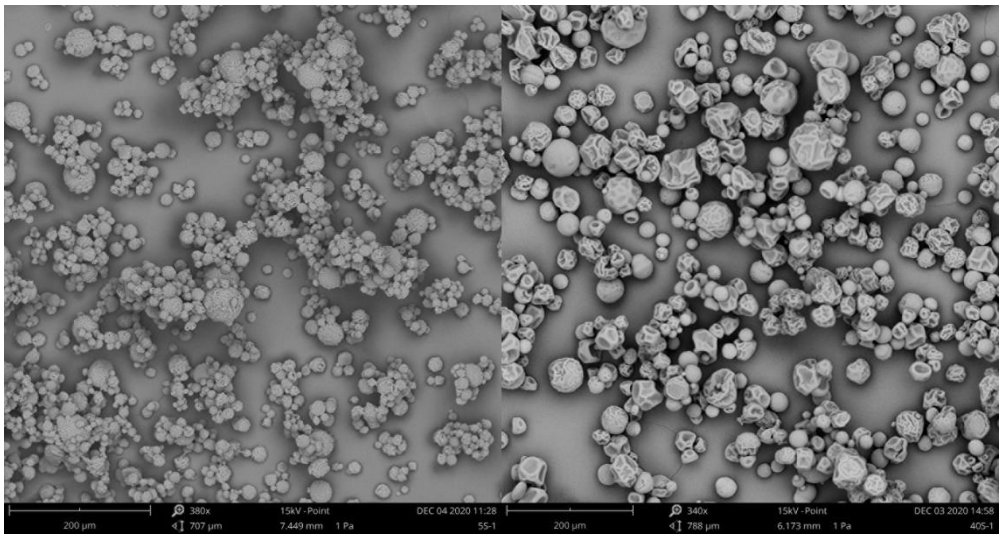

Figure 39. SEM images of sucrose powder obtained from the 5% (w/w) solution (left) and the 40% (w/w) solution (right), atomized at a flowrate of 1 mL/min at 3 W.

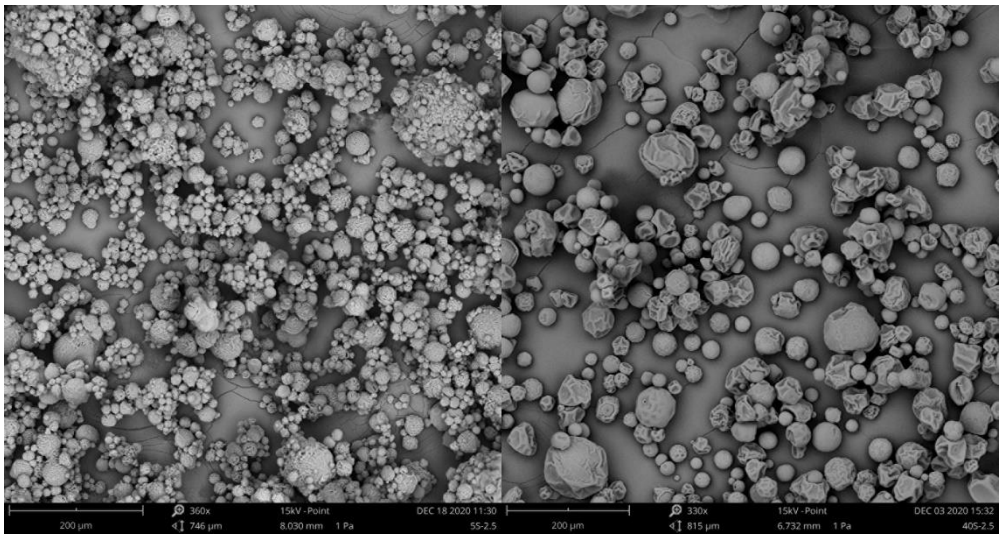

Figure 40. SEM images of sucrose powder obtained from the 5% (w/w) solution (left) and the 40% (w/w) solution (right), atomized at a flowrate of 2.5 mL/min at 3 W.

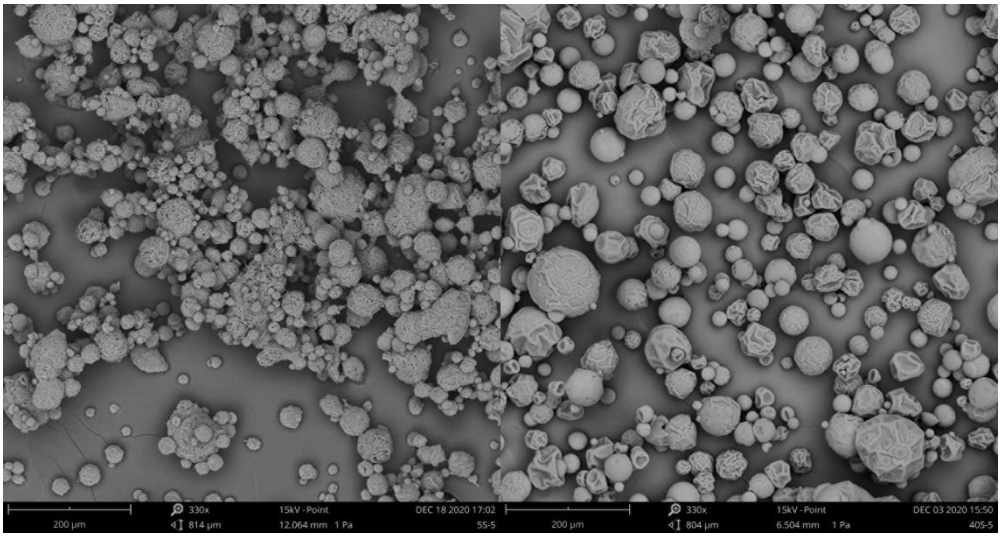

Figure 41. SEM images of sucrose powder obtained from the 5% (w/w) solution (left) and the 40% (w/w) solution (right), atomized at a flowrate of 5 mL/min at 3 W.

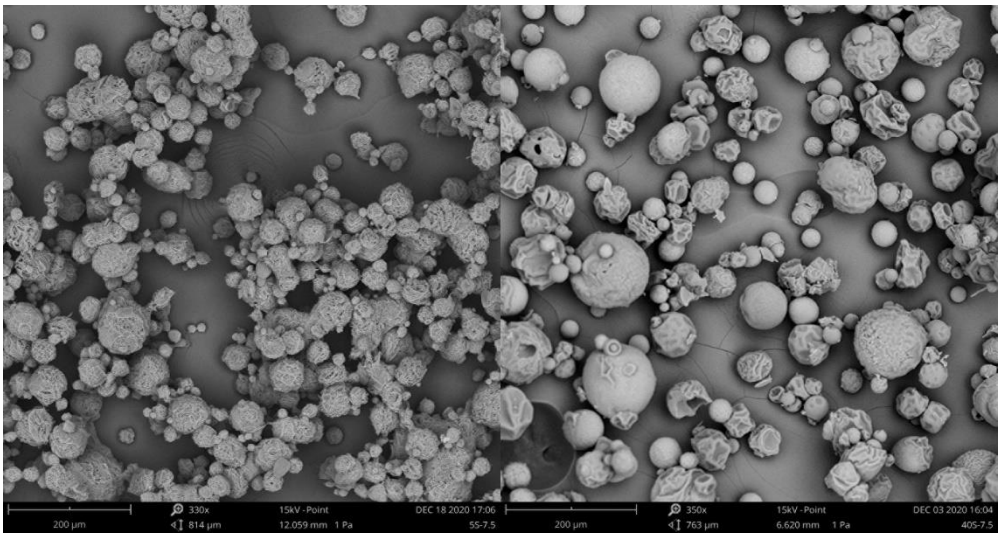

Figure 42. SEM images of sucrose powder obtained from the 5% (w/w) solution (left) and the 40% (w/w) solution (right), atomized at a flowrate of 7.5 mL/min at 3 W.

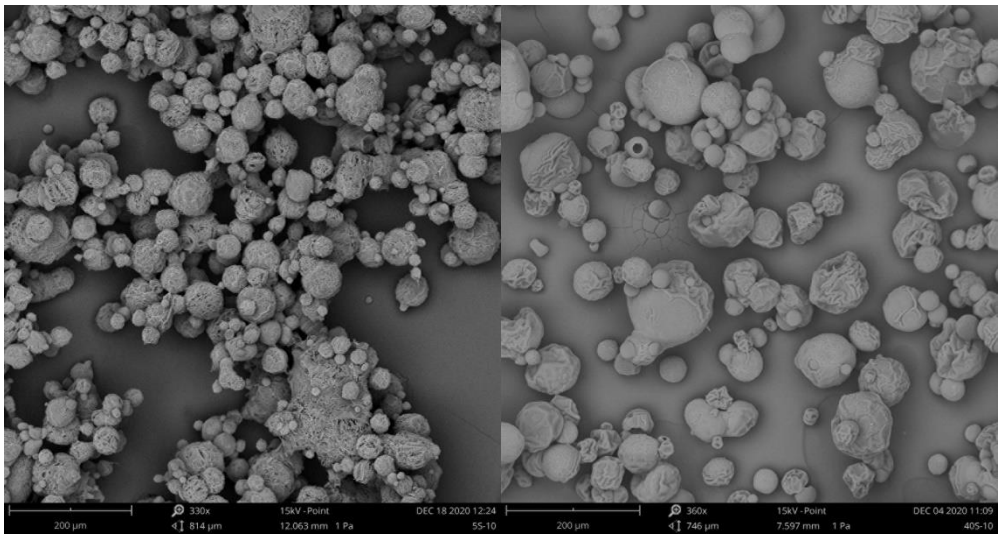

Figure 43. SEM images of sucrose powder obtained from the 5% (w/w) solution (left) and the 40% (w/w) solution (right), atomized at a flowrate of 10 mL/min at 3 W.

Visually, both solutions followed the same trend of forming clusters at low flowrates. However, the amount and frequency with which these aggregates formed were significantly higher in the 5 %(w/w) solution. Additionally, the particles formed from a higher viscosity fluid were also visually larger in size. The smaller particle size could be a factor for the increased formation of clusters at lower viscosities. Table 2 provides the particle diameter of the powder obtained for both the 5% (w/w) and the 40% (w/w) sucrose solution. The average particle size and its standard deviation were also obtained by using a Lognormal distribution because it provided a better fit for the experimental results.

Table 2. Geometric particle size of sucrose powder produced from a 5% (w/w) solution and a 40% (w/w) solution atomized at different flowrates using an ultrasonic atomizer operated at 3 W.

Flowrate (mL/min) [Q]	5% sucrose solution		40% sucrose solution	
	Mean (µm) [M]	Std. Deviation (µm) [σ]	Mean (µm) [M]	Std. Deviation (µm) [σ]
1.0	9.58	0.37	21.93	0.29
2.5	11.22	0.43	22.14	0.39
5.0	17.00	0.43	26.51	0.34
7.5	23.60	0.46	28.07	0.45
10.0	21.18	0.70	29.82	0.57

As was expected, an increase in the viscosity of the solution had a large effect on the particle average size, slightly greater in fact than the one flowrate has. This is consistent with the theory because higher viscosity fluids will dissipate more energy from the cavitation bubbles, which in turn will cause the particles formed to be larger at the same flowrate. Moreover, this means that even if the liquid film on the nozzle is thinner, more energy will be required to atomize it and the sample will not be destroyed. Furthermore, the tendency to reach a peak value was not seen for the 40% solution. This could be attributed to the fact that the viscous forces will also be increased, which will then take a higher fraction of the power used for atomization to produce the film oscillation and will therefore delay the liquid film thickness at which the gravity will contribute in a significant manner.

Images 44 to 48 show the particle size distribution obtained for the 5% (w/w) and 40 %(w/w) sucrose solutions at different flowrates.

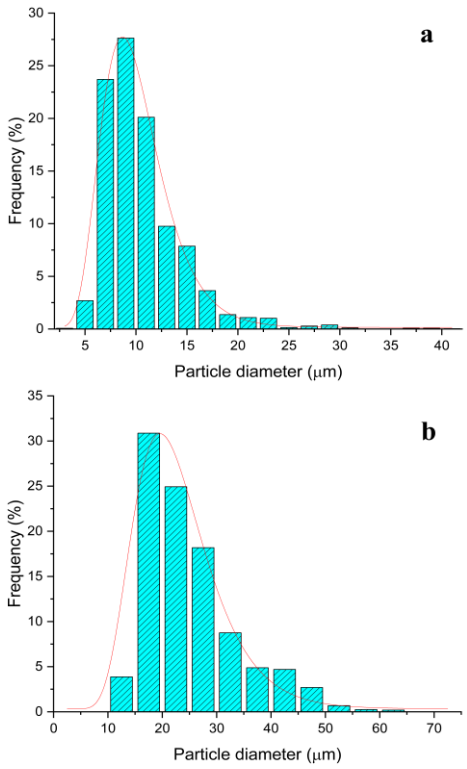

Figure 44. Particle size distribution of sucrose powder obtained from the 5 % (w/w) solution (a) and the 40% (w/w) solution (b), atomized at a flowrate of 1 mL/min at 3 W.

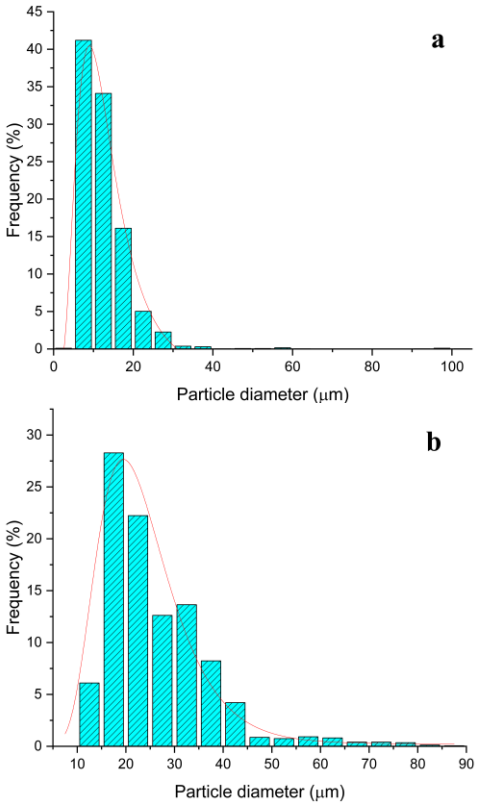

Figure 45. Particle size distribution of sucrose powder obtained from the 5 % (w/w) solution (a) and the 40% (w/w) solution (b), atomized at a flowrate of 2.5 mL/min at 3 W.

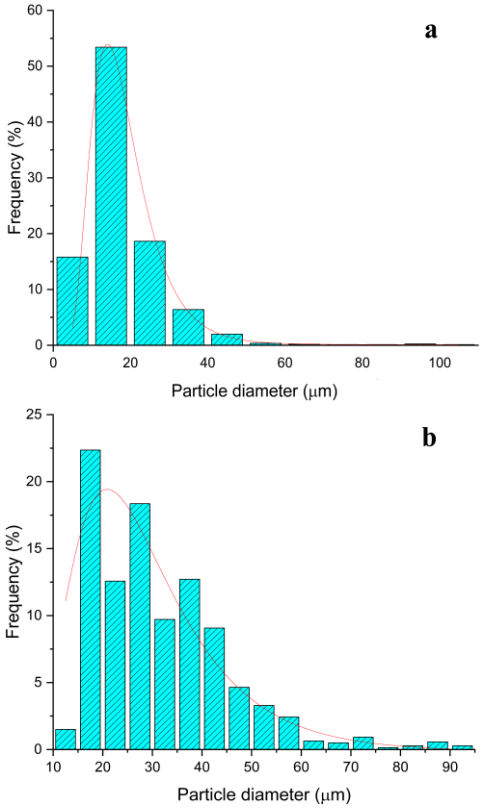

Figure 46. Particle size distribution of sucrose powder obtained from the 5 % (w/w) solution (a) and the 40% (w/w) solution (b), atomized at a flowrate of 5 mL/min at 3 W.

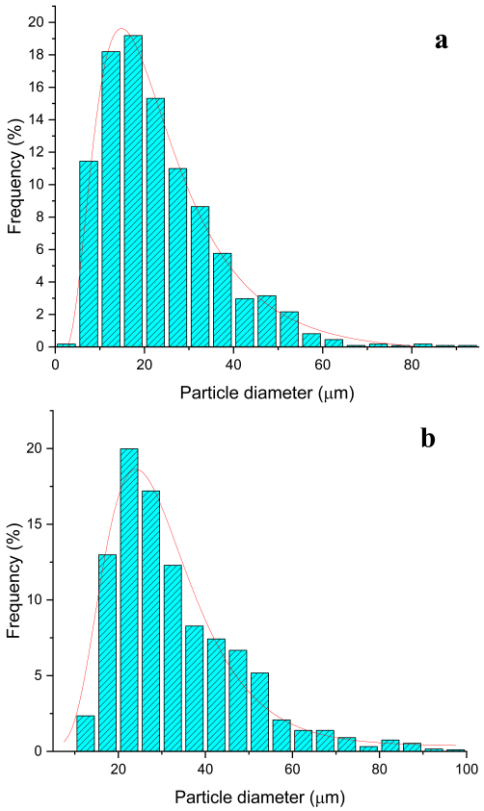

Figure 47. Particle size distribution of sucrose powder obtained from the 5 % (w/w) solution (a) and the 40% (w/w) solution (b), atomized at a flowrate of 7.5 mL/min at 3 W.

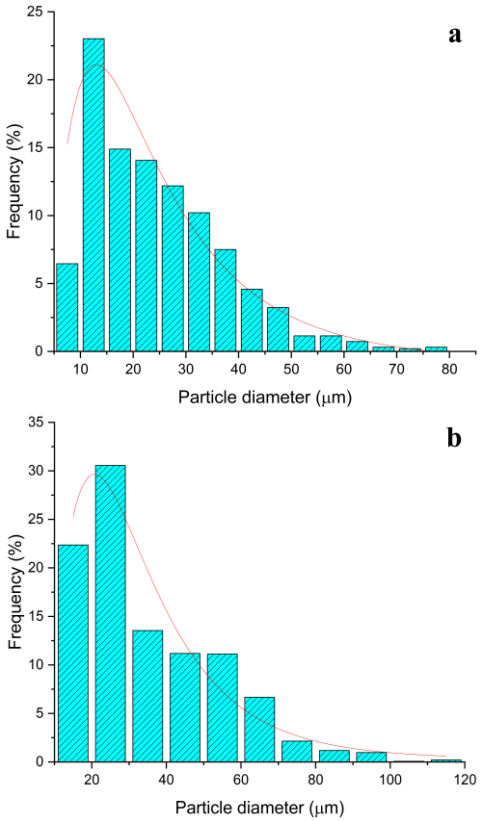

Figure 48. Particle size distribution of sucrose powder obtained from the 5 % (w/w) solution (a) and the 40% (w/w) solution (b), atomized at a flowrate of 10 mL/min at 3 W.

These images show that increasing the viscosity slightly decreased the uniformity of the particles. This can be explained by considering that a part of the energy used to atomize a solution of higher viscosity will not be used for the actual atomization process but will be dissipated into the fluid, reducing the energy from the cavitation bubbles and the capillary waves, and causing the system to behave as if a lower power input is being used.

4.1.3. Influence of the feed flowrate

The influence of the flowrate has been a part of the discourse for the other phenomena present in the study. This section will discuss the individual influence that the feed flowrate had on the finished product.

From the previous result, we can see that increasing the flowrate generally increases the final particle size of the powder. This makes sense given that a higher amount of fluid is entering the system, resulting in a thicker liquid film which helps dissipate part of the energy supplied. An indefinite increase in flowrate however will not cause an increase in particle size as it was seen for the 5 % (w/w) mannitol powders and the 5% (w/w) sucrose powders. As commented before, after reaching a determined flowrate the gravitational forces that act in the fluid will compensate the amount of energy that is used to make the nozzle oscillate and will allow the energy to go in its entirety towards the atomization of the fluid.

Additionally, increasing the flowrate also decreased the particle size distribution uniformity. This can be explained by considering the same principle we used in the previous argument. A larger amount of fluid entering the system will mean that more energy from the cavitation is dissipated and therefore will function as if the power supplied is lower than the actual value. Since the uniformity of the method comes from the regularity at which the cavitation bubbles and capillary waves form, the influence of the gravitational forces, while allowing more net energy to be transmitted to the fluid, will not help with the uniformity of the distribution.

4.2. Specific surface area

The second part of the study focused on the changes in the specific surface area of the particle, with the relevant parameters being the same as the ones used for the particle size distribution analysis.

4.2.1. Influence of the feed flowrate

This section will analyze the effect flowrate had on the specific surface area of the powders produced using the 5% (w/w) mannitol solution and the 5% (w/w) sucrose solution, both atomized at 3 W. The adsorption isotherms of all the samples studied mostly followed a typical type II pattern, with the exceptions being those of sucrose at 1 mL/min and 2.5 mL/min, both are shown in figure 49.

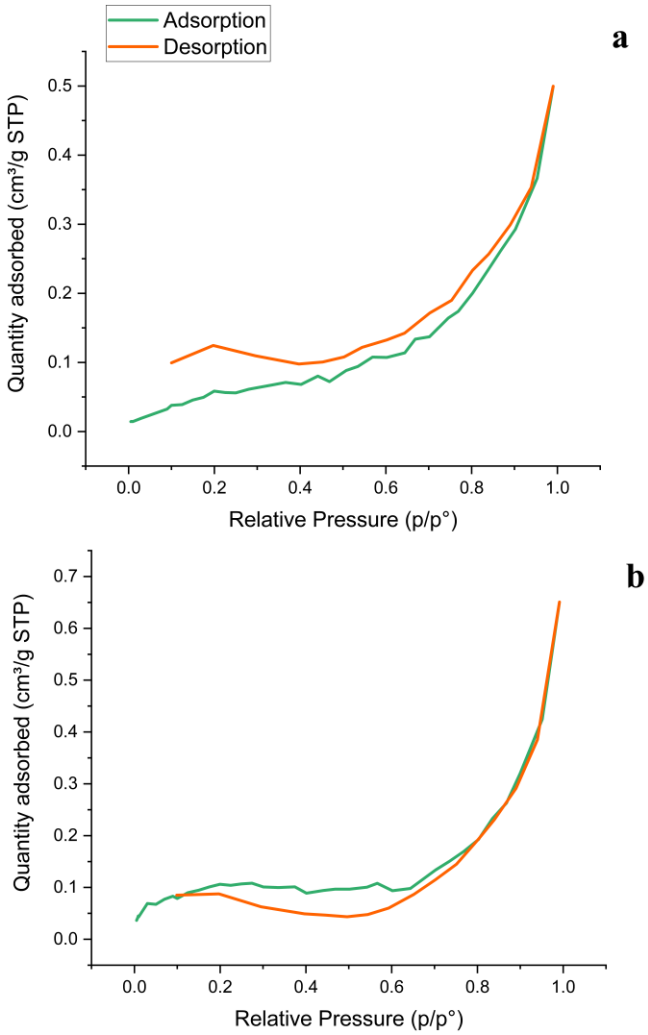

Figure 49. Adsorption isotherms of sucrose powder obtained from a 5% (w/w) solution produced at a flowrate of 1 mL/min (a) and 2.5mL/min (b), atomized at 3 W.

The first image shows an incomplete adsorption-desorption loop, this could indicate that the time used assigned to the process was not enough to allow the nitrogen to desorb, and this makes sense given that the sample had an intricate network of clusters that made the diffusion of the gas more difficult at this flowrate. The second image denotes a hysteresis, which according to Gleysteen and Deitz (1945) could mean that capillary condensation occurred or that there was multimolecular adsorption. In this case, the most probable option would be the second one because, as stated by Gleysteen and Deitz (1945), in cases where a multimolecular layer is formed the desorption process would have to occur from the modified layer, therefore causing the desorption isotherm to be above the adsorption one for a certain time until a sufficiently low relative pressure was achieved.

The numerical values of the specific surface area obtained through BET analysis for the 5% (w/w) mannitol and 5% (w/w) sucrose solutions atomized at 3 W and different flowrates are shown in table 3.

Table 3. The specific surface area of powders generated using a 5% (w/w) mannitol solution and a 5% (w/w) sucrose solution atomized at 3 W for different flowrates.

Flowrate (mL/min) [Q]	**Mannitol (m^2/g) [S_{BET}]**	**Sucrose (m^2/g) [S_{BET}]**
1.0	7.5798 ± 0.0580	0.2292 ± 0.0102
2.5	6.1389 ± 0.0861	0.3659 ± 0.0107
5.0	7.5269 ± 0.0538	1.3706 ± 0.0251
7.5	6.3668 ± 0.0434	1.2832 ± 0.0207
10.0	5.5516 ± 0.0248	2.3091 ± 0.0164

From these results, we can observe that mannitol had, on average, a larger surface area than sucrose due to its superior porosity. Even though this was expected, since mannitol solutions at 5% (w/w) have similar values of viscosity, density, and surface tension (Pegram and Record, 2009) to those of sucrose solutions at the same concentration and temperature (1.151 mPa.s (Jiang, Zhu, and Ma, 2013) and 1.144 mPa.s (Swindells, 1958) respectively), a similar trend was expected. However, whilst the surface area of mannitol continuously decreased in value (apart from the one obtained at 5 mL/min), the one of sucrose increased. This difference in results is not attributed to the atomization process since all the relevant physical-chemical properties that influence it are approximately equal, but to the nature of the solute.

Sucrose's behavior could be explained by assuming that the clusters formed at lower flowrates obstructed the pores present in the larger particles, thus lowering their surface area. Moreover, the de-clustering effect of the increase in flowrate had a profound impact on the surface area. This is highlighted by figures 42 and 43, which showed that even with similar average particle size, the samples produced at 7.5 mL/min had a considerably lower surface area than the ones produced at 10 mL/min.

On the other hand, the specific area of mannitol decreased together with the increase in flowrate, apart from the particles produced at 5 mL/min. This makes sense given that a smaller particle size at the same porosity will result in a lower specific surface area. The increase in surface area at 5 mL/min can be caused by the lesser degradation noted for the particles produced at this flowrate.

4.2.2. Influence of the viscosity

From the SEM images presented in the analysis of the influence viscosity has on the particle size, we can observe that an increase in concentration caused the formation of clusters to be decreased. This caused the adsorption isotherms to have a type II pattern from the first flowrate, and a radical increase in the resulting specific surface area, which can be seen in the following table:

Table 4. The specific surface area of sucrose powder generated using a 5% (w/w) solution and a 40% (w/w) solution atomized at 3 W for different flowrates.

Flowrate (mL/min) [Q]	**5% Sucrose (m^2/g) [S_{BET}]**	**40 %Sucrose (m^2/g) [S_{BET}]**
1.0	0.2292 ± 0.0102	1.4737 ± 0.0142
2.5	0.3659 ± 0.0107	1.9659 ± 0.0276
5.0	1.3706 ± 0.0251	4.5365 ± 0.0201
7.5	1.2832 ± 0.0207	8.5312 ± 0.0412
10.0	2.3091 ± 0.0164	8.9679 ± 0.0489

We can observe from the experimental results that an increase in concentration drastically increased the specific surface area. We can attribute this to fewer clusters that were formed at higher concentrations, which can be seen from the SEM images we obtained. These images show that there is a prominent decrease in the number of clusters from 7.5 mL/min onwards for the 40% (w/w), which would then explain the sudden jump in surface area at this flowrate.

CHAPTER 5: CONCLUSIONS AND RECOMMENDATIONS

This thesis focused on supplying information about the spray freeze-drying process, its relevant parameters (specifically those that influenced the atomization), and the resulting impact they had on the particle size distribution and specific surface area.

5.1 Conclusions

After carrying out the experiments and analyzing the results, the following conclusions can be drawn:

- Within a specific range, an increase in the power employed for atomization will both decrease the average particle size and will make the particles more uniform in their distribution. After the range is exceeded, there will not be any notable decrease in particle size and the sample could be disintegrated.
  .
- Increasing the viscosity of a solution will also increase the average particle size of the powder but will decrease its uniformity slightly. It will also decrease the tendency of a solution to form clusters.

- Increasing the feed flowrate results in bigger, less uniform particles. However, there is a critical flowrate after which the particle size will tend to decrease with an increase in flowrate. This critical value is independent of the power, will increase with the viscosity, and to a lesser extent will be modified by the solute that is being used.

- The specific surface area of solutes like sucrose benefit from an increase in feed flowrate and a surge in viscosity. For solutes like mannitol, the specific surface area will decrease with a rise in feed flowrate.

5.2 Recommendations

Taking into consideration the results obtained, there are some further tests that could be performed to have a clearer idea of the effect these parameters have on the final product. To better understand the effect these parameters have on amorphous solutions, a different solute such as trehalose should be used. Additionally, subsequent tests should work with systems like sucrose + mannitol to see the effects of the process on a mixture. Another test that could prove beneficial would be introducing a protein together with a cryoprotectant and then verifying its activity after the drying process. Increasing the flowrate range and power input at which the sucrose solutions were injected would also be of interest.

LIST OF FIGURES

LIST OF TABLES

REFERENCES

Adali, M. B., Barresi, A. A., Boccardo, G., & Pisano, R. (2020). Spray Freeze-Drying as a Solution to Continuous Manufacturing of Pharmaceutical Products in Bulk. *Processes, 8*(6), 709-736. doi:https://doi.org/10.3390/pr8060709

Alia, M. E., & Lamprecht, A. (2014). Spray freeze drying for dry powder inhalation of nanoparticles. *European Journal of Pharmaceuticals and Biopharmaceuticals, 87*, 510-517.

Alzamora, S. M., Vergara-Balderas, F., & Welti-Chanes, J. (2008). Freeze Drying. In Y. H. Hui, C. Clary, M. M. Farid, O. O. Fasina, A. Noomhorm, & J. Welti-Chanes, *Food Drying Science and Technology - Microbiology, Chemistry, Applications* (p. 403-416). DEStech Publications. Tratto da https://app.knovel.com/hotlink/khtml/id:kt011EP197/food-drying-science-technology/freeze-dry-introduction

Anandharamakrishnan, C., Gimbun, J., Stapley, A. G., & Rielly, C. D. (2009, 12). Application of Computational Fluid Dynamics (CFD) Simulations to Spray-Freezing Operations. *Drying Technology, 28*, 94–102. doi:10.1080/07373930903430843

Avvaru, B., Patil, M. N., Gogate, P. R., & Pandit, A. B. (2006). Ultrasonic atomization: Effect of liquid phase properties. *Ultrasonics, 44*, 146–158. doi:10.1016/j.ultras.2005.09.003

Azad, A. K., Rasul, M. G., Khan, M. M., Mondal, S. K., & Islam, R. (2016). Chapter 10 - Modeling and Simulation of Heat and Mass Flow by ASPEN HYSYS for Petroleum Refining Process in Field Application. (M. M. Khan, & N. M. Hassan, A cura di) *Thermofluid Modeling for Energy Efficiency Applications*, 227–257. doi:10.1016/B978-0-12-802397-6.00010-5

Bayvel, L., & Orzechowski, Z. (1993). *Liquid Atomization* (1 ed.). CRC Press. doi:10.1201/9780203748787

Bhandari, B. R., Patel, K. C., & Chen, X. D. (2008). Spray drying of food materials-process and product characteristics. *Drying Technologies in Food Processing*, 113-159. Retrieved from https://books.google.it/books?id=yB-VhPpQxv0C&printsec=frontcover&hl=it#v=onepage&q&f=false

Bhatnagar, B. &. (2008). Study of the Individual Contributions of Ice Formation and Freeze-Concentration on Isothermal Stability of Lactate Dehydrogenase during Freezing. *Journal of pharmaceutical sciences.*(97), 798-814. doi:10.1002/jps.21017.

Bhattacharya, S. (2018). Cryoprotectants and Their Usage in Cryopreservation Process. In Y. Bozkurt, *Cryopreservation Biotechnology in Biomedical and Biological Sciences.* IntechOpen. doi:10.5772/intechopen.80477

Bjelošević, M., Seljak, K. B., Trstenjak, U., Logar, M., Brus, B., & Ahlin Grabnar, P. (2018). Aggressive conditions during primary drying as a contemporary approach to optimise freeze-drying cycles of biopharmaceuticals. *European Journal of Pharmaceutical Sciences, 122*, 292–302. doi:10.1016/j.ejps.2018.07.016

Boguslavskii, Y. U., & Eknadiosyants, O. K. (1969). Physical Mechanism of Acoustic Atomization of Loquid. *Akusticheskij Zhurnal, 15*, 17–24.

Capozzi, L., Trout, B. L., & Pisano, R. (2019, 1). From Batch to Continuous: Freeze-Drying of Suspended Vials for Pharmaceuticals in Unit-Doses. *Ind. Eng. Chem. Res., 58*, 1635–1649. doi:10.1021/acs.iecr.8b02886

Chalmers, B. (1964). *Principles of Solidification.* Wiley. Tratto da https://books.google.com/books?id=OWnxAAAAMAAJ

Charlesworth, D. H., & Marshall Jr., W. R. (1960, 3). Evaporation from drops containing dissolved solids. *AIChE J., 6*, 9–23. doi:10.1002/aic.690060104

Chen, S.-L., & Chen, C.-L. (1999, 10). Effect of Nucleation Agents on the Freezing Probability of Supercooled Water inside Capsules. *null, 5*, 339–351. doi:10.1080/10789669.1999.10391242

Chen, X. D. (2008). *Drying Technologies in Food Processing.* (1st ed.. ed.). Hoboken: John Wiley & Sons, Incorporated.

Cheng, F., Zhou, X., & Liu, Y. (2018, 1). Methods for Improvement of the Thermal Efficiency during Spray Drying. *E3S Web of Conferences, 53*, 01031. doi:10.1051/e3sconf/20185301031

Dawoodbhai, S., & Rhodes, C. T. (1989, 1). The Effect of Moisture on Powder Flow and on Compaction and Physical Stability of Tablets. *Drug Development and Industrial Pharmacy, 15*, 1577–1600. doi:10.3109/03639048909052504

Donohue, M., & Aranovich, G. (1998). Classification of Gibbs adsorption isotherms. *Advances in Colloid and Interface Science, 76*, 137-152. doi:10.1016/S0001-8686(98)00044-X.

Eckhardt, B. O. (1991). Effect of Freezing on Aggregation of Human Growth. *Hormone. Pharm Res*(8), 1360-1364. doi:https://doi.org/10.1023/A:1015888704365

Franks, F. (1992). Freeze-Drying : A Combination of Physics, Chemistry, Engineering and Economics. *Japanese Journal of Freezing and Drying, 38*, 5–16. doi:10.20585/touketsukansokaishi.38.0_5

Gharsallaoui, A., Roudaut, G., Chambin, O., Voilley, A., & Saurel, R. (2007). Applications of spray-drying in microencapsulation of food ingredients: An overview. *Food Research International, 40*, 1107–1121. doi:10.1016/j.foodres.2007.07.004

Giner-Santonja, G., Karlis, P., Stubdrup, K., Brinkmann, T., & Roudier, S. (2019, 12). *Best Available Techniques (BAT) Reference Document for the Food, Drink and Milk Industries.* doi:10.2760/243911

Gleysteen, L. F., & Deitz, V. R. (1945, 11). Hysteresis in the physical adsorption of nitrogen on bone char and other adsorbents. *Journal of the Franklin Institute, 240*, 416–417. doi:10.1016/0016-0032(45)90543-6

Gogate, P. (2015). The use of ultrasonic atomization for encapsulation and other processes in food and pharmaceutical manufacturing. (J. A. Gallego-Juárez, & K. F. Graff, Eds.) *Power Ultrasonics, 30*, 911-935. doi:https://doi.org/10.1016/B978-1-78242-028-6.00030-2

Haseley, P., & Oetjen, G.-W. (2018, 2). *Freeze-Drying.* Wiley-VCH Verlag GmbH & Co. KGaA. doi:10.1002/9783527808946

Hickling, R. (1965). Nucleation of Freezing by Cavity Collapse and its Relation to Cavitation Damage. *Nature, 206*, 915–917. doi:10.1038/206915a0

Hindmarsh, J., Russell, A., & Chen, X. (2007). Fundamentals of the spray freezing of foods—microstructure of frozen droplets. *Journal of Food Engineering, 78*(1), 136-150. doi:https://doi.org/10.1016/j.jfoodeng.2005.09.011.

Hozumi, T., Saito, A., Okawa, S., & Eshita, Y. (2005). Effects of shapes of electrodes on freezing of supercooled water in electric freeze control. *International Journal of Refrigeration, 28*, 389–395. doi:10.1016/j.ijrefrig.2004.08.009

Hozumi, T., Saito, A., Okawa, S., & Matsui, T. (2002). Freezing phenomena of supercooled water under impacts of ultrasonic waves. *International Journal of Refrigeration, 25*, 948–953. doi:10.1016/S0140-7007(01)00104-9

Hozumi, T., Saito, A., Okawa, S., & Watanabe, K. (2003). Effects of electrode materials on freezing of supercooled water in electric freeze control. *International Journal of Refrigeration, 26*, 537–542. doi:10.1016/S0140-7007(03)00008-2

Hu, Y., Zhang, Z., Zhang, Y., Fan, S., & Liang, D. (2006, 3). Viscosity and Density of the Nonelectrolyte System Mannitol + Sorbitol + Sucrose + H2O and Its Binary and Ternary Subsystems at 298.15 K. *Journal of Chemical & Engineering Data, 51*, 438–442. doi:10.1021/je0503608

Huang, L. X., & Mujumdar, A. (2005). Development of a new innovative conceptual design for horizontal spray dryer via mathematical modeling. *Drying Technology, 23*, 1169–1187. doi:10.1081/DRT-200059328

Huang, L., Kumar, K., & Mujumdar, A. S. (2003). Use of Computational Fluid Dynamics to Evaluate Alternative Spray Dryer Chamber Configurations. *Drying Technology, 21*, 385–412. doi:10.1081/DRT-120018454

International Atomic Energy Agency. (1978). *Particle Size Analysis in Estimating the Significance of Airborne Contamination.* Vienna: IAEA.

Ishwarya, S. P., Anandharamakrishnan, C., & Stapley, A. G. (2015). Spray-freeze-drying: A novel process for the drying of foods and bioproducts. *Trends in Food Science & Technology, 41*, 161–181. doi:10.1016/j.tifs.2014.10.008

Jangam, S., Mujumdar, A., & B. Adhikari. (2016). Drying: Physical and Structural Changes. (B. Caballero, P. M. Finglas, & F. Toldrá, A cura di) *Encyclopedia of Food and Health*, 446-455. doi:https://doi.org/10.1016/B978-0-12-384947-2.00241-5

Jehinder, J., & Umadevi, M. (2012, 8). Synthesis and characterization of monodispersed silver nanoparticles. *Advances in Natural Sciences: Nanoscience and Nanotechnology, 3*, 035013. doi:10.1088/2043-6262/3/3/035013

Jennings, T. A. (1988, 7). Discussion of Primary Drying during Lyophilization. *PDA J Pharm Sci Technol, 42*, 118. Tratto da http://journal.pda.org/content/42/4/118.abstract

Jiang, X., Zhu, C., & Ma, Y. (2013). Densities and Viscosities of Erythritol, Xylitol, and Mannitol in l-ascorbic Acid Aqueous Solutions at T = (293.15 to 323.15) K. *Journal of Chemical & Engineering Data, 58*, 2970–2978. doi:10.1021/je400395u

Kumar, K. N., Mallik, S., & Sarkar, K. (2017, 12). Role of freeze-drying in the presence of mannitol on the echogenicity of echogenic liposomes. *The Journal of the Acoustical Society of America, 142*, 3670–3670. doi:10.1121/1.5017607

Kuu, W. Y. (2018, January 16). *United States of America Patent No. US9869513B2.* Retrieved from https://patents.google.com/patent/US9869513B2/en

Kuu, W., Doty, M., Rebbeck, C., Hurst, W., & Cho, Y. (2013, 8). Gap-freezing approach for shortening the lyophilization cycle time of pharmaceutical formulations–Demonstration of the concept. *Journal of pharmaceutical sciences, 102*. doi:10.1002/jps.23610

Lang, R. J. (1962). Ultrasonic Atomization of Liquids. *The Journal of the Acoustical Society of America, 34*, 6–8. doi:10.1121/1.1909020

Leuenberger, H. (1986, September 2). *United States of America Patent No. 4608764.* Retrieved from https://patents.google.com/patent/US4608764A/en

Leuenberger, H. (2002). Spray Freeze-drying – The Process of Choice for Low Water Soluble Drugs? *Journal of Nanoparticle Research, 4*, 111–119. doi:https://doi.org/10.1023/A:1020135603052

Lewin, L. M., & Mateles, R. I. (1962). Freeze drying without a vacuum, a preliminary investigation. *Food Technology, 16*, 94.

Liapis, A., & Bruttini, R. (2009). A mathematical model for the spray freeze drying process: The drying of frozen particles in trays and in vials on trays. *International Journal of Heat and Mass Transfer, 52*, 100-111. doi:https://doi.org/10.1016/j.ijheatmasstransfer.2008.06.026

Liu, G. (1992). Energy conservation in spray drying. *Dyestuff industry, 29*, 49.

Liu., W. (2001). The practical technology of spray drying. *China Light Industry Press*.

Magri, G., Franzé, S., Musazzi, U. M., Selmin, F., & Cilurzo, F. (2019). Data on spray-drying processing to optimize the yield of materials sensitive to heat and moisture content. *Data in Brief, 23*, 103792. doi:10.1016/j.dib.2019.103792

Malecki, G. J., Shinde, P., Morgan, A. L., & Farkas, D. F. (1970). Atmospheric fluidized bed freeze drying. *Food Technology, 24*, 601-603.

Maury, M., Murphy, K., Kumar, S., Shi, L., & Lee, G. (2005, 4). Effect of process variables on the powder yield of spray dried trehalose on a laboratory spray-drier. *European journal of pharmaceutics and biopharmaceutics : official journal of Arbeitsgemeinschaft für Pharmazeutische Verfahrenstechnik e.V, 59*, 565–73. doi:10.1016/j.ejpb.2004.10.002

Meryman, H. T. (1959, 9). Sublimation Freeze-Drying without Vacuum. *Science, 130*, 628. doi:10.1126/science.130.3376.628

Millqvist-Fureby, A., Malmsten, M., & Bergenståhl, B. (1999). Spray-drying of trypsin – surface characterisation and activity preservation. *International Journal of Pharmaceutics, 188*, 243–253. doi:10.1016/S0378-5173(99)00226-4

National Center for Biotechnology Information. (2004, 09 16). *PubChem*. Tratto il giorno 01 21, 2021 da https://pubchem.ncbi.nlm.nih.gov/compound/Mannitol.

Oetjen, G.-W., & Haseley, P. (2004). *Freeze Drying* (2nd ed.). Weinheim: WILEY-VCH Verlag GmbH & Co. KGaA.

Patel, S. M., Bhugra, C., & Pikal, M. J. (2009). Reduced Pressure Ice Fog Technique for Controlled Ice Nucleation during Freeze-Drying. *AAPS PharmSciTech, 10*, 1406. doi:10.1208/s12249-009-9338-7

Patel, S., Doen, T., & Pikal, M. (2010, 3). Determination of End Point of Primary Drying in Freeze-Drying Process Control. *AAPS PharmSciTech, 11*, 73–84. doi:10.1208/s12249-009-9362-7

Pegram, L. M., & Record, M. T. (2009). Using surface tension data to predict differences in surface and bulk concentrations of nonelectrolytes in water. *The journal of physical chemistry. C, Nanomaterials and interfaces, 113*(6), 2171–2174. doi:https://doi.org/10.1021/jp8073305

Pikal, M., Shah, S., Roy, M., & Putman, R. (1990). The secondary drying stage of freeze drying: drying kinetics as a function of temperature and chamber pressure. *International Journal of Pharmaceutics, 60*(3), 203-207. doi:https://doi.org/10.1016/0378-5173(90)90074-E

Pikal, M., Tang, X., & Nail, S. (2005). *United States of America Patent No. US 6971187 B1.*

Pisano, R. (2019). Alternative methods of controlling nucleation in freeze drying. *Lyophilization of Pharmaceuticals and Biologicals. Methods in Pharmacology and Toxicology.*

Pisano, R. (2020). Continuous Manufacturing of Lyophilized Products: Why and How to Make it Happen. *Am. Phar. Rev, 23*, 20–22. Tratto il giorno 03 11, 2021 da https://www.americanpharmaceuticalreview.com/Featured-Articles/563771-Continuous-Manufacturing-of-Lyophilized-Products-Why-and-How-to-Make-it-Happen/

Pisano, R., Arsiccio, A., Capozzi, L. C., & Trout, B. L. (2019). Achieving continuous manufacturing in lyophilization: Technologies and approaches. *European Journal of Pharmaceutics and Biopharmaceutics, 142*, 265-279. doi:https://doi.org/10.1016/j.ejpb.2019.06.027.

Pisano, R., Fissore, D., & Barresi, A. A. (2011). Heat transfer in freeze-drying apparatus.

Pisecký, J. (2012). *Handbook of milk powder manufacture.* Copenhagen: GEA Process Engineering A/S. Retrieved 09 9, 2020, from https://www.gea.com/en/expert-knowledge/milk-powder-manufacture/index.jsp

Qi Lin, S. X., & Chen, X. D. (2002). Improving the Glass-Filament Method for Accurate Measurement of Drying Kinetics of Liquid Droplets. *Chemical engineering research & design, 80*, 401–410. doi:10.1205/026387602317446443

Quast, D. G., & Karel, M. (1968, 3). Dry Layer Permeability and Freeze-Drying Rates in Concentrated Fluid Systems. *Journal of Food Science, 33*, 170–175. doi:10.1111/j.1365-2621.1968.tb01344.x

Rajan, R., & Pandit, A. B. (2001). Correlations to predict droplet size in ultrasonic atomisation. *Ultrasonics, 39*, 235–255. doi:10.1016/S0041-624X(01)00054-3

Rambhatla, S., Ramot, R., Bhugra, C., & Pikal, M. J. (2004). Heat and mass transfer scale-up issues during freeze drying: II. Control and characterization of the degree of supercooling. *AAPS PharmSciTech, 5*, 54–62. doi:10.1208/pt050458

Ranz, W. E., & Marshall, W. R. (1952). Evaporation from drops. *Chemical Engineering Progress, 48*, 141–173.

Rey, L., & May, J. C. (2010, 4). *Freeze-drying/lyophilization of pharmaceutical and biological products: Third edition.* Informa Healthcare.

Sano, Y., & Keey, R. B. (1982). The drying of a spherical particle containing colloidal material into a hollow sphere. *Chemical engineering science, 37*, 881–889. doi:10.1016/0009-2509(82)80176-0

Shi, M., & Wang, X. (2004, 12). Investigation on Moisture Transfer Mechanism in Porous Media During Rapid Drying Process. *Drying Technology., 22*, 111–122. doi:10.1081/DRT-120028222

Skoog, D. A., Crouch, S. R., & Holler, F. J. (2017). *Principles of instrumental analysis.*

Storey, R. A., & Ymen, I. (2011). *Solid state characterization of pharmaceuticals.* Chichester, UK: John Wiley & Sons. doi:10.1002/9780470656792

Swindells, J. F. (1958). *Viscosities of sucrose solutions at various temperatures: tables of recalculated values.* Wahington: United States. National Bureau of Standards.

Trelea, I. C., Passot, S., Fonseca, F., & Marin, M. (2007, 6). An Interactive Tool for the Optimization of Freeze-Drying Cycles Based on Quality Criteria. *Drying technology, 25*, 741–751. doi:10.1080/07373930701370100

(2014, 8 5). *Patent No. US8794013B2.* Retrieved from https://patents.google.com/patent/US8794013B2/un

van Winden, E. C. (2003). Freeze-Drying of Liposomes: Theory and Practice. In *Methods in Enzymology* (Vol. 367, p. 99–110). Academic Press. doi:10.1016/S0076-6879(03)67008-4

Velić, D., Bilic, M., Tomas, S., & Planinić, M. (2003, 11). *Energy saving in spray drying process.*

Vijay, G. A., Moorthi, N. S., & Manivannan, A. (2015). Internal and external flow characteristics of swirl atomizers: A review. *Atomization and Sprays, 25*(2), 153-188. doi:10.1615/AtomizSpr.2014010219

Vishali, D. A., Monisha, J., Sundari, S. S., Moses, J. A., & Chinnaswamy, A. (2019, 3). Spray freeze drying: Emerging applications in drug delivery. *Journal of Controlled Release, 300*. doi:10.1016/j.jconrel.2019.02.044

Wang, Z., Finlay, W., Peppler, M., & Sweeney, L. (2006). Powder formation by atmospheric spray-freeze-drying. *Powder Technology, 170*(1), 45-52. doi:https://doi.org/10.1016/j.powtec.2006.08.019

Wei, S., Zhong, C., & Su-Yi, H. (2005, 7). Molecular dynamics simulation of liquid water under the influence of an external electric field. *null, 31*, 555–559. doi:10.1080/0892702500138483

Woodward, H. T. (1963). Freeze drying without vacuum. *Food Engineering, 35*, 96-97.

Yu, Z., Johnston, K. P., & O.Williams III, R. (2006). Spray freezing into liquid versus spray-freeze drying: Influence of atomization on protein aggregation and biological activity. *European Journal of Pharmaceutical Sciences, 27*(1), 9-18. doi:https://doi.org/10.1016/j.ejps.2005.08.010.